

Aus der Klinik für Psychiatrie und Psychotherapie
(Prof. Dr. med. J. Wiltfang)
der Medizinischen Fakultät der Universität Göttingen

Neuropathological and behavioral alterations in two transgenic mouse models of Alzheimer's disease

INAUGURAL-DISSERTATION

zur Erlangung des Doktorgrades
der Medizinischen Fakultät der
Georg-August-Universität zu Göttingen

vorgelegt von

Julius Nicolai Meißner

aus

Göttingen

Göttingen 2016

Dekan:	Prof. Dr. rer. nat. H. K. Kroemer
Referent/in	Prof. Dr. rer. nat. T. A. Bayer
Ko-Referent/in:	Prof. Dr. T. F. Outeiro
Drittreferent/in:	Prof. Dr. med. M. Oppermann

Datum der mündlichen Prüfung: 19.07.2016

Hiermit erkläre ich, die Dissertation mit dem Titel "Neuropathological and behavioral alterations in two transgenic mouse models of Alzheimer's disease" eigenständig angefertigt und keine anderen als die von mir angegebenen Quellen und Hilfsmittel verwendet zu haben.

Göttingen, den

Contents

Contents	I
List of figures	IV
List of tables	V
List of abbreviations	VI
1 Introduction	1
1.1 Clinical aspects of Alzheimer's disease	1
1.1.1 Epidemiology	2
1.1.2 Diagnosis	2
1.1.3 Therapy	4
1.1.4 Neuropathology of Alzheimer's disease	4
1.2 Pathogenesis of Alzheimer's Disease	5
1.2.1 Amyloid precursor protein	5
1.2.2 Processing of the amyloid precursor protein	6
1.2.3 Genetics of Alzheimer's disease	7
1.2.4 Amyloid cascade hypothesis	7
1.2.5 The modified amyloid hypothesis	8
1.2.6 A β toxicity	8
1.2.7 A β variants	9
1.2.8 Pyroglutamate modified A β	10
1.2.9 The TBA42 mouse model	10
1.2.10 A β clearance	11
1.2.11 LRP1	11
1.2.12 The 5xFAD <i>Lrp1</i> ^{BE-/-} mouse model	11
1.3 Project objectives	12
1.3.1 Project I: Quantification of neurodegeneration and analysis of behavioral deficits in the TBA42 mouse model	13
1.3.2 Project II: Exploring in vivo effects of impaired A β clearance induced by knockout of brain endothelial <i>LRP1</i> in 5xFAD mice	13
2 Materials and methods	15
2.1 Animal breeding and genotyping	15
2.1.1 DNA extraction	15
2.1.2 DNA concentration determination	16
2.1.3 Polymerase chain reaction	16
2.1.4 Agarose gel electrophoresis	17
2.2 Preparation of CNS-tissue	18
2.3 Stereology	19
2.3.1 Preparation of cryosections	19

2.3.2	Cresyl violet staining.....	19
2.3.3	Optical fractionator workflow.....	20
2.4	Immunohistochemistry	22
2.4.1	Fixation and paraffin embedding of CNS tissue.....	22
2.4.2	Preparation of paraffin sections	22
2.4.3	3,3'-Diaminobenzidine (DAB) immunohistochemistry	22
2.5	4-6-diaminidino-2-phenylindole (DAPI) staining	23
2.6	Quantifications	24
2.7	Behavioral analyses.....	25
2.7.1	Balance beam	25
2.7.2	Inverted grip hang.....	25
2.7.3	String suspension	26
2.7.4	Morris water maze	27
2.7.5	Cross maze	28
2.7.6	Elevated plus maze	28
2.8	Data analysis.....	29
2.9	Software	29
3	Results	30
3.1	Project I: Quantification of neurodegeneration and analysis of behavioral deficits in the TBA42 mouse model.....	30
3.1.1	A β deposition in the hippocampal CA1 region and spinal cord of TBA42 mice	30
3.1.2	Obvious neuron loss depicted by DAPI staining	32
3.1.3	Stereological quantification of neuron loss	32
3.1.4	Severe motor deficits in aged TBA42 mice.....	33
3.1.5	Reduced anxiety in aged TBA42 mice.....	34
3.1.6	Impaired working memory in aged TBA42 mice.....	36
3.1.7	TBA42 mice display spatial learning deficits.....	37
3.2	Project II: Exploring in vivo effects of impaired Aβ clearance induced by knockout of brain endothelial <i>LRP1</i> in 5xFAD mice	42
3.2.1	Unaltered plaque pathology and gliosis in 5xFAD/ <i>Lrp1</i> ^{BE-/-} mice.....	42
3.2.2	Morris water maze	43
4	Discussion	45
4.1	Project I: Quantification of neurodegeneration and analysis of behavioral deficits in the TBA42 mouse model.....	45
4.1.1	The TBA42 mouse model.....	46
4.1.2	Neuron loss in aged TBA42 mice.....	47
4.1.3	Impaired motor function in TBA42 mice	48

4.1.4	Reduced anxiety behavior in the TBA42 model	49
4.1.5	Cognitive decline in aged TBA42 mice.....	50
4.1.6	TBA42 is a valid model of AD.....	52
4.1.7	A β _{pE3-42} as a potential drug target	53
4.2	Project II: Exploring in vivo effects of impaired Aβ clearance induced by knockout of brain endothelial <i>LRP1</i> in 5xFAD mice	55
4.2.1	Plaque pathology in 5xFAD/ <i>Lrp1</i> _{BE^{-/-}}	56
4.2.2	Gliosis in 5xFAD/ <i>Lrp1</i> _{BE^{-/-}} mice.....	57
4.2.3	Cognitive decline in 5xFAD/ <i>Lrp1</i> _{BE^{-/-}} mice	57
4.2.4	Restoring BBB clearance as a potential treatment and prevention of AD	58
5	Summary	60
6	Literature	62

List of figures

Figure 1.1 Project objectives.....	14
Figure 2.1 Stereological quantifications of the neuron number in the hippocampal CA1 region.	20
Figure 2.2 Quantification procedure.....	24
Figure 2.3 Setup of motor test apparatuses.	26
Figure 2.4 Morris water maze apparatus.	28
Figure 3.1 Expression of A β in hippocampus and spinal cord of TBA42 mice.....	31
Figure 3.2 Age-dependent neuron loss in TBA42 mice.....	32
Figure 3.3 Quantification using unbiased stereology.	33
Figure 3.4 Severe motor deficits in TBA42 mice.....	35
Figure 3.5 Reduced Anxiety in aged TBA42 mice.....	36
Figure 3.6 Impaired working memory in aged TBA42 mice.....	37
Figure 3.7 Cued training showed that all mice have appropriate motor abilities and intact vision.	39
Figure 3.8 Impaired spatial learning in aged TBA42 mice.....	40
Figure 3.9 Impaired spatial reference memory in aged TBA42 mice.....	41
Figure 3.10 <i>LRP1</i> knockout does not lead to altered plaque loads and gliosis in 5xFAD mice..	42
Figure 3.11 Spatial learning deficits in 5xFAD/ <i>Lrp1</i> _{BE} ^{-/-}	43
Figure 3.12 Impairment of spatial reference memory deficits in 5xFAD/ <i>Lrp1</i> _{BE} ^{-/-}	44

List of tables

Table 1 PCR-mixture used for genotyping of TBA42 mice.....	17
Table 2 PCR protocol used for genotyping of TBA42 mice	18
Table 3 Definition of stereological parameters.....	21
Table 4 Stereological parameters for quantification of neurons in the CA1 region.....	21
Table 5 String suspension scoring system.....	26

List of abbreviations

Abbreviation	Description
A β	amyloid beta
A β _{pE3-42}	amyloid beta with a pyroglutamate residue at position 3
AD	Alzheimer's disease
ANOVA	Analysis of variance
ApoE	apolipoprotein E
APP	amyloid precursor protein
asf	area sampling fraction
BBB	blood brain barrier
BE	brain endothelium
CNS	central nervous system
CSF	cerebrospinal fluid
DAB	3,3'-Diaminobenzidine
DAPI	4-6-Diaminidino-2-Phenylindole
ddH ₂ O	distilled, deionized water
DNA	deoxyribonucleic acid
EOAD	early-onset Alzheimer's disease
FAD	familial Alzheimer's disease
KI	knock in
LOAD	late-onset Alzheimer's disease
LTP	long term potentiation
LRP1	low density lipoprotein receptor-related protein 1
MANOVA	multivariate analysis of variance
MRI	magnetic resonance imaging
MWM	Morris water maze
NMDA	N-methyl-D-aspartate
PBS	phosphate buffered saline
PCR	polymerase chain reaction
PSEN	Presenilin

1 Introduction

Alzheimer's disease (AD) is named after the German physician Alois Alzheimer. In 1906 he presented a single case study of one of his patients. Auguste Deter developed a cognitive decline and behavioral symptoms. After his patient's death Alzheimer examined her brain and found neuron loss, extracellular amyloid plaques and intracellular neurofibrillary tangles (Alzheimer 1907; Alzheimer et al. 1995), which today are commonly accepted neuropathological hallmarks of AD (Montine et al. 2012). It took up until 1992, when John Hardy and Gerald Higgins formulated the amyloid cascade hypothesis, to identify the accumulation of amyloid beta ($A\beta$) as the key event in the pathogenesis of AD (Hardy and Higgins 1992). Today, more than 100 years after its description AD is the most prevalent form of dementia (Reitz et al. 2011) and therapeutic options are urgently needed. However, to date no disease modifying strategy is available.

1.1 Clinical aspects of Alzheimer's disease

Alzheimer's disease is classified as a degenerative disorder of the brain that progresses gradually following a slow onset (World Health Organization). It is characterized clinically by a global cognitive impairment. Lasting for longer than six months, this syndrome is referred to as dementia. In order to distinguish Alzheimer's disease from other forms of dementia it is further characterized by neuropathological and neurochemical hallmarks (McKhann et al. 2011; Holtzman et al. 2011). The most commonly observed late-onset Alzheimer's disease (LOAD) begins beyond the age of 65 with an increasing incidence starting at the end of the seventh decade of life. On the contrary an early onset form of Alzheimer's disease (EOAD), which often progresses more rapidly is described (Reitz and Mayeux 2014). According to the National Institute on Aging (NIA) the disease progresses from a preclinical stage to mild cognitive impairment due to AD and finally dementia due to AD (Albert et al. 2011; McKhann et al. 2011). It is assumed that in the preclinical stage the pathological process resulting in the development of AD is initiated as early as 20 to 30 years before the first symptoms occur (Blennow et al. 2006). Mild cognitive impairment due to AD progresses to dementia due to AD with a conversion rate of 10 to 15 % per year (Petersen 2004), which finally results in the death of patients (Holtzman et al. 2011).

1.1.1 Epidemiology

Alzheimer's disease is the most prevalent form of dementia, accounting for approximately 70 % of the cases (Reitz et al. 2011). Globally the estimated prevalence was 23.4 million in 2006 (Ferri et al. 2006). By the year 2050 however, this number is predicted to increase dramatically by the factor four (Reitz and Mayeux 2014), in the light of demographic ageing in developed countries (Reitz et al. 2011). For Germany in 2007 the prevalence of dementias of all etiologies was 1.07 million in over 60 year-old persons with an incidence of 244.000. Interestingly, the prevalence rates in Eastern-Germans aged above 85 years was higher than in Western-Germans (Ziegler and Doblhammer 2009). The incidence of Alzheimer's disease increases progressively with age, rising from approximately 0.5% in persons aged 65-70 to 7-8% in over 85 year old individuals (Mayeux and Stern 2012). In general women are at higher risk to develop AD (Farrer et al. 1997).

In addition to ageing a number of other non-genetic risk factors for developing AD are described. Risk factors for atherosclerosis like hypertension, hypercholesterolemia and smoking also increase the risk for developing AD later in life (Kivipelto et al. 2001; Kivipelto et al. 2005) and persons suffering from heart failure (Qiu et al. 2006) or diabetes mellitus are at greater risk for developing AD (Leibson et al. 1997). Furthermore, a history of traumatic brain injury predisposes for the development of AD (Plassman et al. 2000; Jellinger et al. 2001; Sivanandam and Thakur 2012; Gupta and Sen 2016).

1.1.2 Diagnosis

Alzheimer's disease is diagnosed applying cognitive tests, followed by laboratory tests and imaging procedures, in order to allow an early diagnosis, distinguish between different forms of dementia and monitor disease progression (Leitlinie Demenzen 2009). Taking prevalence and clinical features into account, most relevant differential diagnoses are vascular dementia (Qiu et al. 2007) and frontotemporal dementia (Weder et al. 2007). Typical slow onset, gradual progression, and the exclusion of other explanatory medical findings hint towards "probable AD dementia". An AD family history can further strengthen the diagnosis, while an abrupt onset, epilepsy, paresis and sensory deficits in early stages make AD less probable (McKhann et al. 2011). Pre-existing psychiatric conditions like depressions and an intake of anticholinergic medication may increase the risk for later developing dementia in general (Carrière et al. 2009) or AD in particular (Ownby et al. 2006).

Presence and severity of cognitive impairment in AD patients can be quantified with cognitive tests. The Mini-Mental State Examination is most commonly used and provides a scale ranging from 0 (severe impairment) to 30 (no impairment) (Folstein et al. 1975). The test, among others like the clock-drawing test (Sunderland et al. 1989) or the Cambridge Cognitive Examination, is especially suitable as a screening test (Mitchell 2009, Aprahamian et al. 2010, 2010; Martinelli et al. 2014). Behavioral components of AD can be quantified by comprehensive tests (Reisberg et al. 1997; Blazina et al. 1995) or focusing specific aspects of behavioral abnormalities in AD (Cohen-Mansfield 1997; Clarke et al. 2007). However, results from cognitive tests can be confounded by educational level and dementia can be caused by other pathologies than AD. Therefore, further diagnostic tests should be considered in order to specify the diagnosis (McKhann et al. 2011). The detection of prodromal AD cases (Hampel et al. 2009) is especially important for proper stratification, aiding study design of clinical trials, testing preventive or therapeutic strategies (Hampel et al. 2010; Hampel et al. 2011). Alzheimer's disease cerebrospinal fluid (CSF) biomarkers are particularly specific for the disease since changes derive from deposits of amyloid protein and intracellular neurofibrillary tangles (Genius et al. 2012). Interestingly, CSF levels of $A\beta_{42}$ (Blennow and Hampel 2003; Andreasson et al. 2007) and the ratio of $A\beta_{1-42}/A\beta_{1-40}$ are decreased (Mattsson et al. 2009). Concentrations of total Tau-protein (T-Tau) and phosphorylated Tau (p-Tau) are increased, but certain p-Tau species are more specific for AD (Arai et al. 2000; Hu et al. 2002).

Using structural magnetic resonance imaging (MRI) atrophy of hippocampus and amygdala, typically found in the late-onset form of the disease (Reitz and Mayeux 2014) and the precuneus, commonly affected in early onset forms (Karas et al. 2007; Mungas et al. 2005) can be visualized. Using positron emission tomography (PET), protein aggregates amyloid plaques can be visualized with FDDNP ((2-(1-{6-[(2-[fluorine-18]fluoroethyl)(methyl)amino]-2-naphthyl}-ethylidene)malononitrile) (Shoghi-Jadid et al. 2002; Shin et al. 2010) or PIB (pittsburgh compound B) (Edison et al. 2008; Rowe et al. 2007; Klunk et al. 2004) respectively. Single photon emission computed tomography (SPECT) tracers targeting components of the cholinergic system (Colloby et al. 2010) also deliver an altered signal in AD. However proven to be useful, biomarkers have to be obtained in standardized procedure (Genius et al. 2012), which partly have yet to be defined (Frisoni et al. 2013).

1.1.3 Therapy

To date no disease modifying therapy or preventive strategy of Alzheimer's disease is available and patients are solely treated symptomatically. Inhibitors of the acetylcholinesterase are administered to treat patients with mild to moderate AD, addressing an acetylcholine deficiency, induced by neurodegeneration in the basal forebrain. Although effects are small, patients treated for 6 or 12 months with donepezil, galantamine or rivastigmine, improve significantly in AD-tests (Birks 2006). These substances should be applied in the highest tolerated dose (Leitlinie Demenzen 2009). Moderate to severe cases of AD are treated with memantine, a non-competitive glutamate N-methyl-D-aspartate (NMDA) receptor agonist. The substance has a small beneficial effect on cognition, activities of daily living and behavior (McShane et al. 2006). Furthermore, agitation and psychosis that occur regularly in AD (Levy et al. 1996) should be treated with selective serotonin reuptake inhibitors (SSRIs) like sertraline and citalopram (Seitz et al. 2011). The usage of antipsychotic drugs like haloperidol or olanzapine has to be limited in time and dosage, since the risk of mortality is significantly increased (Kales et al. 2014). According to the literature available, no definite conclusion on a beneficial effect of cognitive training and cognitive rehabilitation can be drawn (Bahar-Fuchs et al. 2013). Instead, there are studies indicating that physical exercise can have a beneficial effect in AD patients (Rolland et al. 2007). Many clinical trials have been and are still trying to address the need for new therapeutics of AD. Promising therapeutic approaches include targeting the production of A β , its oligomerization and facilitation of its clearance (Schneider et al. 2014).

1.1.4 Neuropathology of Alzheimer's disease

A definite diagnosis of AD requires post mortem neurohistopathological investigation of the brain. The AD defining neuropathological pathology can be classified as low, intermediate or high according to the ABC score (Montine et al. 2012). It is determined by the phase of A β plaque deposition (Thal et al. 2002), the stage of NFT deposition (Braak and Braak 1991) and the abundance of neuritic plaques (Mirra et al. 1991; Montine et al. 2012). A β plaque deposition starts in the neocortex (Phase 1), progresses to allocortical brain regions and diencephalic nuclei, the striatum and cholinergic nuclei of the basal forebrain (Phase 2). Later stages are characterized by plaque deposits in brain stem nuclei (Phase 4) and the cerebellum (Phase 5) (Thal et al. 2002). In contrast, neurofibrillary tangle pathology starts in the transentorhinal region (Stages I-II) and extends to the entorhinal region (Stages III-IV). Eventually neurofibrillary tangles are found in the isocortex (Stages IV-V) (Braak and Braak 1991). The classifi-

cation of the density of neuritic plaques ranges from sparse (1-5 neuritic plaques/mm²) and intermediate (6-20 neuritic plaques/mm²) to high (>20 neuritic plaques/mm²) (Mirra et al. 1991). Besides these criteria used for post-mortem diagnosis of AD a number of further neuropathological hallmarks is found. For example, Cerebral amyloid angiopathy is the commonly observed deposition of A β in cerebral vessels (Ellis et al. 1996). Additionally, an inflammatory response is seen in AD brains (Akiyama et al. 2000).

1.2 Pathogenesis of Alzheimer's Disease

The influential amyloid cascade hypothesis proposes that A β is the causative agent of AD pathology (Hardy and Higgins 1992). A β was shown to be the major component of senile plaques (Masters et al. 1985). Interestingly, A β is constantly produced in the brain by cleavage of its precursor protein (Haass et al. 1992) and is found in healthy individuals throughout life (Seubert et al. 1992). Following production it is removed from the brain by various clearance mechanisms (Deane et al. 2009; Lee and Landreth 2010; Tarasoff-Conway et al. 2015). A change in the delicate homeostasis between A β production and its clearance leads to an elevated steady state of A β concentrations (Selkoe 2000). According to the amyloid cascade hypothesis A β accumulation causes a series of downstream effects that eventually cause dementia (Hardy and Selkoe 2002). Changes on either side of the equilibrium of A β production and A β clearance can cause AD. Overproduction however is a rare cause mainly limited to familial Alzheimer's disease (FAD), early onset cases, while impaired clearance of A β is assumed to cause the majority of sporadic late-onset cases of the disease (Bates et al. 2009).

1.2.1 Amyloid precursor protein

The amyloid precursor protein (APP) is a type I membrane protein expressed in various cell types throughout the body (Mattson 1997). Several physiological functions in neurons have been attributed to the protein involving neurotrophic activity (Mucke et al. 1996), neurite outgrowth (Milward et al. 1992), neuronal differentiation (Hung et al. 1992) and cell adhesion (Storey et al. 1996; Coulson et al. 1997). The neuronal isoform comprises 695 amino acids. It consists of a large N-terminal portion that is located extracellularly, a 24 amino acid hydrophobic stretch that anchors the protein in intracellular membranes and in the plasmamembrane, and a small C-terminal intracellular domain. The A β fragment includes the last 28 resi-

dues of the extracellular portion and the first 12-14 residues of the transmembrane domain (Selkoe 1998).

1.2.2 Processing of the amyloid precursor protein

An amyloidogenic and a non-amyloidogenic pathway of APP processing are classically described. The turnover of APP by each of the two pathways is inversely correlated as the respective enzymes involved compete for APP as a substrate. Due to its localization within the center of its precursor protein two proteolytical cleavages are necessary to liberate A β . Firstly, APP is cleaved extracellularly by the beta-secretase β -site APP-cleaving enzyme 1 (BACE1) (Vassar et al. 1999; Kandalepas and Vassar 2012), resulting in the release of the N-terminal APPs β and the production of a membrane-bound C-terminal fragment (CTF- β). Secondly, the membrane embedded γ -secretase catalyzes the cleavage of the C-terminal fragment within the transmembrane domain (Selkoe and Wolfe 2007), which leads to the release of A β into the extracellular space. The residual cytoplasmatically located polypeptide is referred to as amyloid precursor protein intracellular domain (AICD). Gamma-secretase is a multi-subunit protein complex comprised of presenilin-1 (De Strooper et al. 1998) or presenilin-2 (Yan et al. 1999) harboring the active site of the complex and its limiting cofactors (Francis et al. 2002; Takasugi et al. 2003) Nicastrin (Yu et al. 2000; Edbauer et al. 2002), anterior pharynx-defective 1 (Aph-1) (Goutte et al. 2002; Francis et al. 2002) and presenilin enhancer 2 (Pen-2) (Francis et al. 2002). Peptides produced by γ -secretase most commonly end after amino acid 40 (90 %) and amino acid 42 (10 %) (Thinakaran and Koo 2008).

The non-amyloidogenic pathway is initiated by alpha-secretase cleavage of APP between Lys16 and Leu 17 within the A β -domain, interfering with A β production (Allinson et al. 2003). This leads to the release of the sAPP α ectodomain (Sisodia 1992) that in addition serves in promoting neuroprotection (Furukawa et al. 1996; Mattson et al. 1999) and memory enhancement (Thinakaran and Koo 2008). The residual membrane bound C-terminal fragment (CTF- α) is referred to as C83 (Vassar et al. 1999). Subsequent proteolytic cleavage results in the formation of AICD and the non-pathogenic p3 (Haass et al. 1992). Various zinc metalloproteinases harbor alpha secretase activity including the ADAM-family (a disintegrin and metalloproteinase) (Allinson et al. 2003).

Recently a third physiological APP processing pathway was described. The first step of APP cleavage by membrane-bound matrix metalloproteinases leads to the formation of CTF- η . The generated C-terminal fragment is further cleaved by ADAM and BACE, which results in the

formation of $A\eta$ - α and $A\eta$ - β . $A\eta$ - α is found in AD-brains and impairs neuronal function (Willem et al. 2015).

1.2.3 Genetics of Alzheimer's disease

A number of mutations have been described accounting for early-onset Alzheimer's disease. All of these mutations were identified in genes responsible for the generation of $A\beta$ by proteolytical cleavage of APP or APP itself (Karch et al. 2014). More than 30 mutations in the APP gene account for approximately 16 % of the cases of EOAD (Raux et al. 2005). Those are heterozygous missense mutations in or near the $A\beta$ coding regions (Jack et al. 2013) and APP gene duplications (Kasuga et al. 2009; Rovelet-Lecrux et al. 2006; Rovelet-Lecrux et al. 2007; Sleegers et al. 2006; Cabrejo et al. 2006) as well as recessive mutations (Tomiyama et al. 2008; Di Fede et al. 2009). By these mutations $A\beta$ production and the ratio of $A\beta_{42}$ to $A\beta_{40}$ can be altered or the aggregation propensity of $A\beta$ is increased (Bettens et al. 2013). Due to its localization on chromosome 21, more APP is produced in persons with trisomy 21 causing a genetic form of AD (Olson and Shaw 1969). Mutations in *PSEN* and *PSEN2* encoding the presenilin subunits of gamma secretase lead to an increased $A\beta_{42}/A\beta_{40}$ ratio (De Strooper et al. 1998; Bentahir et al. 2006; Kumar-Singh et al. 2006; Scheuner et al. 1996). For sporadic and familial LOAD the apolipoprotein E4 (apoE4) allele is a well-established risk factor (Corder et al. 1993; Strittmatter et al. 1993; Scheuner et al. 1996). Three different *apoE* alleles are found in human named apoE2, apoE3 and apoE4 (Nickerson et al. 2000). As compared to the most frequent genotype, e3e3, the age-adjusted relative risk for developing AD of individuals with one e4 allele is three, those with two e4 allele have a 15 fold higher risk to develop AD. In individuals aged between 60 and 69 the risk is even 35 times higher than in e3e3 carriers (Farrer et al. 1997). The life time risk of developing AD is 35 % in female e3e4 carriers and 68 % in female e4e4 carriers (Genin et al. 2011).

1.2.4 Amyloid cascade hypothesis

The amyloid cascade hypothesis states that $A\beta$ accumulation in the brain is an early event in the pathogenesis of AD driving downstream processes that eventually lead to dementia. It is proposed that $A\beta$ production, due to mutations in APP, PSEN1 and PSEN2 genes, is increased and accumulation of the peptide leads to the oligomerization and deposition as extracellular plaques. According to the hypothesis these $A\beta$ deposits induce synaptic and neuronal

injury that is accompanied by alterations in neuronal ionic homeostasis, oxidative injury, and altered activities of kinase and phosphatase activities, resulting in the formation of neurofibrillary tangles. Eventually, dementia is caused by widespread neuronal dysfunction and cell death (Hardy and Higgins 1992; Hardy and Selkoe 2002). Evidence supporting the hypothesis is provided by the fact that autosomal dominant EOAD is exclusively caused by mutations in genes involved in A β production. Additionally the hypothesis is consistent with findings on a role of apoE facilitated A β deposition (Holtzman et al. 2000) and results showing that mutations in the gene encoding tau induce frontotemporal dementia but not A β deposition as it is seen in AD (Hutton et al. 1998), indicating that tau pathology is a downstream event in the pathogenesis of AD.

1.2.5 The modified amyloid hypothesis

Although the amyloid cascade hypothesis is explanatory for the general role of A β as the pathogenic agent in AD, it is inconsistent with the finding that severity of the disease as measured by clinical features in AD-patients is well reflected by the extent of neurofibrillary tangle pathology (Braak and Braak 1991), but not by the extent of A β plaque deposition (Giannakopoulos et al. 1997). In contrast it was observed that intraneuronal accumulation of A β precedes NFT and plaque pathology (Gouras et al. 2000) and that intraneuronal A β deposits are correlated with apoptotic cell death in AD brains (LaFerla et al. 1997; Chui et al. 2001). Cell culture studies show that A β can also be produced intracellularly (Greenfield et al. 1999) and can be taken up from the extracellular space (Knauer et al. 1992). Taken together, these findings led to the formulation of the modified β -amyloid hypothesis highlighting the role of intracellular A β in the etiology of AD (Wirths et al. 2004).

Studies have also shown that A β plaque deposition correlates poorly with neurodegeneration in AD patients (Lesné et al. 2013) and in AD mouse models (Schmitz et al. 2004; Moechars et al. 1999). In contrast, a correlation is seen when levels of soluble forms of A β are analyzed (Haass and Selkoe 2007). A major role A β toxicity of soluble A β oligomers (Haupt et al. 2012) and β -sheet containing amyloid fibrils (Klein 2002) has been suggested.

1.2.6 A β toxicity

Early studies showed that soluble monomeric A β , as it is released by APP-cleavage from neurons, is not toxic but may rather be neurite-promoting. Subsequently A β becomes toxic due to

polymerization (Pike et al. 1991). In the course of fibril-formation soluble oligomers, which are a heterogeneous group of non-fibrillar polypeptides, are formed (Fändrich 2012). Different kinds of such oligomers are found in AD brains and impair synapse structure and function (Shankar et al. 2008; Noguchi et al. 2009). The level of soluble A β in brains correlates with severity of AD (McLean et al. 1999; Mc Donald, Jessica M et al. 2010), while plaques are assumed to serve as A β reservoirs standing in a dynamic equilibrium with soluble oligomers (Benilova et al. 2012). Mechanisms of A β oligomer induced synaptic dysfunction and cytotoxicity discussed are a disruption of LTP by affecting NMDA-receptor and AMPA-receptor function (Yamin 2009) or the upregulation of the nicotinic acetylcholine receptor (Dineley et al. 2001). Furthermore, a disruption of Calcium signaling (Demuro et al. 2010), induction of apoptosis by activation of caspases (Nakagawa et al. 2000) and mitochondrial dysfunction (Reddy and Beal 2008) have been reported. Moreover soluble A β oligomers induce hyperphosphorylation of tau (De Felice, Fernanda G et al. 2008; Zempel et al. 2010; Jin et al. 2011), linking A β depositon to neurofibrillary tangle pathology.

1.2.7 A β variants

In addition to A β_{1-40} and A β_{1-42} , many species with a truncated N- or C-terminus were identified in AD (Masters et al. 1985; Prelli et al. 1988; Miller et al. 1993). An extended C-terminus of A β_{1-42} elevates the aggregation propensity as compared to the shorter A β_{1-40} (Pike et al. 1995), and deposition of A β_{1-42} was found to be an early event in plaque formation (Iwatsubo et al. 1994). N-terminally truncated and modified versions were also identified in AD brains (Saido et al. 1995; Näslund et al. 1994). While A β_{1-40} , A $\beta_{\text{pE3-42}}$, A β_{4-40} , and A β_{1-42} are the most abundant species (Portelius et al. 2010), it was shown that N-terminal truncation increases aggregation propensity and toxicity of A β (Pike et al. 1995). Further posttranslational modifications including isomerization (Kuo et al. 1998) and racemization (Mori et al. 1994) of amino acid residues promote stability and formation of A β (Kuo et al. 1998). A β species modified by metal induced oxidation (Dong et al. 2003) and phosphorylation (Kumar et al. 2011) also have been identified in AD-brains. Another mechanism of increased pathogenicity of modified A β variants is an altered interaction with apoE (Munson et al. 2000).

1.2.8 Pyroglutamate modified A β

There is accumulating evidence pointing to a major role of pyroglutamate modified A β in the pathogenesis of AD. A $\beta_{\text{pE3-42}}$ is abundantly found in AD-brains (Saido et al. 1995; Harigaya et al. 2000). A pyroglutamate residue in A β is generated from a glutamate residue at position 3 of A β that by the catalytic activity of the enzyme glutaminyl cyclase (Schilling et al. 2008). A $\beta_{\text{pE3-42}}$ is more neurotoxic than full length A β peptide (Russo et al. 2002). This property is due to altered oligomerization kinetics and an up to 250-fold acceleration in the formation of aggregates as compared to the unmodified full-length peptide (Schilling et al. 2006). Furthermore, A $\beta_{\text{pE3-42}}$ has an increased hydrophobicity compared to the respective unmodified peptides leading to a decreased solubility (Schlenzig et al. 2009). In consequence more toxic high molecular weight oligomers are produced by this A β species (Bouter et al. 2013). To study in vivo effects of A $\beta_{\text{pE3-42}}$ transgenic mouse models have been developed. Constructs encoding A β_{3-42} with glutamine at position 3 that serves as a substrate for QC (Cynis et al. 2008b) were used. Intracellular presence of A $\beta_{\text{pE3-42}}$ induced a neuron loss in these models (Alexandru et al. 2011; Wirths et al. 2009).

1.2.9 The TBA42 mouse model

To study the exclusive impact of pyroglutamate modified A β_{3-42} the TBA42 mouse model has been developed by the group of Prof. Bayer (Wittnam et al. 2012). In TBA42 mice a transgenic vector encoding murine thyrotropin-releasing hormone-A β (mTRH-A β_{3-42}) under the control of the murine Thy1.2 regulatory sequence (Cynis et al. 2006; Wirths et al. 2009; Alexandru et al. 2011) is expressed. N-truncated A $\beta_{\text{pE3-42}}$ with a glutamine at position 3 is liberated into the secretory pathway (Cynis et al. 2006). The peptide is converted into A $\beta_{\text{pE3-42}}$ by the catalytic activity of the enzyme glutaminyl cyclase (Sevalle et al. 2009; Cynis et al. 2006; Jawhar et al. 2011). Glutamine is used instead of the naturally occurring glutamate, since it is a better substrate for QC (Schilling et al. 2004; Huang et al. 2005) and is also converted at a higher rate spontaneously (Cynis et al. 2006). In TBA42 mice A $\beta_{\text{pE3-42}}$ is deposited primarily intraneuronally within the hippocampus, spinal cord and cerebellar nuclei. Extracellular A β is only sparsely deposited and no A β plaques are formed. In the hippocampus a marked gliosis is induced by the presence of pyroglutamate modified A β (Wittnam et al. 2012).

1.2.10 A β clearance

AD is triggered by the accumulation of A β in the brain (Hardy and Higgins 1992). Recent evidence suggests that this accumulation in the most common, sporadic, late-onset form of the disease is due to an impaired clearance of the peptide, but not its overproduction (Mawuenyega et al. 2010). Pathways of A β clearance are the cleavage by proteolytically active enzymes, the cellular uptake A β followed by its proteasomal degradation (Wang et al. 2006), interstitial fluid bulk flow (Weller et al. 2008; Hawkes et al. 2012), cerebrospinal fluid absorption into the circulatory system (Pollay 2010) and efflux via the blood brain barrier (BBB) (Tarasoff-Conway et al. 2015; Deane et al. 2009; Zlokovic 2011). The latter mechanism is addressed by the neurovascular hypothesis of Alzheimer's Disease proposing that impaired clearance of A β by the low density lipoprotein receptor-related protein 1 (LRP1) at the BBB induces more A β deposition, which leads to the progression of AD (Zlokovic 2005).

1.2.11 LRP1

LRP1 is a member of the LDL receptor family, which serves as a receptor in cell signaling and as a cargo transporter (Dieckmann et al. 2010; Boucher and Herz 2011). The protein is ubiquitously expressed in human tissues, including neurons and the brain endothelium (Moestrup et al. 1992). LRP1 interacts with a variety of ligands including A β (Zlokovic et al. 2010). Genetic studies have linked *LRP1* to sporadic late-onset AD and cerebral amyloid angiopathy (Kang et al. 1997; Lambert et al. 1998; Christoforidis et al. 2005). Interestingly, expression of LRP1 in the brain and brain capillaries decreases with age (Silverberg et al. 2010) and is reduced in AD-brains (Donahue et al. 2006). One mechanism of LRP1-mediated A β clearance is the cellular uptake and subsequent degradation of A β (Nazer et al. 2008; Kanekiyo et al. 2013). Transcytotic transport across the blood brain barrier however is assumed to be the major route of A β elimination followed by periperal degradation of the peptide in liver, spleen and kidneys (Shibata et al. 2000; Bell et al. 2007). Thus far the contribution to A β clearance by the different LRP1-mediated mechanisms could not be dissected quantitatively, since LRP1-inhibitors do not lower BBB-clearance selectively (Qosa et al. 2014).

1.2.12 The 5xFAD *Lrp1*_{BE}^{-/-} mouse model

In order to study the role of brain endothelial LRP1 in the clearance of A β across the blood brain barrier an inducible *LRP1*-knockout model was developed by the group of Prof. Pietrzik

(Storck et al. 2016). *Lrp1*^{fl/fl} mice that harbor a Cre/loxP recombination system, allowing for an inducible, tissue specific knockout of *LRP1* (Rohmann et al. 1998) were bred with *Slco1c1*-CreER^{T2} mice that express Cre recombinase exclusively in endothelial cells of brain vessels and the choroid plexus but not in other vascular components (Ridder et al. 2011). The generated *Slco1c1*-CreER^{T2} x *Lrp1*^{fl/fl} mice were named *LRP1*_{BE}^{fl/fl}. By induction with the selective estrogen receptor modulator Tamoxifen, brain endothelial *LRP1* is fully knocked out in *Lrp1*^{fl/fl}, producing *Lrp1*_{BE}^{-/-} mice. In neurons, microglia, the vast majority of astrocytes and non-endothelial components of the brain vasculature of *Lrp1*_{BE}^{-/-} mice *LRP1* is still present and the permeability of the BBB is not influenced. *LRP1* knockout leads to a lowering in the rate of clearance of radiolabeled [¹²⁵I] A β ₁₋₄₂ in *Lrp1*_{BE}^{-/-} mice as compared to *Lrp1*_{BE}^{fl/fl} mice. *Lrp1*_{BE}^{fl/fl} mice were then crossed with 5xFAD mice (Storck et al. 2016). The 5xFAD model harbors the five FAD mutations, three in APP, K670N/M671L (Swedish), I716V (Florida), V717I (London) and two in PS1, M146L and L286V. These 5xFAD mice display an early plaque pathology and gliosis (Oakley et al. 2006). Seven months old 5xFAD/*Lrp1*_{BE}^{-/-} mice had elevated brain levels of soluble and insoluble A β ₁₋₄₀ and higher levels of insoluble A β ₁₋₄₂ (Storck et al. 2016).

1.3 Project objectives

The aim of this thesis was to extend the knowledge about pathogenic effects of cerebral A β deposition, induced by its overproduction one hand and its clearance on the other hand. For this purpose, the thesis was divided into two parts and neuropathological and behavioral features were analyzed in two transgenic murine mouse models (Figure 1.1).

Firstly, the pathological effects of the expression of A β ₃₋₄₂, which forms soluble oligomers, in the TBA42 mouse model were investigated. The peptide is an abundant variant of A β found in AD brains (Portelius et al. 2010). The expression in brain and spinal cord of TBA42 mice was confirmed. Additionally, a quantification of neurons in the hippocampal CA1 region and a series of cognitive and sensorimotor tests was conducted at three different ages to test the hypothesis that A β ₃₋₄₂ is toxic *in vivo* and leads to age dependent neuropathological and behavioral alterations. Three, six and twelve month old mice were tested

Secondly, the effects of the knock-out of *LRP1*, which mediates the clearance of A β from the brain, were studied in the 5xFAD mouse model. The hypotheses that elevated cerebral A β levels induced by knockout of *LRP1* (Storck et al. 2016) leads to an aggravated cognitive phe-

notype, but not a difference in plaque deposition in 5xFAD mice were tested in the second project. Four groups of seven month old animals were tested Wildtype (WT), $Lrp1_{BE}^{-/-}$, 5xFAD/ $Lrp1_{BE}^{-/-}$ and 5xFAD/ $Lrp1_{BE}^{fl/fl}$.

1.3.1 Project I: Quantification of neurodegeneration and analysis of behavioral deficits in the TBA42 mouse model

1. To confirm the pattern of A β deposition in TBA42 mice.
2. To assess an age-dependent neuron loss in the CA1 region of the hippocampus of TBA42 mice possibly induced by
3. To characterize an age-dependent cognitive, behavioral and motor deficits of TBA42 mice.

1.3.2 Project II: Exploring in vivo effects of impaired A β clearance induced by knockout of brain endothelial *LRP1* in 5xFAD mice

1. To quantify the effect of the knockout of *LRP1* on plaque deposition and inflammation in 5xFAD mice.
2. To analyze the effect of the knock-out of *LRP1* on learning, memory and motor abilities in 5xFAD mice.

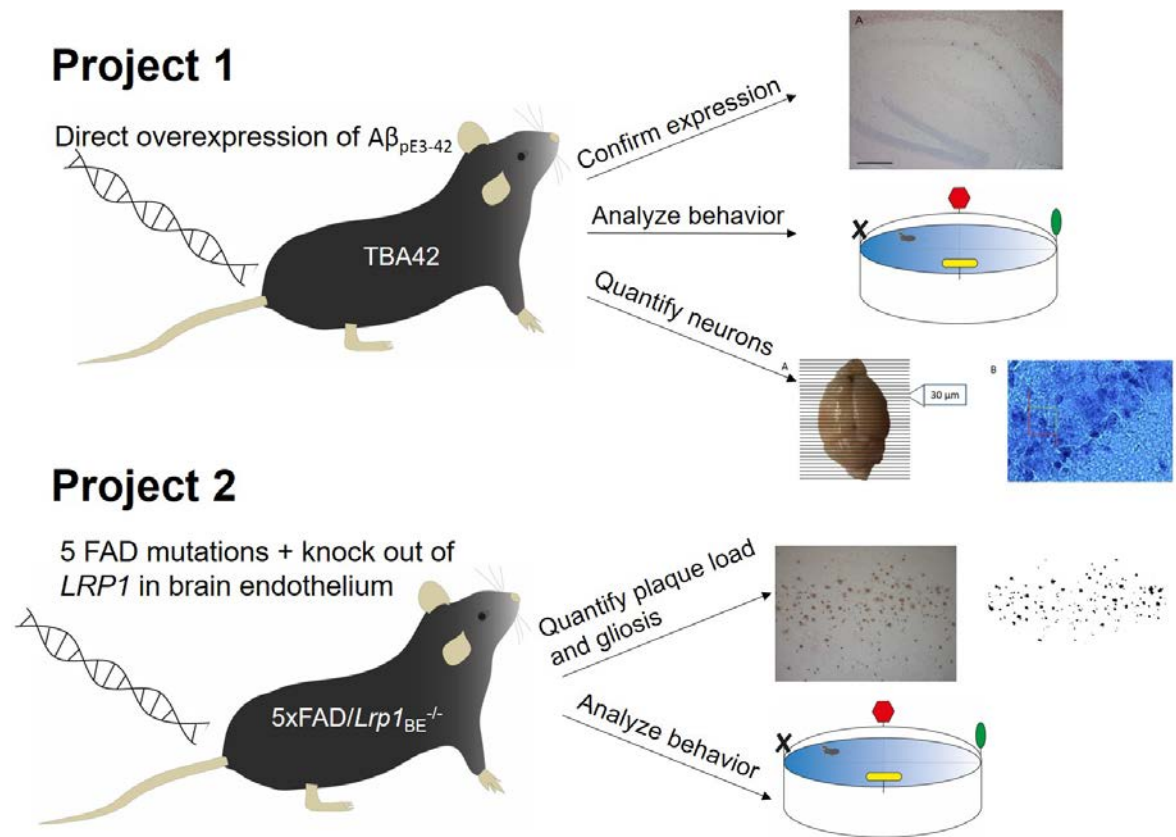


Figure 1.1 Project objectives

2 Materials and methods

2.1 Animal breeding and genotyping

All animals were of the species *Mus musculus*. Wildtype mice were of the inbred strain C56Bl/6J (Jackson Laboratories, Bar Harbor, ME, USA). For the first project heterozygous transgenic TBA42 mice were bred on wild-type background in order to obtain heterozygous transgenic TBA42 mice. Wildtype littermates were used as control animals for behavioral testing and stereological quantification. Transgenic mice were identified by PCR-Genotyping. Mouse tail biopsies were taken in order to obtain chromosomal DNA, which was analyzed by PCR, amplifying A β DNA-sequence and subsequently visualized by gel electrophoresis. Animals were housed at a 12-h day/12-h night cycle in a constant environment with *ad libitum* access to water and a standard laboratory diet.

For the second project, *Lrp1*_{BE}^{-/-} and 5xFAD *Lrp1*_{BE}^{-/-} mice were fed with a diet that contained 400 mg tamoxifen citrate per kilogram dry weight (CRE Active TAM400, LASvendi, Soest, Germany), while wildtype controls and *Lrp1*_{BE}^{fl/fl} were fed a standard laboratory diet.

All animals were handled according to the guidelines of the “Society for Laboratory Animals Science” (GV-SOLAS) and the guidelines of the “Federation of European Laboratory Animal Science Association” (FELASA). Studies were approved by the responsible authorities. Reference numbers: Project 1: G15/1760 LAVES; Project 2: G12-1-051 Rhineland-Palatinate.

2.1.1 DNA extraction

Deoxyribonucleic acid (DNA) extraction was conducted by alkaline lysis of mouse tail biopsy tissue. Tissue samples were incubated in 500mM lysis buffer containing (100mM Tris/HCl (pH 8.5, Roth, Karlsruhe, Germany), 5mM EDTA (AppliChem, Darmstadt, Germany), 0,2 % sodium dodecyl sulfate (SDS, Biomol, Hamburg, Germany), 200 mM NaCl (Roth, Karlsruhe, Germany)) and 5 μ l Proteinase K (20 mg/ml stock, Peqlab, Erlangen, Germany) at 55 °C for 20 hours in a Thermomixer Compact (Eppendorf, Hamburg, Germany). Samples were subsequently centrifuged in a Heraeus Biofuge Stratos (Thermo Fisher Scientific, Waltham, MA, USA) at 17.000 rounds per minute for 20 minutes at 4 °C. Supernatants were transferred to a new tube. Afterwards, DNA was precipitated with 500 μ l ice cold 70 % isopropanol (Roth,

Karlsruhe, Germany) solution. Samples were vortexed (Vortex Genie 2, Scientific Industries, Bohemia, NY, USA) and centrifuged at 13.000 rpm for 10 minutes at room temperature in a Heraeus Biofuge Pico centrifuge (Thermo Fisher Scientific, Waltham, MA, USA). Supernatants were discarded and the DNA pellet was washed with 500 µl of 70 % Ethanol (Merck, Darmstadt, Germany). After another centrifugation step (13.000 rpm, 10 min., at room temperature) supernatants were discarded and the DNA pellet was dried at 37 °C on a Thermo-mixer Compact (Eppendorf, Hamburg, Germany) for 1 hour. DNA was suspended in 40 µl of distilled, deionized water (ddH₂O) and stored over night at 4 °C.

2.1.2 DNA concentration determination

For concentration and purity determination of DNA an Eppendorf Biophotometer (Eppendorf, Hamburg, Germany) was used. For this purpose, a blank value was measured using 80 µl molecular grade water in a UVette® (Eppendorf) cuvette. Thereafter in the same cuvette 2 µl of DNA sample was diluted in 78 µl of ddH₂O for the photometrical measurement. The A260/A280 light absorbance ratio was measured for each DNA sample to determine purity. A value of 1.8 was indicative of acceptable purity. The DNA concentration was measured at OD260 and samples were diluted to a final concentration of 20 ng/µl with molecular weight water.

2.1.3 Polymerase chain reaction

Polymerase chain reaction (PCR) was performed on a SensoQuest LabCycler (SensoQuest, Göttingen, Germany) in 20 µl PCR tubes (Greiner Bio-One, Kremsmuenster, Austria) to amplify the transgene fragment from the chromosomal DNA of TBA42 mice. The PCR reaction mixture contained the extracted murine DNA and the following reagents (Table 1): Taq thermostable DNA polymerase (Axon Labortechnik, Kaiserslautern, Germany), 10x reaction buffer (Mg²⁺ free, Axon), MgCl (Axon), dNTP mix (Invitrogen), ddH₂O and Aβ PCR Primers (forward: 5' GTGACTCCTCAGCTTCCAC 3'; reverse: 5' GTTACGCTATGACAACACC 3'). Thirty-four PCR amplification cycles were used (Table 2).

Table 1 PCR-mixture used for genotyping of TBA42 mice

Reagent	Concentration	Volume (μ l)
DNA	20 μ g/ μ l	2
Primer forward	10 μ mol/ μ l	1
Primer reverse	10 μ mol/ μ l	1
dNTPs	2mM	2
MgCl ₂	25mM	1.6
10 x Buffer		2
H ₂ O		10.2
Taq-Polymerase	5U/ μ l	0.2
PCR Mixture		20

2.1.4 Agarose gel electrophoresis

PCR products were analyzed by agarose gel electrophoresis. For this purpose, 2 % agarose gel was prepared by cooking 2 grams of agarose (Lonza, Basel, Switzerland) in 100 ml of 1XTBE buffer until the agarose was dissolved. Once the agarose solution was cooled down but still fluid it was poured into a casting tray with a 20 pocket casting comb. Before the gel became solid 5 μ l of ethidium bromide solution (10 mg/ml; Roth, Karlsruhe, Germany) were added to the gel, dispensed and air bubbles were removed using a pipette tip. After it was set, the agarose gel was transferred into an electrophoresis chamber (Bio-Rad, Hercules, CA, USA) filled with 1XTBE buffer. 10 μ l of PCR product were mixed with 2 μ l of 6 x loading buffer (Life Technologies, Carlsbad, CA, USA) and each well was filled with one 12 μ l sample. Additionally, 5 μ l of a DNA ladder (Bioron, Ludwigshafen, Germany) were added to another well. The gel chamber was closed and connected to a Power Pack P 25 power supply (Biometra, Goettingen, Germany). The gel was run at 100 V until DNA bands had properly separated. DNA was visualized in a Gel Doc 2000 (BioRad, Hercules, CA, California) UV transilluminator (366 nm) and all gels were documented using Quantity One software (version 4.3, Biorad).

10XTBE buffer: 108 g Tris (Roth, Karlsruhe, Germany) and 55 g boric acid (Sigma, St. Louis, MO, USA) were dissolved in 900 ml ddH₂O. 40 ml 0,5 M Na₂EDTA (pH 8.0; Roth, Karlsruhe, Germany) was added to the solution and the volume was adjusted to 1 l with ddH₂O. Before use the solution was diluted 1:10 in ddH₂O to obtain 1XTBE buffer.

Table 2 PCR protocol used for genotyping of TBA42 mice

Step	Temperature(°C)	Time (s)	Number of Cycles
Initialization	94	180	1
Denaturation	94	45	34
Annealing	58	60	34
Elongation	72	60	34
Final Elongation	72	300	1
Final Hold	4	∞	1
PCR Procedure		2 hours 26 minutes	

2.2 Preparation of CNS-tissue

Mice were sacrificed via transcardiac perfusion followed by decapitation. Mice were anesthetized with a mixture of 10 % ketamine (Medistar, Ascheberg, Germany) and 2 % xylazinehydrochloride (Xylarium, 23.3 mg/ml, Ecuphar, Oostkamp, Belgium) diluted in Aqua ad injectabilia (B. Braun, Melsungen, Germany). The anesthetic was administered by intraperitoneal injection at a dosage of 100 mg/kg ketamine and 10 mg/kg xylazinehydrochloride. When mice were deeply anesthetized, the perfusion surgery was started. Mice were secured by their limbs on a perfusion tray using thin needles. The abdominal skin was incised and the thoracic skin was removed, in order to expose the ribcage. The abdominal wall was subsequently opened and the diaphragm was cut in order to access the thoracic cavity. The ribcage was partially removed and the beating heart was exposed. Surgical scissors were used to cut open the right atrium and the syringe attached to the perfusion pump was inserted into the left ventricle. Perfusion was first conducted with 30 ml ice cold 0.01 M phosphate buffered saline (PBS) to wash out the animals' blood. The perfusion process was monitored by observing a color-change of the animal's liver, from dark red to gray. Next, the pump was stopped and was now connected to a cylinder containing a 4% paraformaldehyde (PFA, Roth, Karlsruhe, Germany) in 0.01 M PBS solution. The perfusion process was continued and 40 ml of the fixation agent were applied as described above. Proper fixation was indicated by a stiffening of the animal's limbs and tail. Thereafter, mice were removed from the perfusion tray and decapitated using large surgical scissors. Subsequently, mouse brains and spinal cords were quickly dissected on ice. Starting from the spinal canal and ending at the temporal part of the orbital cavity, two lateral incisions along the temporal skullbase were made. The skullcap was additionally loosened by cutting the osseous connection between the eyes. The skullcap could now be removed using fine forceps. Subsequently, the brain was gently extracted from the cranial cavity.

Olfactory bulbs and cranial nerves were resected and brain hemispheres were separated along the interhemispherical fissure using a scalpel. For spinal cord preparation, back muscles were removed to expose the vertebral column. Vertebral arcs were incised laterally and removed. Cervicothoracic spinal cord tissue was subsequently sampled. Thereafter right brain hemispheres and spinal cords were transferred into embedding cassettes (Simport, Beloeil, QC, Canada) and stored in Histofix® solution (Roth, Karlsruhe, Germany) for 96 hours at 4 °C. Subsequently the tissue was embedded using an EG1140 H Embedding Station (Leica, Wetzlar, Germany). Left brain hemispheres that were eventually used for Stereology, were post-fixed in 10 ml 4 % paraformaldehyde in 0.01 M PBS solution overnight and later transferred into 30 % sucrose (Roth, Karlsruhe, Germany) in 0.01 M PBS solution for cryoprotection. Subsequently, brain hemispheres were quickly frozen on dry ice and stored at -80 °C.

2.3 Stereology

2.3.1 Preparation of cryosections

For stereology left brain hemispheres were frontally cut into 30 µm sections on a CM1850 UV cryostat (Leica, Wetzlar, Germany) (Figure 2.1 A). Every tenth section was systematically sampled into 4 ml Rotilab screw threads (Roth, Kaiserslautern, Germany). Thereafter brain tissue was transferred into -80 °C and sections were stored until further processing. Before staining, sections were mounted onto Superfrost® slides (Thermo Fisher Scientific, Waltham, MA, USA). For this purpose, ice cold 0.01 M PBS was added to one screw thread sections and the embedding material was allowed to dissolve. Sections were then transferred to a culture dish and carefully mounted using a fine paintbrush. When residual PBS had evaporated sections were stored in a dry box at 37 °C for 16 hours.

2.3.2 Cresyl violet staining

Cryosections were stained with cresyl violet in order to unspecifically visualize neuronal nuclei. For delipidation sections were incubated in Solution A for 2 x 10 minutes. Delipidation was achieved by incubating sections in solution B for 20 minutes. Thereafter sections were transferred back to solution A for 2 x 10 minutes. Staining was performed by incubating sections for 2 x 8 minutes at room temperature in cresyl violet staining solution. Remaining staining solution was subsequently washed away 3 times for 1 minute in solution A. Sections were now

dehydrated in alcohol (3 min in 100 % ethanol (CVH, Hannover, Germany), 10 min in 100 % isopropanol (Roth, Karlsruhe, Germany) and 2 x 5 min in xylol (Roth)). After dehydration xylol was allowed to evaporate and sections subsequently were covered with cover slips (Menzel-Gläser GmbH, Braunschweig, Germany) using Roti Histokitt (Roth, Karlsruhe, Germany). The mounting medium was allowed to harden overnight under a fume hood and sections were covered with aluminium foil to avoid light exposure.

Solution A: 13.61 g Natrium Trihydrate (Roth) diluted in 100 ml ddH₂O. 40 ml of the generated 1 M Natrium Acetate solution was mixed with 9.6 ml 100 % acetic acid (Merck, Darmstadt, Germany). The volume was adjusted 10 l with ddH₂O.

Solution B: 2 ml Triton X-100 (Roth) dissolved in 10 ml ddH₂O. 2.5 ml of the generated solution were mixed with 50 ml ddH₂O and 150 ml 100% ethanol (Roth).

Staining solution: 0.1 g cresyl violet (Fluka, St. Louis, MO, USA) was added to 1l work solution A and stirred for 1 hour.

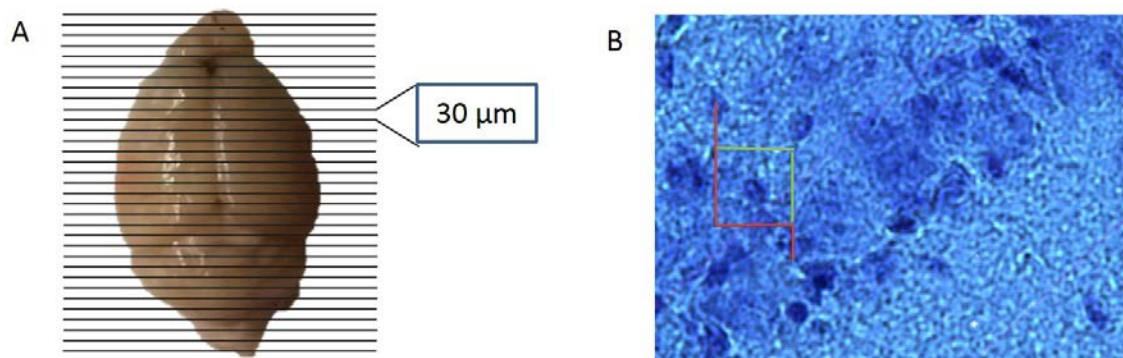


Figure 2.1 Stereological quantifications of the neuron number in the hippocampal CA1 region. Brains were cut frontally and every tenth 30 µm sections were sampled (A). Using a high magnification lens (100 x magnification), neuronal nuclei were sampled (B). Cells within the box or touching the green line were counted. Cells located outside the box or touching the red line were not counted. Counting areas were automatically and randomly selected.

2.3.3 Optical fractionator workflow

Unbiased stereological analysis was performed, using design-based stereology to quantify neuron number in the hippocampal CA1 region. An Olympus BX51 stereology station (Olympus, Shinjuku, Japan) with a motorized microscope stage, which allows for automatic sampling and Stereo Investigator 7 software (MicroBrightField Bioscience, Williston, VT, USA) was used. Sections that contained CA1 tissue (Bregma -1.22 mm to -3.80 mm) were identified at 4 x

magnification and the CA1 region was delineated. Counting was then performed at high magnification using a 100 x oil lens (Figure 2.1 B). Within a 49 x 105 micrometer sampling grid, randomly distributed counting frames (14 x 14 micrometer) were used. Optical dissector probes were used to sample neuronal nuclei and the total neuron number was estimated using a 2 micrometer top guard zone. Counting was performed according to the principles of stereology (West et al. 1991; Schmitz and Hof 2005). The section thickness was evaluated on every sampling site. The hippocampal cell layer CA1 of TBA42 mice and wildtype littermate controls were analyzed in sex- and age-matched groups (n = 3 per group). Samples were blinded to avoid a counting bias. The total neuron number was calculated using the following formulas (1), 2)) and parameters (Table 3, Table 4):

$$1) P = asf \times ssf \times tsf$$

$$2) N = \sum_{i=1}^n (P \times Q) i$$

Table 3 Definition of stereological parameters

Stereological parameters	
asf	Area sampling fraction (xy/XY)
ssf	Section sampling fraction
tsf	Thickness sampling fraction (T/Z)
Z	Dissector height
P	Number of neurons
T	Mean section thickness
Q	Total markers counted (neuron number)

Table 4 Stereological parameters for quantification of neurons in the CA1 region

Parameter	CA1
Sampling grid (x) (μm)	49
Sampling grid (y) (μm)	105
Sampling grid area (xy) (μm ²)	5145
Counting frame width (X) (μm)	14
Counting frame height (Y) (μm)	14
Counting frame area (XY)(μm ²)	196
asf	26.25
ssf	10
Z (μm)	Total markers counted (neuron number)

2.4 Immunohistochemistry

2.4.1 Fixation and paraffin embedding of CNS tissue

After preparation of CNS tissue as described above, embedding cassettes were transferred to the TP 1020 Automatic Tissue Processor (Leica, Wetzlar, Germany) for dehydration in a series of ethanol baths and paraffin emersion. The following steps were programmed: five minutes in 4 % histofix (Roth, Karlsruhe, Germany), 30 minutes in tap water, 1 hour in 50 %, 60 %, 70 %, 80 % and 90 % ethanol solutions (CVH, Hannover, Germany), 2 x 1 hour in 100 % ethanol, 1 hour in xylol (Roth) and 2 x 1 hour in melted paraffin (Roth). Following this procedure CNS tissue was embedded cut side down in molten paraffin wax on an EG1140 H embedding station (Leica, Wetzlar, Germany).

2.4.2 Preparation of paraffin sections

Paraffin embedded tissue was cut to produce 4 μm sections using a HMI 335E microtome (Thermo Fischer Scientific, Watham, MA, USA). Sections were carefully transferred to a water bath containing ddH₂O at room temperature and mounted onto Superfrost® slides (Thermo Fisher Scientific). Sections were subsequently fixed onto the slides in a 54 ° C water bath (Medax, Olching, Germany). Sections were dried on a heating block for approximately 20 minutes at 54 ° C and at 37 ° C overnight.

2.4.3 3,3'-Diaminobenzidine (DAB) immunohistochemistry

3,3'-Diaminobenzidine (DAB) immunostaining was conducted on 4 μm paraffin sections. First, sections were deparaffinized in xylol (Roth, Karlsruhe, Germany) for 2 x 5 min, subsequently rehydrated in a series of ethanol (CVH, Hannover, Germany) baths (10 min 100 %, 5 min 95 %, 5 min 70 %) and washed in ddH₂O. Endogenous peroxidases were blocked in 30 % H₂O₂ in 0.01 M PBS. Antigen retrieval was achieved by boiling sections in 10mM citrate buffer (pH 6.0, Roth) for 10 minutes (800 W until boiling, 80 W for 8 minutes). After sections were cooled down section were washed in ddH₂O. Membranes were permeabilized using 0.1 % Triton X-100 (Roth) in 0.1 M PBS and subsequently washed in PBS. For A β staining additional antigen retrieval was achieved by incubating sections for 3 minutes in 88 % formic acid (Roth). Following another washing step (2 x 10 minutes in 0.01 M PBS) sections were circled with a lipid pen (Pap Pen, Kisker Biotech, Steinfurt, Germany) and unspecific antigen epitopes

were blocked using 100 μ l of 0.01 M PBS containing 10 % fetal cow serum (Thermo Fischer Scientific, Waltham, MA, USA) and 4 % skim milk powder (Roth). Primary antibodies were diluted in 10 % fetal cow serum in 0.01 M PBS solution and, after removing the blocking solution sections were incubated at room temperature for 16 hours. After washing three times with 0.1 % Triton X-100 in 0.01 M PBS and with 0.01 M PBS, sections were incubated with the respective biotinylated secondary antibody 37 ° C for 1 hour. Secondary antibodies were diluted in 0.01 M PBS containing 10 % fetal cow serum. Avidin-biotin complex solution was prepared according to the manufacturer's instructions using VECTASTAIN Elite ABC Kit (Vector Laboratories, Burlingame, CA, USA). In brief, each solution was added to a 0 % fetal cow serum in 0.01 M PBS solution at a concentration of 1:100 and the solution was incubated for 30 minutes at 4 ° C. Sections were washed three times in 0.01 M PBS and subsequently incubated with 100 μ l of avidin-biotin complex solution per section for 1.5 hours at 37 ° C. After incubation sections were washed in 0.01 M PBS to remove unbound antibodies. Antibody binding was visualized using DAB. The DAB solution was prepared by adding 100 μ l of DAB stock solution (25mg/ml DAB in 50 mM Tris/HCl, Sigma, St. Louis, MO, USA) and 2.5 μ l 30 % H₂O₂ to 5 ml 50 mM Tris/HCl (pH 7.5, Roth). Sections were incubated in 100 μ l DAB solution until the staining was detected by eyesight. The DAB staining was followed by three 5 min washing steps in 0.01 M PBS. A counterstaining was performed using hematoxylin. Subsequently, sections were washed under tap water for 5 minutes. Dehydration was achieved using a series of ethanol (CVH) baths: 1 minute in 70 % ethanol, 5 minutes in 95 % ethanol, 10 minutes in 100 % ethanol, and 2 x 5 minutes in xylol (Roth). Slides were covered using two drops of Roti®-Histokitt mounting medium (Roth) and a cover slip. Bright field images were acquired using a BX-51 microscope (Olympus, Shinjuku, Japan) equipped with a camera.

2.5 4-6-diaminidino-2-phenylindole (DAPI) staining

4-6-diaminidino-2-phenylindole (DAPI) staining was performed on 4 μ m paraffin sections. First sections were deparaffinized in xylol (Roth, Karlsruhe, Germany) for 2 x 5 min, subsequently rehydrated in a series of ethanol (CVH, Hannover, Germany) baths (10 min 100 %, 5 min 95 %, 5 min 70 %) and washed for 1 minute in ddH₂O and for 1 minute in 0.01 M PBS. The staining solution contained 1.5 mg/l DAPI (Sigma, St. Louis, MO, USA) in ddH₂O. After staining, slides were washed twice in 0.01 M PBS. Subsequently, fluorescent mounting medium (Dako, Glostrup, Denmark) was added to cover the slides with a cover slips (Menzel-

Gläser GmbH, Braunschweig, Germany). Images were acquired using a BX-51 microscope (Olympus, Shinjuku, Japan) equipped with a mercury arc lamp, a filter box and a camera.

2.6 Quantifications

A β plaque load was measured on images of the hippocampal region, taken from sagittal paraffin sections of mouse brains spaced a minimum 20 μ m apart. Sections were stained using the polyclonal A β antibody 24311 (AG Bayer) (Stainings by Nils Schubert). Three sections per animal were analyzed. Using NIH ImageJ software (version 1.49c), images were converted into an eight-bit black and white format, using a predefined frame area (Figure 2.2). Thresholds were set to a fixed value. Thresholds were selected to maximize the stained area detected, while minimizing the contribution of intracellular A β deposits and background staining. Plaque load was defined as the area of the image occupied by A β staining. For microglia and astrocyte staining the procedure was conducted accordingly on sections stained with Iba1 (polyclonal from rabbit, Waco) and GFAP (polyclonal from mouse, Chemicon) antibodies (Stainings by Nils Schubert). The following quantification parameters were defined in an IJM macro file:

```
makeOval(69, 585, 2571, 1275);
waitForUser( "Quantification", "OK to continue");
run("8-bit");
run("Clear Outside");
setAutoThreshold("Default");
//run("Threshold...");
setThreshold(0, 110);
run("Colors...", "foreground=black background=white")
run("Convert to Mask");
run("Measure");
run("Open Next");
```

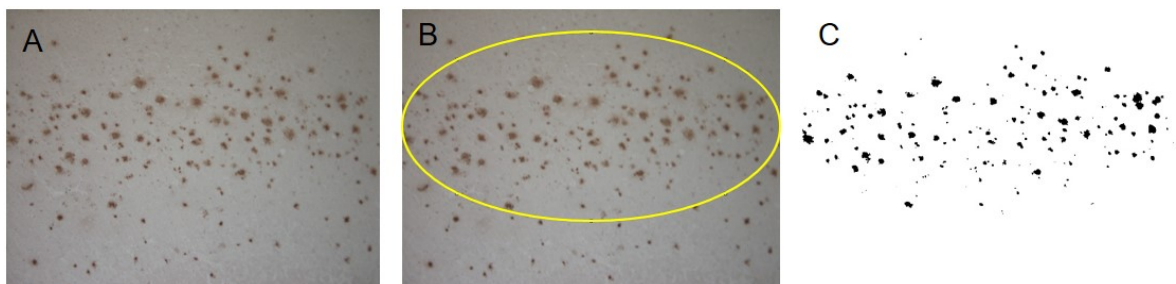


Figure 2.2 Quantification procedure. Images were opened using image J software (A). Using a macro file the area of interest was labeled using a predefined frame (B). The labeled area of the image was converted into an eight-bit black and white format and the area covered was calculated automatically (C).

2.7 Behavioral analyses

In all behavioral tests TBA42 transgenic animals were tested at 3 different ages (TBA 42: 3 months $n = 11$, 6 months $n = 12$, 12 months $n = 8$) and compared to age matched wildtype mice (Wildtype: 3 months $n = 12$, 6 months $n = 10$, 12 months $n = 10$). For the LRP1 project four groups of seven month-old female mice were used: Wildtype (WT) ($n=6$), $Lrp1_{BE}^{-/-}$ ($n=5$), $5xFAD/Lrp1_{BE}^{-/-}$ ($n=7$) and $5xFAD/Lrp1_{BE}^{n/n}$ ($n=7$). Each individual mouse received only one round of testing and was subsequently sacrificed.

2.7.1 Balance beam

The balance beam was used to assess general motor function and balance in TBA42 mice compared to wildtype littermates. The balance beam apparatus consisted of a 1 cm wooden dowel that was laterally supported by two 44 cm columns, each carrying an escape platform. The 50 cm beam was installed spanning a padded surface (Figure 2.3 A) and cleaned with 70 % ethanol (Merck, Darmstadt, Germany) solution after every trial. Three trials were given to each mice on one day with an average inter-trial interval of 10 minutes. At the beginning of the procedure mice were released onto the center of the beam and the time mice remained on the apparatus was stopped. When mice did not fall within 60s or managed to escape onto the platform a maximum time of 60s was documented. Falling latencies of the three trials were thereafter averaged.

2.7.2 Inverted grip hang

Vestibular function and muscle strength were tested with the inverted grip hanging test (Figure 2.3 B). The testing apparatus consisted of a wire grid 45 cm long and 30 cm wide with a grid spacing of 1 cm². The grid was suspended 40 cm above a padded surface using foam supports. Mice were released in the center of the grid, which was inverted subsequently. The time the mice that mice held on to the grid was recorded during a single 60 second trial. When mice were able to remain on the grid for the entire testing period or escaped over the edge of the grid, the maximum time of 60 seconds was given. Otherwise, the latency to fall from the grid was recorded. Between testing the mice, the apparatus was cleaned with 70 % ethanol (Merck, Darmstadt, Germany) to diminish odor cues.

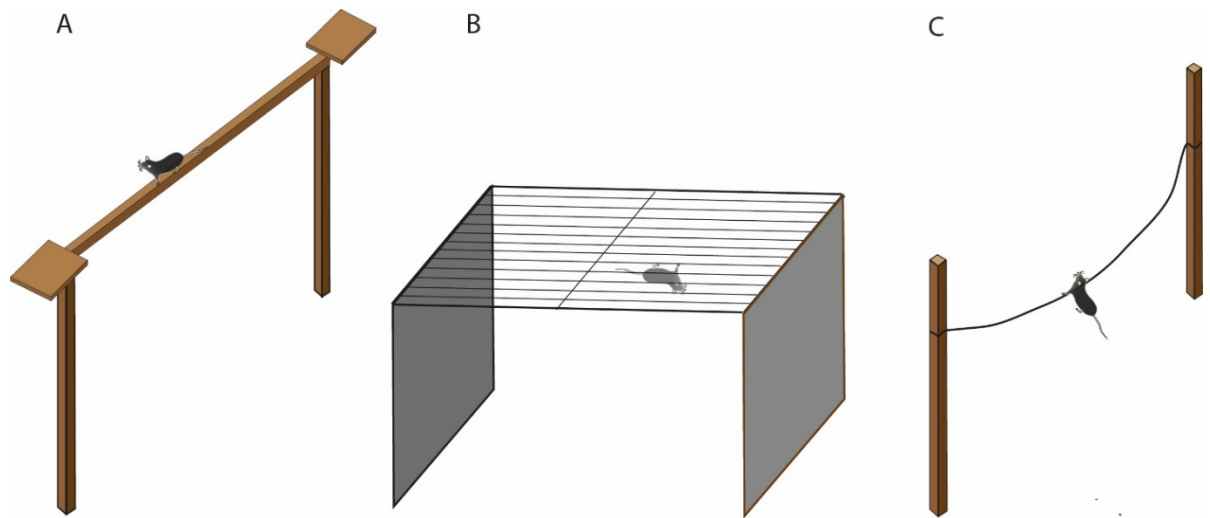


Figure 2.3 Setup of motor test apparatuses. Balance beam (A), Inverted grid (B) and String suspension (C).

2.7.3 String suspension

Sensory-motor abilities of TBA42 mice were additionally analyzed using the string suspension test. A 0.5 cm string was spanned between two wooden support columns (Figure 2.3 C). The apparatus was cleaned with 70 % ethanol (Merck, Darmstadt, Germany) solution between trials. Mice were allowed to grasp the string with forepaws and subsequently released onto the string. A rating system was used to categorize the animal's sensory-motor abilities (Table 5).

Table 5 String suspension scoring system.

Rating	Criteria
0	Unable to remain on string
1	Hangs by frontpaws or hindpaws
2	Hangs by frontpaws or hindpaws, attempts to climb on string
3	Sits on string and is able to hold balance
4	Four paws and tail around string, lateral movement
5	Escapes

2.7.4 Morris water maze

Spatial learning and spatial reference memory in TBA42 and wildtype control mice for project 1 and in wildtype, *Lrp1*_{BE}^{-/-} and 5xFAD/*Lrp1*_{BE}^{-/-}, 5xFAD/*Lrp1*_{BE}^{fl/fl} for project 2 were assessed using the Morris water maze (MWM) (Morris 1984). Mice learn to navigate to a hidden platform (diameter 10 cm) in a circular 1.1 m diameter pool filled with non-transparent water. Non-toxic white acrylic paint was added to the water that had room temperature. The pool was segmented and four virtual quadrants were defined. Based on their relative position to the goal platform they were named left, right, opposite and target quadrant. The target quadrant contained the goal platform.

The testing procedure started with three days of cued training (Figure 2.4 A) during which the goal platform was highlighted with a triangular flag. The location of the platform as well as the position from where the mice were introduced into the pool was altered between trials. Four training trials per day were conducted. Mice that did not find the platform within 60 seconds were gently guided to it. All mice were allowed to stay on the platform for 10 seconds before being transferred back to their cage. Between the trials mouse were allowed to dry under a heat lamp and rest for 10 minutes. Mice that showed decreased escape latencies during the cued training qualified for the acquisition training.

Twenty-four hours after the last day of cued training, mice performed 5 days of acquisition training (Figure 2.4 B). For this part of testing the flag was removed from the platform and cues were attached to the outside of the pool. The platform position remained in the same location in the target quadrant for each mouse throughout the entire acquisition training. Trials were conducted as during the cued training phase.

Twenty-four hours after finishing the acquisition trial, a probe trial was performed (Figure 2.4 C) for analyzing spatial reference memory. The platform was removed and mice were released into the water from a new entry point. Mice were allowed to swim for 1 minute while their route was recorded. ANY-Maze software (Stoelting, Wood Dale, IL, USA), which was connected to a camera (Computar, Commack, NY, USA) was used to record and calculate the distance travelled, escape latency, swimming speed and time that mouse spent in the different quadrants.

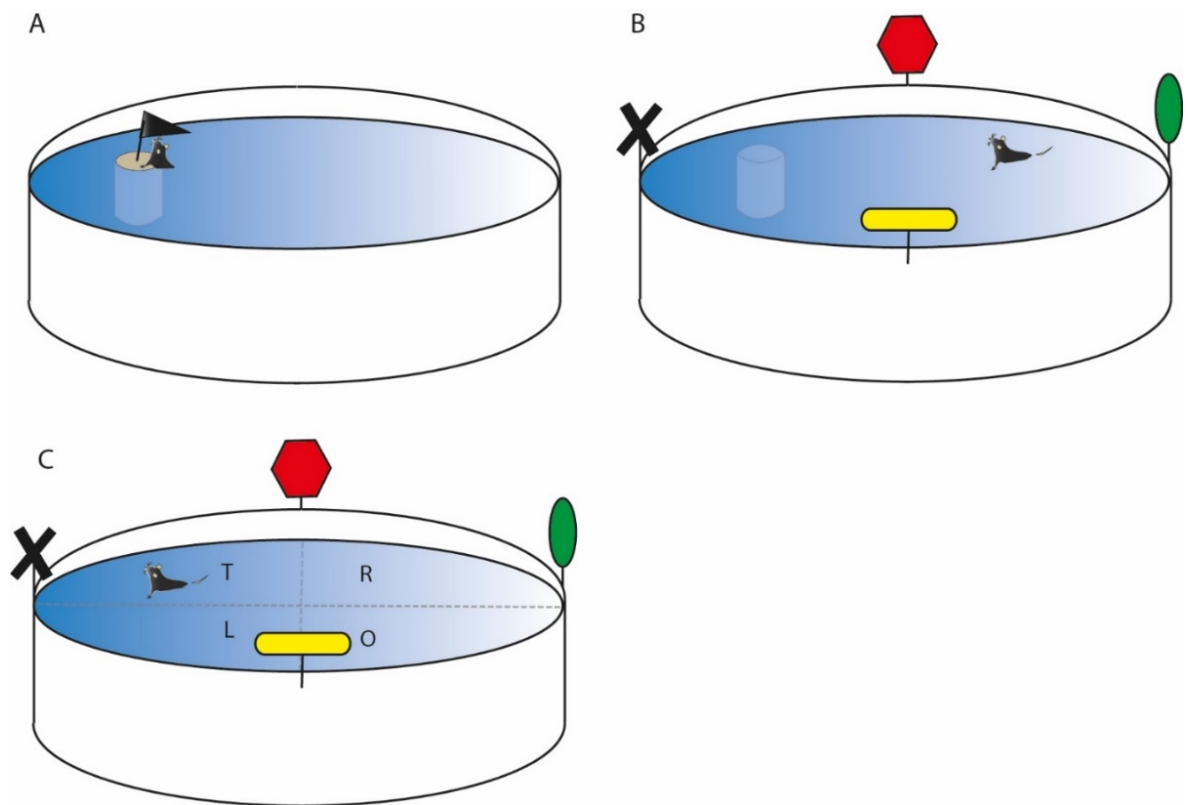


Figure 2.4 Morris water maze apparatus. Cued training (A), Acquisition training (B), Probe trial (C).

2.7.5 Cross maze

Spontaneous alternation rates of mice were analyzed using a cross maze apparatus, which is built of a black plastic material. The maze had four arms arranged in a 90 ° angle extending from a central area that measured measuring 8 x 8 cm (arm size: 30 cm length, 8 cm width, 15 cm height). During the test sessions, each mouse was placed in one of the four arms and was able to move through the maze. A complete alternation was defined as four subsequent entries into different arms in overlapping sets (for example 3, 1, 4, 2 or 1, 2, 4, 3 but not 3, 1, 2, 1). Distance travelled and routes were recorded using the automated ANY-maze video tracking software (Stoelting, USA) connected to a camera (Computar, Commack, NY, USA). The alternation percentage was calculated as the ratio of complete alternations and the total number of recorded arm entries. In order to remove odor cues the apparatus was cleaned with 70 % ethanol (Merck, Darmstadt, Germany) solution after each animal tested.

2.7.6 Elevated plus maze

The elevated plus maze was used to study exploratory behavior, locomotor activity, and anxiety levels. The maze was shaped like a “+” with two alternating open and two alternating

closed arms that extended from a central area. The apparatus was raised 75 cm above ground level. Each one of the arms measured 15 cm in length expanding from a 5 x 5 cm central zone. Closed arms were bounded by a transparent 15 cm acrylic glass wall. For testing mice were placed on the area and were allowed to explore the maze for 5 minutes. Anxiety is measured by the time mice spend in the open arms of the maze. Lower anxiety levels correspond to a greater amount of time spent in the open arms (Karl et al. 2003).

The ratio of time spent in the open arms to the total testing time and the percentage of open arm entries to the total arm entries were measured using the automated ANY-maze video tracking software (Stoelting, USA) and a camera that recorded mouse paths (Computar, Commack, NY, USA). Odor cues were removed with 70 % ethanol (Merck, Darmstadt, Germany) solution after each animal tested.

2.8 Data analysis

Details on the statistical analyses and the number of biological replicates (n) are indicated in the respective results section. Levels of significance are indicated as follows: *** $p < 0.001$, ** $p < 0.01$, * $p < 0.05$. Data was analyzed by one-way analysis of variance (ANOVA) followed by Bonferroni multiple comparisons, two-way ANOVA, repeated measures analysis of variance (MANOVA) and unpaired T-test using GraphPad Prism v.5 (GraphPad Software, San Diego, CA, USA) and repeated measures analysis of variance (MANOVA) using Statistica v.12 (StatSoft, Tulsa, Oklahoma, USA).

2.9 Software

The following software was used: GraphPad Prism v.5.04 (GraphPad Software, San Diego, CA, USA), Statistica v.12.0 (StatSoft, Tulsa, Oklahoma, USA), ANY-Maze software (Stoelting, Wood Dale, IL, USA), Microsoft Office 365 (Microsoft, Redmond, WA, USA), Adobe Illustrator CS6 (Adobe Systems, San Jose, CA, USA)

3 Results

Parts of this work have been published:

Meißner JN, Bouter Y, Bayer TA (2015): Neuron Loss and Behavioral Deficits in the TBA42 Mouse Model Expressing N-Truncated Pyroglutamate Amyloid- β 3-42. *J Alzheimers Dis.* 45, 471–482

Storck SE, Meister S, Nahrath J, **Meißner JN**, Schubert N, Di Spiezio A, Baches S, Vandenbroucke RE, Bouter Y, Prikulis I, Korth C, Weggen S, Heimann A, Schwaninger M, Bayer TA, Pietrzik CU (2016): Endothelial LRP1 transports amyloid-beta1-42 across the blood-brain barrier. *J Clin Invest.* 126, 123–136

3.1 Project I: Quantification of neurodegeneration and analysis of behavioral deficits in the TBA42 mouse model

The TBA42 mouse model is a transgenic mouse model that does not rely on the overexpression of mutated genes that are involved in the production of A β by proteolytic cleavage of the amyloid precursor protein. Instead the model overexpresses only a single transgene, which results in the formation of the N-terminally truncated and pyroglutamate modified A β species A β_{pE3-42} (Wittnam et al. 2012). It was the aim of the first project to deliver a detailed characterization of the TBA42 mouse model. For this purpose, the presence of A β_{pE3-42} in the hippocampus was confirmed. This was followed by a quantification of neuron numbers in the hippocampal CA1 region at three time points, analyzing brains of young (3 months) and older (6 and 12 months) animals. Finally, the behavioral phenotype, with an emphasis on cognitive and motor functions, of TBA42 mice and wildtype control mice at the same age points was assessed.

3.1.1 A β deposition in the hippocampal CA1 region and spinal cord of TBA42 mice

Immunohistochemical DAB-staining was used to confirm the pattern of expression of the transgene in the TBA42 mouse model previously described (Wittnam et al. 2012). Using the polyclonal pan-A β antibody 24311 (host rabbit, AG Bayer) antibody A β deposits were visualized. As previously shown, the strongest expression could be detected in the neuronal CA1 layer of the hippocampus (Figure 3.1 A). In aged TBA42 mice A β was located intracellularly as well as extracellularly (Figure 3.1 B). Intracellular A β was deposited in compact granular struc-

tures. Extracellular A β depositions were found in the CA1 region in the hippocampus as well but not in other brain regions. These extracellular A β deposits should not be referred to as plaques since they were diffusely organized and not as clearly structured as plaques are. Interestingly, in the spinal cord of aged TBA42 mice A β deposition was different from deposition in the hippocampus. Neuronal cells expressing the transgene were located widely distributed within the gray matter of the cervicothoracic spinal cord of TBA42 mice (Figure 3.1 C). A β immunoreactivity was observed in small granular structures within motor neurons (Figure 3.1 D). However, no diffuse extracellular A β deposits were detected. In sum, the high rate of A β expression and deposition within the hippocampal CA1 region and the cervicothoracic spinal cord could be confirmed. Additionally, previous findings that A β plaques were lacking in TBA42 mice were corroborated.

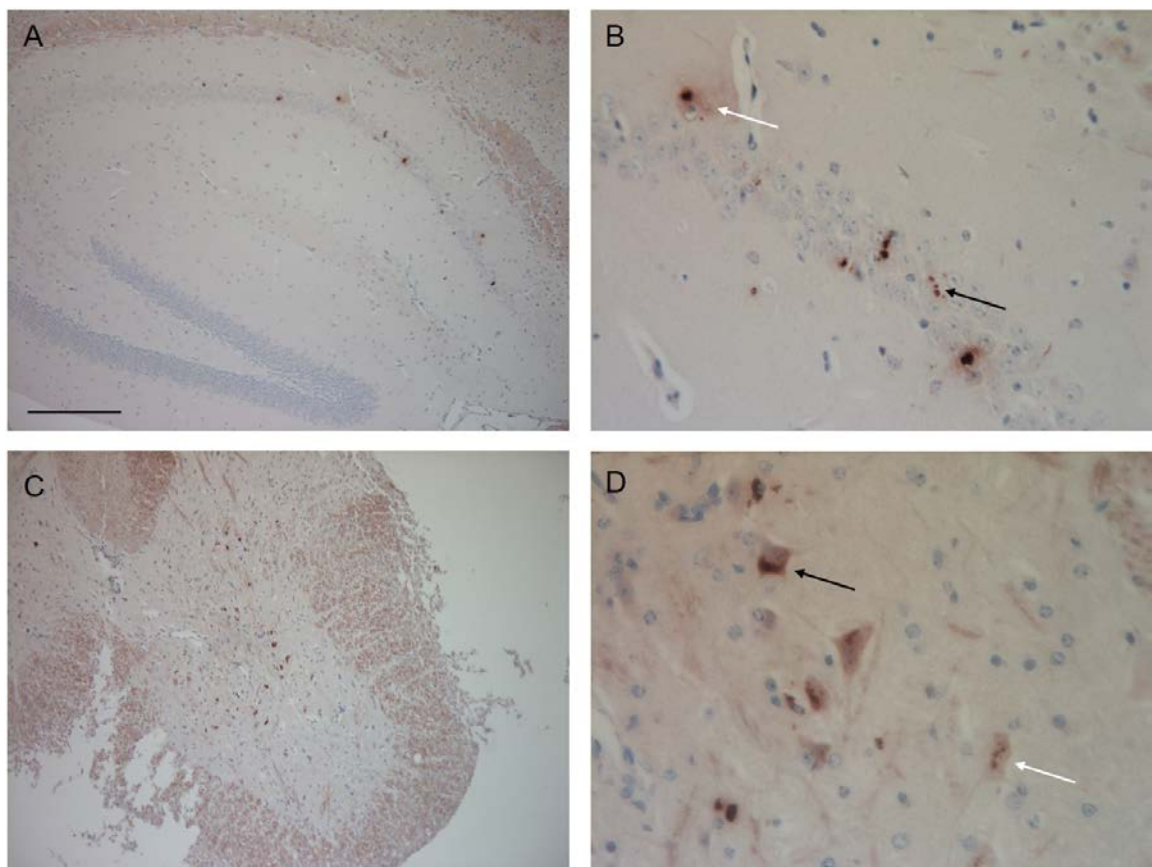


Figure 3.1 Expression of A β in hippocampus and spinal cord of TBA42 mice. Expression of A β in the hippocampal CA1 region of TBA42 mice confirmed by immunohistochemistry (A). Intraneuronal A β formed granular structures (black arrow), while extracellular A β was diffusely deposited (white arrow) (B). In the spinal cord of TBA42 mice A β was present as well (C). Here A β was only found within neurons (arrows), but not extracellularly. Representative brain mounts stained with 24311 A β -antibody. A, C: Scale bar = 200 μ m; B, D: Scale Bar = 33 μ m.

3.1.2 Obvious neuron loss depicted by DAPI staining

To assess a possible neurodegeneration induced by the accumulation of A β , mouse brain sections were histochemically stained using the fluorescent dye 4-6-diaminidino-2-phenylindole (DAPI). In order to obtain information about whether the presence of intraneuronal A β_{pE3-42} leads to the reduction of neuronal cell number in the brain region with the highest transgene expression neuronal nuclei were visualized on paraffin sections of 3, 6 and 12 months old TBA42 mice and wildtype control mice of the same age.

An age dependent neuron loss of the hippocampal CA1 region became obvious in aged TBA42 mice, as this neuronal layer was considerably thinned in brains of these animals when compared to TBA42 mice at the age of 3 and six months (Figure 3.2). Since the A β_{pE3-42} is also found in the spinal cord of TBA42 mice, it is possible that it leads to neuron loss here as well. However, in spinal cord tissue no difference in the number of motor neurons of the ventral horn became obvious. A stereological quantification of the neuron number in the spinal cord was not realizable.

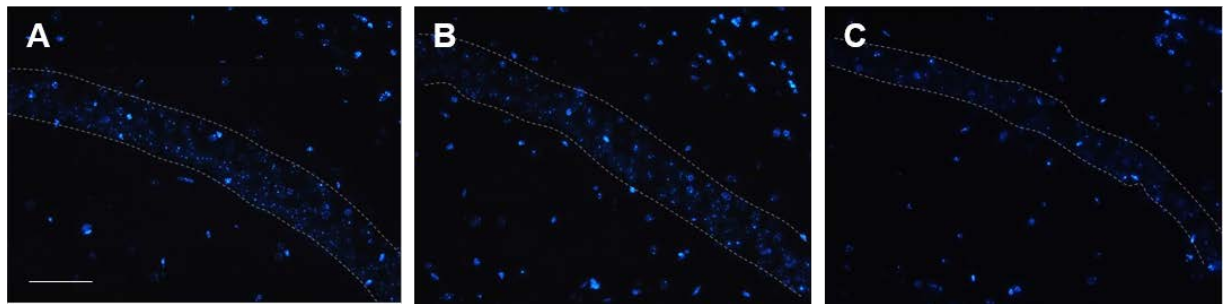


Figure 3.2 Age-dependent neuron loss in TBA42 mice. DAPI staining revealed an age-dependent neuron loss in the hippocampal CA1 region of aged TBA42 mice (C) as compared to 3-month old (A) and 6-month old animals (B). Scale Bar = 50 μ m.

3.1.3 Stereological quantification of neuron loss

Mouse brains were subjected to stereological investigation in order to corroborate the observations about neuronal loss in the CA1 region of the hippocampus of aged TBA42 mice. The number of neurons in the hippocampal CA1 region was investigated in 3, 6 and 12 months old TBA42 mice and wildtype control mice of the respective age using the optical fractionator workflow. By stereological quantification an age-dependent neurodegeneration of the hippocampal CA1 region was observed in aged TBA42 mice (Figure 3.3). Twelve months old TBA42 mice showed a 35 % neuron loss (mean = 184,600, SEM \pm 8,734, p = 0.0019), as compared to wildtype mice (mean = 283,800 SEM \pm 10,360). In contrast, in 3-month old

TBA42 mice, no neuron loss could be detected (TBA42: mean = 274,700 SEM \pm 17,790; wildtype: mean = 287,700 SEM \pm 7,280). Likewise, at the age of 6 months no difference in the total number of neurons between TBA42 (mean = 281,800 SEM \pm 19,750) and wildtype control mice (mean = 284,400, SEM \pm 3,053) was seen.

In sum, the data collected by stereological quantification of the hippocampal neuron number, indicate that a relevant neuron loss is initiated between the age of six and twelve months in the TBA42 mouse model.

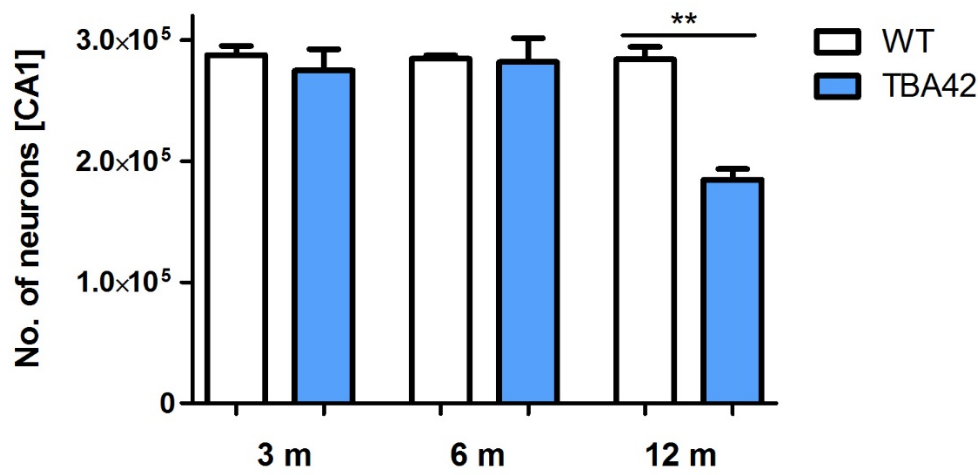


Figure 3.3 Quantification using unbiased stereology. Unpaired t-test ** $p = 0.01$ m = age in months; $n = 3$ per group; 3 months: 3 males, 6 months: 3 males, 12 months: 2 females, 1 male. WT = wildtype Data presented as mean \pm SEM. m = months

3.1.4 Severe motor deficits in aged TBA42 mice

Since a strong intra-neuronal accumulation of A β in spinal cord neurons was seen by immunohistochemistry, sensory-motor abilities of TBA42 and wildtype control mice were assessed using the balance beam, the string suspension and the inverted grip hanging test (Figure 3.4). The balance beam was used to analyze the ability of mice to remain on a wooden rod. 3 months old TBA 42 mice did not show an impairment in this task, whereas 6 months old TBA 42 mice performed worse than wildtype controls ($p < 0.001$). Motor function as measured by the balance beam task was exacerbated in 12 months old TBA 42 mice (Figure 3.4 A). The inverted gri hanging test was also used to assess motor abilities by analyzing the ability of mice to hold on to an inverted metal grid. 3 months old TBA 42 mice did not display an impairment in this task, while 6 months old TBA 42 mice showed a decreased latency to fall ($p <$

0.01), which decreased further at 12 months of age ($p < 0.001$) (Figure 3.4 B). The string suspension test is another sensory-motor test that was used to measure the ability of mice to remain on a wire spanned between two wooden dowels. TBA 42 mice of 3 months already showed poorer performance compared to WT mice ($p < 0.05$). In older TBA42 mice this deficit was even aggravated ($p < 0.001$) (Figure 3.4 C).

In sum, the results from the different sensory-motor tests reveal a severe age-dependent motor deficit induced by the presence of $A\beta_{pE3-42}$ in TBA42 mice.

3.1.5 Reduced anxiety in aged TBA42 mice

The elevated plus maze was used to assess anxiety related behavior of 3-, 6-, and 12-month old TBA42 mice in comparison to age-matched wildtype controls (Figure 3.5 A, B). In the elevated plus maze paradigm the time mice spent in the closed arm of the apparatus is correlated with the level of anxiety. TBA42 mice displayed an age-dependent increase in anxiety behavior (Two-way ANOVA main significant effect of age combined with genotype: $p < 0.05$). In young TBA42 mice, only a trend toward reduced anxiety levels could be detected, transgenic mice spent more time in the open arms of the maze. However, this difference did not reach significance (Figure 3.5 A). In contrast, 6-month old TBA42 mice spent a greater amount of time in the open arms of the elevated plus maze than the control animals (One-way ANOVA followed by Bonferroni multiple comparisons: $p < 0.05$). At an age of 12 months this difference compared to the appropriate control group became more significant (One-way ANOVA followed by Bonferroni multiple comparisons: $p < 0.001$). An age dependent reduction in locomotor activity could be detected irrespective of genotype (Two-way ANOVA main significant effect of age: $p < 0.001$). However, TBA42 mice, compared to same-aged wildtype animals, showed no difference in the total distance travelled at any age tested (Figure 3.5 B). In summary, an age dependent reduction of anxiety levels as reflected by the greater amount of time spent in the open arms of the elevated plus maze was found in TBA42 mice.

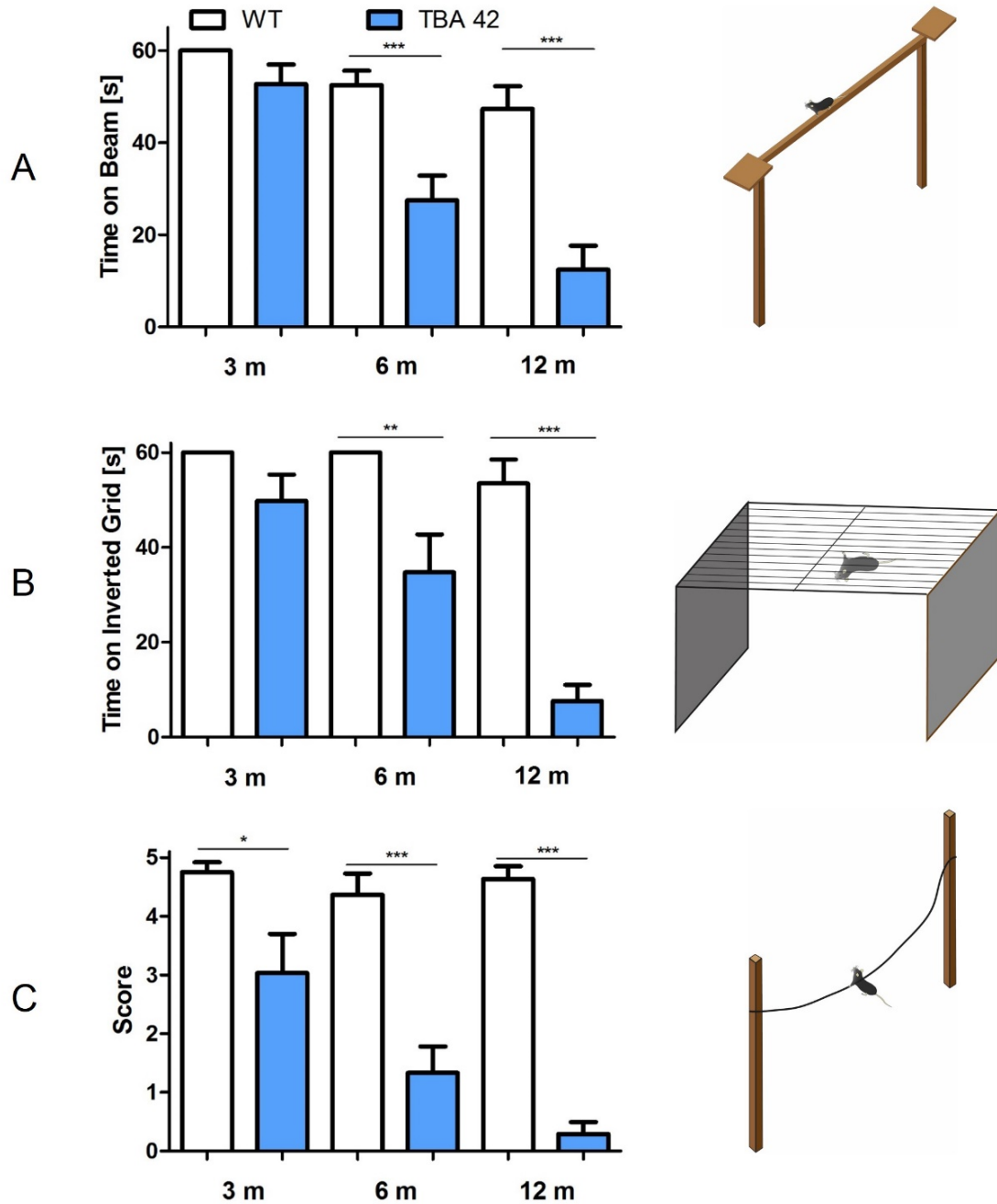


Figure 3.4 Severe motor deficits in TBA42 mice. The balance beam (A) and the inverted grid hanging test (B) revealed a motor deficit in TBA42 mice starting at 6 months of age and progressing in an age dependent manner. In the string suspension test (C) a deficit could already been found at 3 months of age. WT=wildtype. One-way analysis of variance (ANOVA) followed by Bonferroni multiple comparisons. *** $p < 0.001$; ** $p < 0.01$; * $p < 0.05$. 3 months $n = 11-12$, 6 months $n = 10-12$, 12 months $n = 8-10$. Data presented as mean \pm SEM. m = months

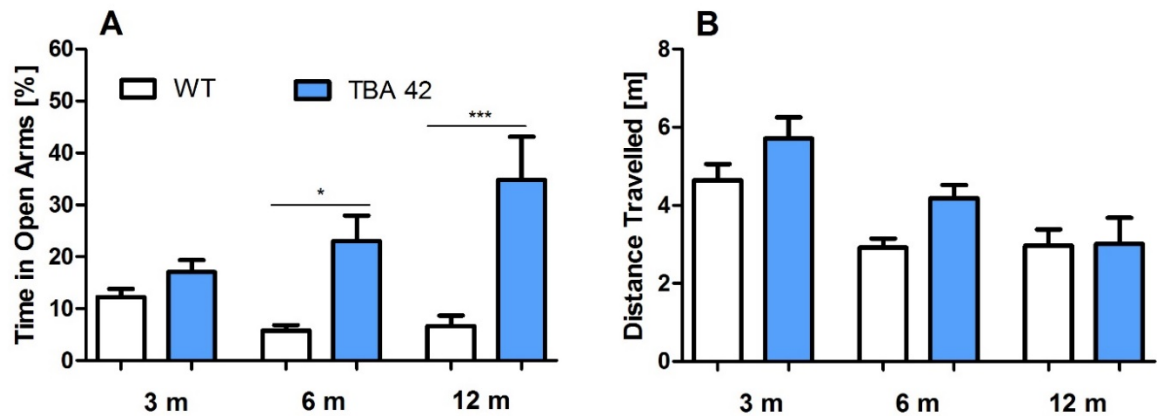


Figure 3.5 Reduced Anxiety in aged TBA42 mice. The elevated plus maze revealed a reduced anxiety in TBA42 mice as reflected by a significantly greater amount of time spent in the open arms (A). No difference in the covered distance was detected (B). *** $p < 0.001$, * $p < 0.05$ Data presented as mean \pm SEM. m = months

3.1.6 Impaired working memory in aged TBA42 mice

Working memory was assessed in wildtype and TBA42 mice using the cross maze task (Figure 3.6 A, B). A reduction in alternation rates could be detected for TBA42 mice (Two-way ANOVA main significant effect of genotype: $p < 0.05$). Alternation rates of 3- and 6-month old TBA42 mice did not differ significantly from age-matched wildtype controls (Figure 3.6 A). However, in 12-month old TBA42 mice, an impaired working memory could be observed as reflected by a reduced alternation rate, which was even below the chance level (One-way ANOVA followed by Bonferroni multiple comparisons: $p < 0.05$), compared to 12-month old wildtype animals. This reduction was not due to a decreased explorative behavior since no difference in the distance travelled between TBA42 and age-matched wildtype mice could be detected (Figure 3.6 B).

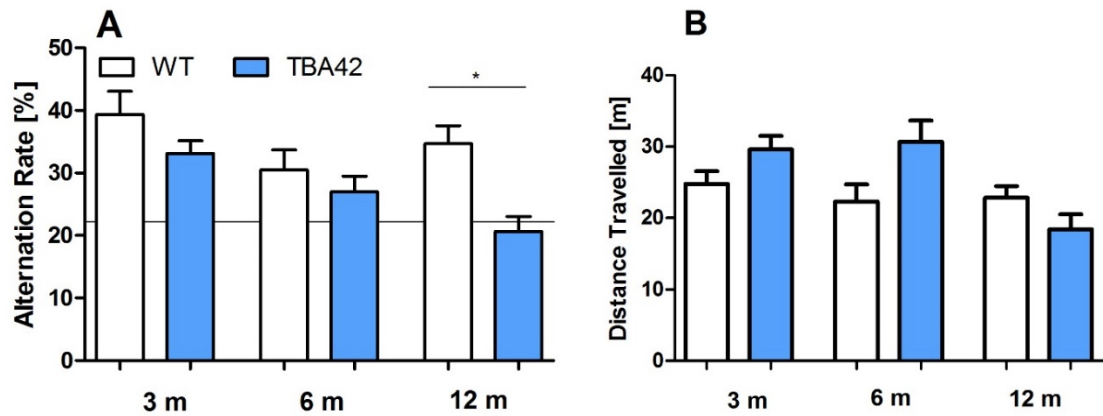


Figure 3.6 Impaired working memory in aged TBA42 mice. The significantly lowered alternation rate of 12-month old TBA42 mice in the cross maze (C) was not due to changes in the total distance travelled (D). No significant changes in alternation rates of wildtype mice were detected. Chance level is indicated by horizontal line at 22.22 %. WT, wildtype. One-way analysis of variance (ANOVA) followed by Bonferroni multiple comparisons. * $p < 0.05$ Data presented as mean \pm SEM. m = months

3.1.7 TBA42 mice display spatial learning deficits

Spatial reference learning was analyzed in TBA42 and wildtype control mice at three age points using the Morris water maze. First, mice performed cued training with a marked platform to familiarize with the pool and to rule out effects from motor or sensory deficits. Both, TBA42 and wildtype mice showed a significant decrease in escape latencies and therefore reached criteria for further testing (Figure 3.7 A, C, E) (Unpaired t-test day 1 versus day 5: 3 and 6 months wildtype and TBA42 $p < 0.001$, 12 months wildtype and TBA42 $p < 0.01$). The cued training showed that all mice tested had appropriate eyesight and motor abilities to swim (Figure B, D, F). However, TBA42 mice swam slower than their littermates (Unpaired t-test: 3 months day 2, day 3 $p < 0.05$, 6 months day 1, day 3 $p < 0.01$, day 2 $p < 0.05$, 12 months day 1 $p < 0.05$)

Twenty-four hours after the cued training was finished, the acquisition training was started, in order to test their ability to learn finding the location of a submerged platform relying on cues (Figure 3.7). Swimming speeds of TBA42 mice differed from wildtype controls (Repeated measures ANOVA: significant main effect of genotype: $p < 0.01$) on day 1 (Unpaired t-test: $p < 0.01$) for 6-month old mice (Figure 3.7 D) and throughout the five days of acquisition training in 12-month old mice (Figure 3.7 F). Twelve month old TBA42 mice displayed an average swimming speed of 0.119m/s over the five days of acquisition training, mice were able to

swim the maximum distance from entry point to goal platform (approximately 85 cm) within 7.1 s. Wildtype mice of the same age displayed a mean swimming speed of 0.160m/s, enabling them to travel the same distance within 5.3 s

Since the escape latency as a measure for learning can be confounded by the reduced swimming speed observed in TBA42 mice, we analyzed the distance travelled by mice to measure learning behavior in a less biased manner. The distance travelled decreased from day 1 to day 5 in both TBA42 and wildtype mice at the ages of 3 and 6 months, respectively (Figure 3.8 A, C; unpaired t-test day 1 versus day 5: 3 months TBA 42 and wildtype $p < 0.001$; 6 months TBA42 $p < 0.001$; 6 months wildtype $p < 0.05$). However, at the age of 12 months, a deficit in learning behavior in TBA42 mice was detected, as they did not show a decreased average distance travelled, while wildtype mice of the same age still did (Figure 3.7 E; main significant effect of genotype: $p < 0.01$. Unpaired t-test day 1 versus day 5: 12-month old wildtype $p < 0.01$). 12-month old TBA42 mice swam significantly slower than their wildtype littermates (Repeated measures ANOVA: significant main effect of genotype: $p < 0.05$) (Figure 3.8 F). Therefore, it can be stated that 12-month old TBA42mice display a deficit in spatial learning.

Twenty-four hours after the last acquisition trial, a probe trial was given to assess spatial reference memory. Three- and 6-month old TBA42 and wildtype mice displayed a significant preference for the target quadrant (Figure 3.9 C), as indicated by the greater amount of time spent in the target quadrant of the pool than in the other quadrants (Unpaired t-test target versus left, right, and opposite quadrant). In contrast, no preference for the target quadrant was found for aged TBA42mice, while it was still observed for aged wildtype mice ($p < 0.001$) (Figure 3.9 E). Swimming speeds in the probe trial did not differ between groups for 3- and 6-month old animals (Figure 3.9 B, D). As observed in the acquisition training, 12-month old TBA42 mice also showed a reduced swimming speed in the probe trial (Unpaired t-test, $p < 0.01$) (Figure 3.9 F). In sum, the results from the probe trial indicate a reduced spatial reference memory in aged TBA42 mice, although an influence of decreased swimming speed cannot be ruled out completely.

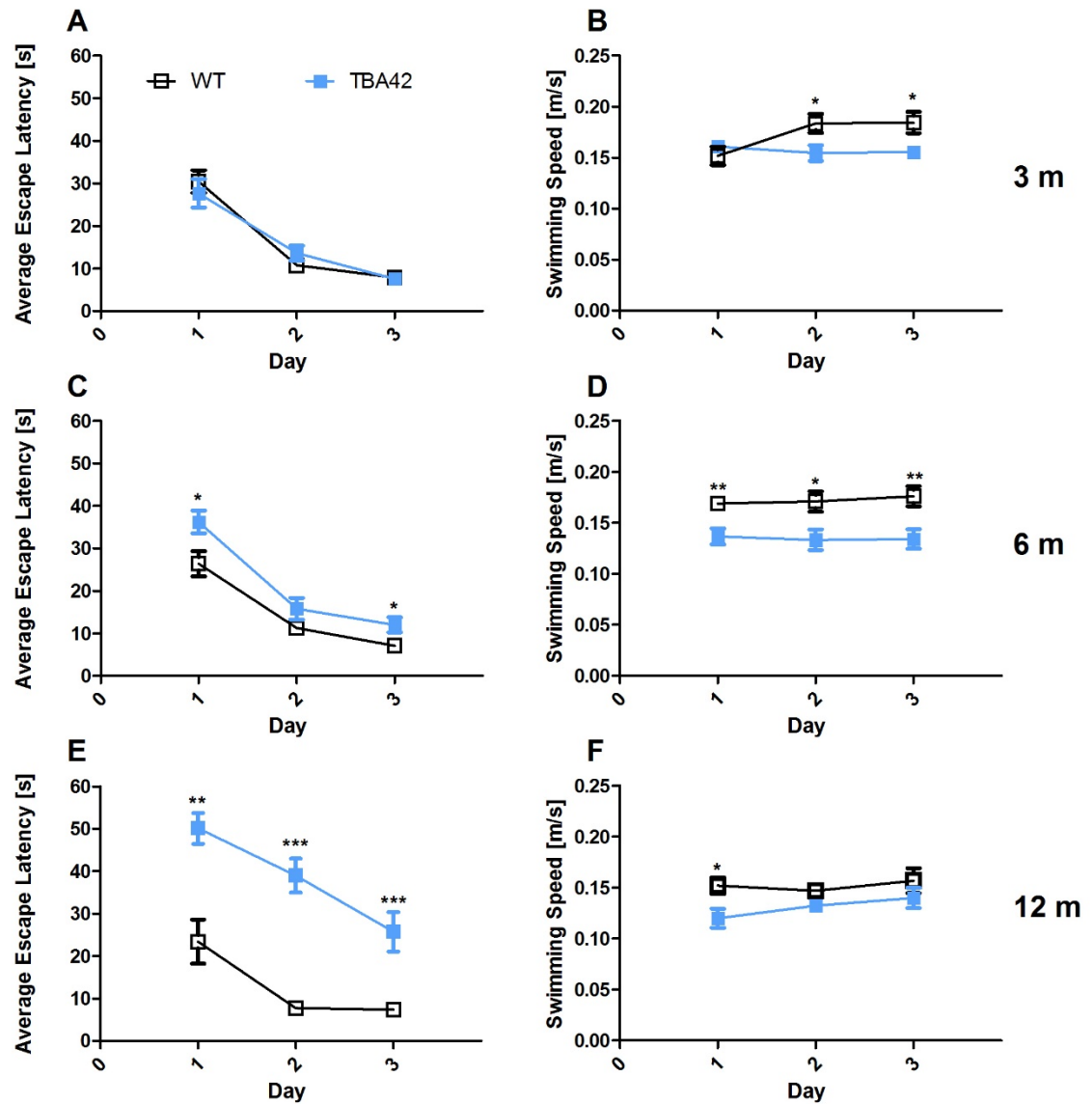


Figure 3.7 Cued Training showed that all mice have appropriate motor abilities and intact vision. The escape latency of mice decreased significantly in all groups tested (A, C, E). During the cued training TBA42 mice swam slower than their age-matched wildtype littermates (3 months on days 2 and 3, 6 months all 3 days, 12 months day 1) Unpaired t-test for each day. *** $p < 0.001$, ** $p < 0.01$, * $p < 0.05$. Data presented as mean \pm SEM. m = months

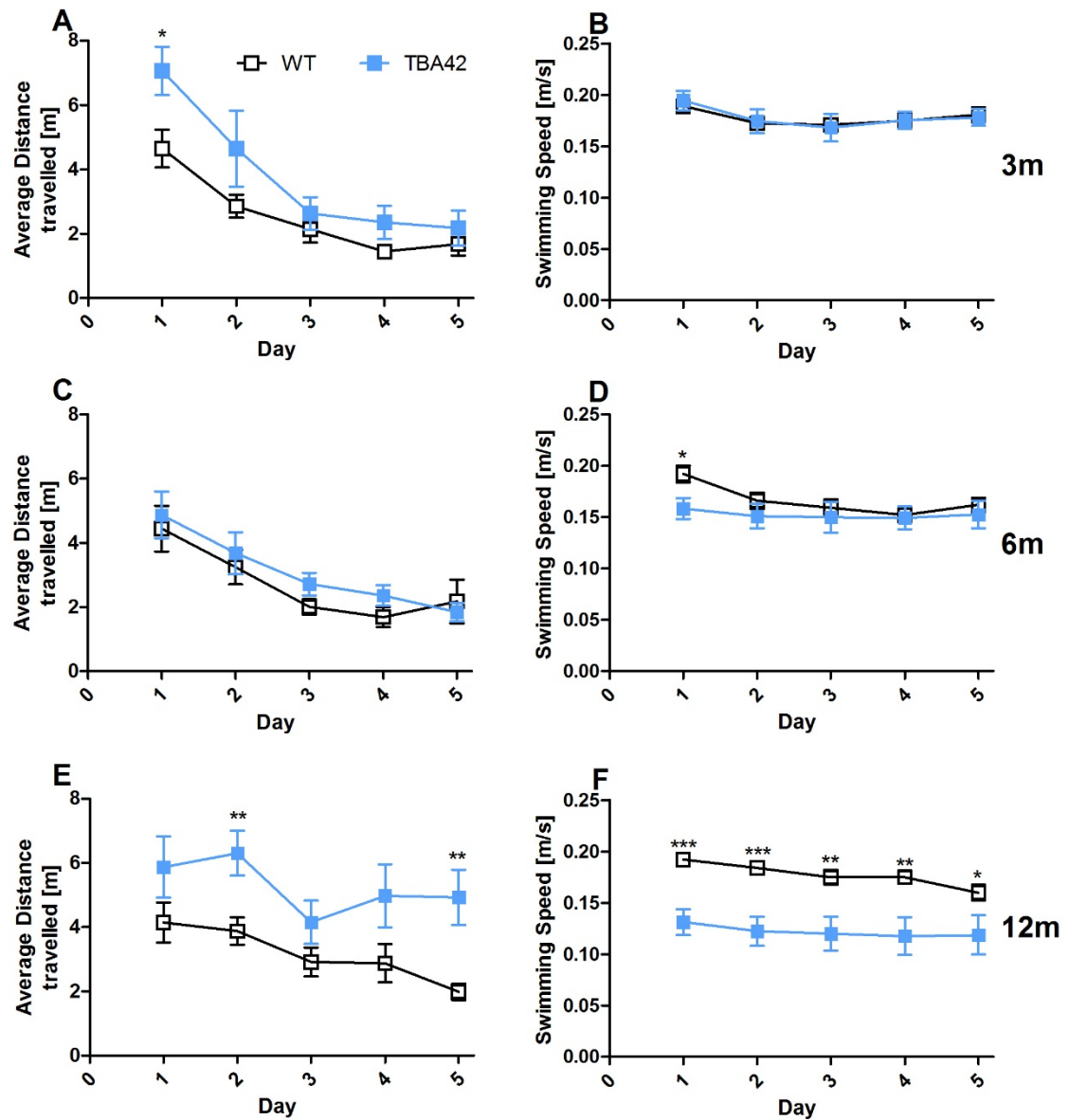


Figure 3.8 Impaired spatial learning in aged TBA42 mice. The distance travelled decreased over the five days of acquisition training in 3-month old (A) and 6-month old (C) TBA42 and wildtype mice. In contrast, in 12-month old TBA42 mice the distance travelled remained on a high level (E), while wildtype mice showed a reduction in this measure. Swimming speeds did not differ in 3- and 6-month old mice (B, D). At 12 months, swimming speeds were significantly lowered in TBA42 mice (F). WT, wildtype Escape latency: Unpaired t-test day 1 versus day 5 for each group and between groups for each day. Swimming speed: Unpaired t-test. *** $p < 0.001$, ** $p < 0.01$, * $p < 0.05$. Data presented as mean \pm SEM. m = months

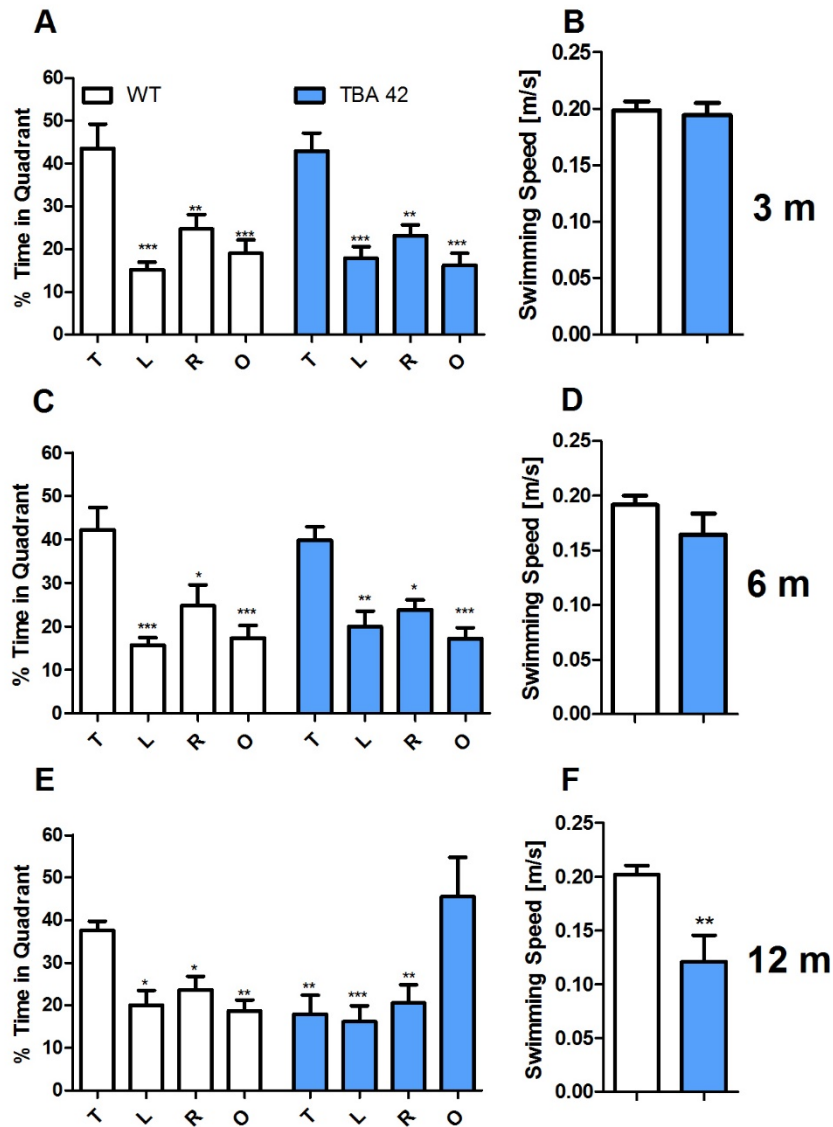


Figure 3.9 Impaired spatial reference memory in aged TBA42 mice. Three- and 6-month old TBA42 and wildtype mice show a preference for the target quadrant, as they spent more time in this quadrant (A, C). At 12 months, wildtype animals show a target quadrant preference, while 12-month old TBA42 no longer spent more time in the target quadrant (E). Swimming speed differed between 12-month old TBA42 mice and wildtype controls (F), while it was unaltered in younger animals (B, D). T, target quadrant; LRO, average of left, right, and opposite quadrant. One-way ANOVA followed by Bonferroni multiple comparisons. *** $p < 0.001$, ** $p < 0.01$, * $p < 0.05$. Data presented as mean \pm SEM. m = months

3.2 Project II: Exploring in vivo effects of impaired A β clearance induced by knock-out of brain endothelial *LRP1* in 5xFAD mice

3.2.1 Unaltered plaque pathology and gliosis in 5xFAD/ *Lrp1*_{BE}^{-/-} mice

This part of the work was performed in collaboration with Nils Schubert (Immunohistochemical stainings by Nils Schubert; Image acquisition, Quantification and Statistical analysis by Julius Nicolai Meißner)

To evaluate the impact of *LRP1* knockout on A β plaque deposition, the plaque load as measured by the area covered with A β immunoreactivity was measured in the hippocampus of 7 months old female 5xFAD/*Lrp1*_{BE}^{fl/fl} and 5xFAD/*Lrp1*_{BE}^{-/-} mice.

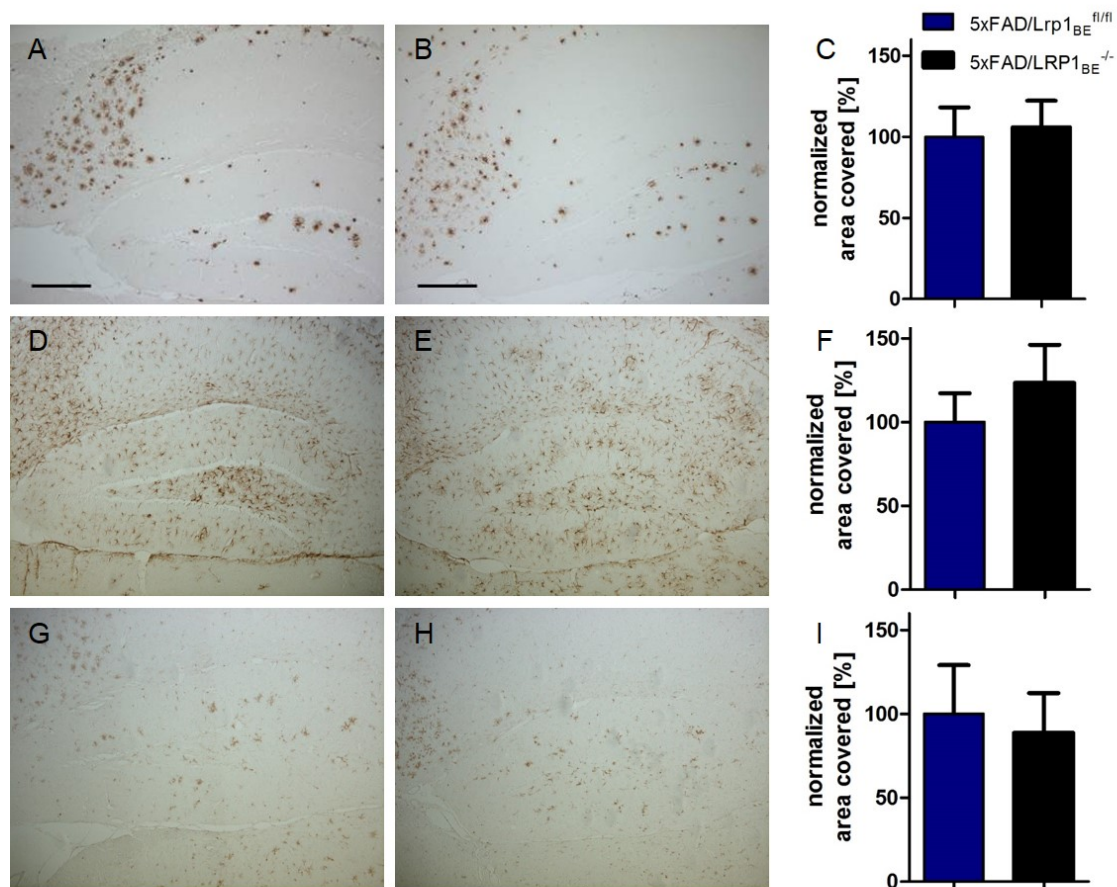


Figure 3.10 *LRP1* knockout does not lead to altered plaque loads and gliosis in 5xFAD mice. Exemplary images from brain mounts that were used for quantifications. Stainings by Nils Schubert. 24311 polyclonal A β antibody in 5xFAD/*Lrp1*_{BE}^{fl/fl} (A) and 5xFAD/*Lrp1*_{BE}^{-/-} (B) mice. GFAP staining in 5xFAD/*Lrp1*_{BE}^{fl/fl} (D) and 5xFAD/*Lrp1*_{BE}^{-/-} (E). Iba1 staining in 5xFAD/*Lrp1*_{BE}^{fl/fl} (G) and 5xFAD/*Lrp1*_{BE}^{-/-} (H). Quantifications revealed no significant difference in plaque load and gliosis. Scale bars 200 μ m. For statistical analysis unpaired t-test was used. Data presented as mean \pm SEM.

3.2.2 Morris water maze

Since the plaque load in 5xFAD mouse brains was unaffected by the conditional knockout of *LRP1* in endothelial cells of brain vessels, but soluble levels of A β were elevated, it was analyzed if brain endothelial *LRP1* knockout affects the cognitive functions by examining spatial learning and spatial reference memory. It was analyzed, whether 5xFAD/*Lrp1*_{BE}^{-/-} displayed memory deficits earlier and spatial learning and memory at 7 months of age was assessed in four experimental groups: Wildtype (WT) (n=6), *Lrp1*_{BE}^{-/-} (n=5), 5xFAD/*Lrp1*_{BE}^{-/-} (n=7) and 5xFAD/*Lrp1*_{BE}^{fl/fl} (n=7). Testing the spatial learning in the acquisition training revealed significantly reduced escape latencies for each genotype except 5xFAD/*Lrp1*_{BE}^{fl/fl} (Figure 3.11 A, Unpaired t-test, Day 1 vs. Day 5, 5xFAD/*Lrp1*_{BE}^{-/-} p = 0.036 5xFAD/*Lrp1*_{BE}^{fl/fl} p = 0.314; *Lrp1*_{BE}^{-/-} p = 0.025; WT p = 0.017). However, on days 3 to 5 5xFAD/*Lrp1*_{BE}^{-/-} mice displayed an increased escape latency when compared to the other groups. The swimming speed did not differ between groups (Figure 3.11 B). These results suggest that spatial learning is impaired in both 5xFAD/*Lrp1*_{BE}^{fl/fl} and 5xFAD/*Lrp1*_{BE}^{-/-} mice.

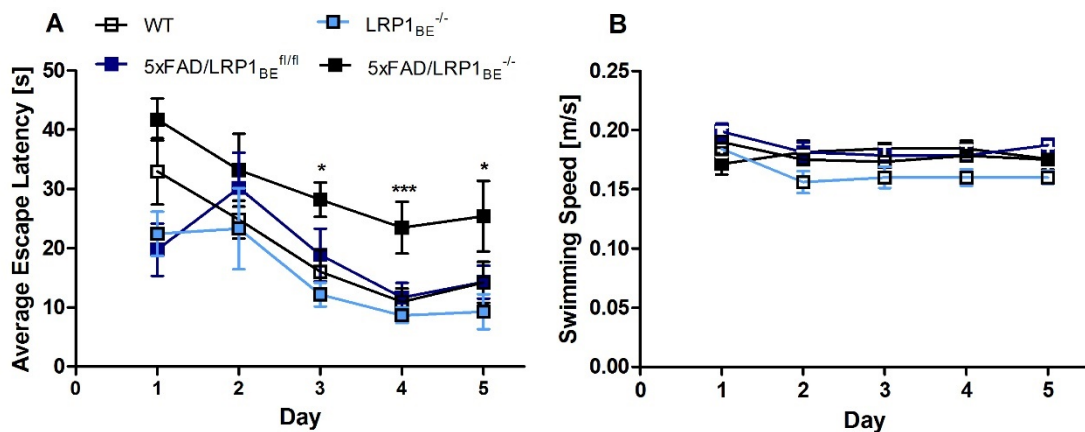


Figure 3.11 Spatial learning deficits in 5xFAD/*Lrp1*_{BE}^{-/-}. Female 7-month-old wildtype (WT) (n=6), *Lrp1*_{BE}^{-/-} (n=5), 5xFAD/*Lrp1*_{BE}^{-/-} (n=7) and 5xFAD/*Lrp1*_{BE}^{fl/fl} (n=7). Animals underwent acquisition training to learn to use cues to navigate a route to a submerged platform. Escape latency decreased significantly in all groups except 5xFAD/*Lrp1*_{BE}^{fl/fl}. Swimming speed was comparable in all mice tested. For statistical analyses, the following tests were used: escape latency day 1 vs. day 5: unpaired t-test; swimming speed and comparisons of escape latency: One-way ANOVA followed by Bonferroni multiple comparisons. ***p<0.001, *p<0.05. Data presented as mean \pm SEM.

The following probe trial revealed that 5xFAD/*Lrp1*_{BE}^{fl/fl} mice displayed a significant preference for the target quadrant, whereas no quadrant preference was found for 5xFAD/*Lrp1*_{BE}^{-/-} mice (Figure 3.12 A). Swimming speeds did not differ between groups (Figure 3.12 B). In summary, the results illustrate that endothelial-specific *Lrp1* knockout in 5xFAD mice, and therefore, reduced clearance of A β peptides, induced an impairment of spatial reference memory as reflected by the absence of a preference for the target quadrant.

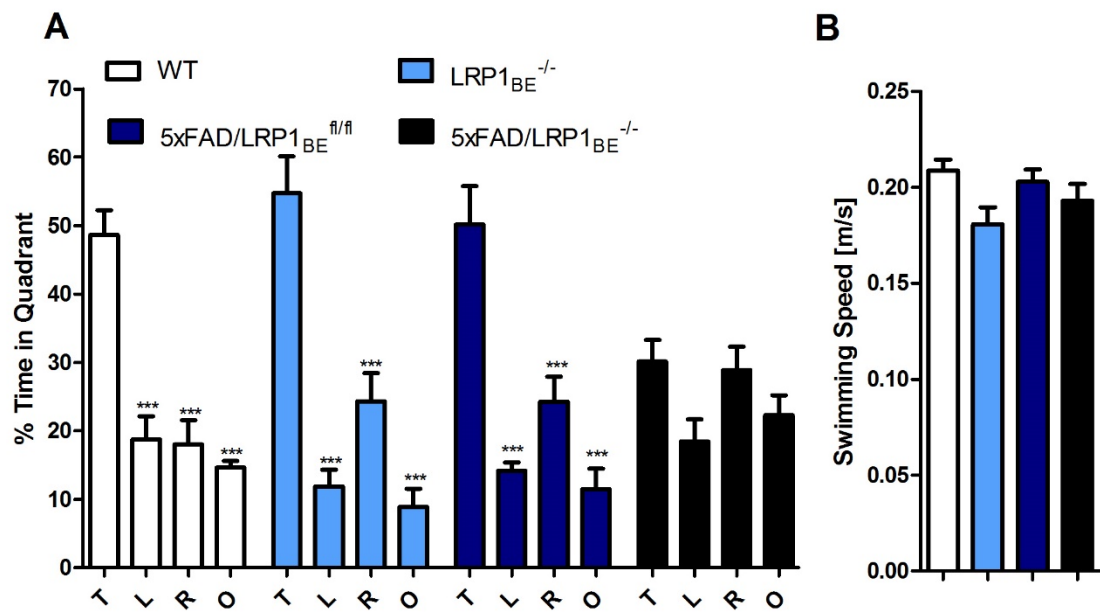


Figure 3.12 Impairment of spatial reference memory deficits in 5xFAD/*Lrp1*_{BE}^{-/-}. The probe trial was performed analyze spatial reference memory. 5xFAD/*Lrp1*_{BE}^{fl/fl}, *Lrp1*_{BE}^{-/-} and wildtype (WT) control mice showed no impairment of spatial reference memory, as reflected by the significant greater percentage of time spent in the target quadrant ($p < 0.001$ target vs. left, right and opposite quadrant). The probe trial revealed an impaired spatial reference memory in 5xFAD/*Lrp1*_{BE}^{-/-} mice as they showed no preference for the target quadrant. Swimming speed did not differ between the groups. Abbreviations: T=target quadrant, L=left quadrant, R=right quadrant, O=opposite quadrant. For statistical analyses of quadrant preference and swimming speed, the following tests were used: One-way ANOVA followed by Bonferroni multiple comparisons. Data presented as mean \pm SEM.

4 Discussion

4.1 Project I: Quantification of neurodegeneration and analysis of behavioral deficits in the TBA42 mouse model

When Masters et al. (1985) purified A β from brains of AD-patients and aged Down syndrome patients their analysis by high-performance liquid chromatography revealed the presence of N-terminally ragged species of the peptide. Mori et al. (1992) first described the presence of pyroglutamate modified A β in AD-brains, overcoming difficulties in sequencing the N-terminus of A β , which is blocked by pyroglutamate formation (Selkoe et al. 1986; Mori et al. 1992). A study performed by Miller et al. (1993) that used matrix assisted, laser-desorption-time-of-flight (MALDI-TOF) mass spectroscopy and protein sequencing further extended the findings on truncated A β , detecting A β species starting with each of the first eleven amino acids. Using species-specific A β antibodies in 28 AD-brains Saido et al. (1995) identified A $\beta_{\text{pE3-42}}$ as the dominant species of A β in AD. Based on data obtained in ELISA experiments it was later estimated that A $\beta_{\text{pE3-42}}$ constitutes approximately 25 % of the total A $\beta_{\text{x-42}}$ deposits (Harigaya et al. 2000). Interestingly, A $\beta_{\text{pE3-42}}$ was reported to be present already in presymptomatic AD patients (Sergeant et al. 2003). N-truncated forms of A β are not only found in human AD brains but also in AD-mouse models. In APP/PS1KI mice Casas et al. (2004) identified different N-terminally ragged A β peptides as early as at 2.5 months using two-dimensional gel electrophoresis and mass spectroscopy. A $\beta_{\text{pE3-42}}$ deposition was also found starting at 6 months and increasing with age. A $\beta_{\text{pE3-42}}$ was also detected in 5xFAD mice using mass spectroscopy (Wittnam et al. 2012)

It is assumed that the formation of A $\beta_{\text{pE3-42}}$ requires two steps. Firstly full length A β is truncated by proteolytic cleavage, which leads to the exposure of the glutamate residue at position 3 (Jawhar et al. 2011). Secondly, pyroglutamate formation via dehydration of glutamate is enzymatically catalyzed by glutaminyl cyclase (QC) (Schilling et al. 2004; Cynis et al. 2008a).

Not only is A $\beta_{\text{pE3-42}}$ a highly abundant A β species in AD brains, moreover it is assumed to be highly pathogenic. The peptide shows a higher hydrophobicity, due to the loss of two positive charges and one negative charge (Schlenzig et al. 2009). An increased propensity to form stable aggregates has been reported (Bouter et al. 2013). The formation of aggregates by A $\beta_{\text{pE3-42}}$ is up to 250 fold accelerated (Schilling et al. 2006). This higher aggregation propensity was shown to be caused by an increased tendency to form a β -sheet containing secondary structure

induced by pyroglutamate formation (Dammers et al. 2015). Cell culture experiments revealed an elevated toxicity as compared to the unmodified full length peptide *in vitro* (Russo et al. 2002; Bouter et al. 2013). Moreover, $A\beta_{pE3-42}$ containing deposits are inaccessible for aminopeptidases, thus clearance by proteolytic cleavage of the peptide is impeded (Jawhar et al. 2011; Cummins and O'Connor 1998). Finally, *In vivo* experiments showed that intraventricular injection of $A\beta_{pE3-42}$ in wildtype mice led to a reduction in working memory, further implying a role of the peptide in AD (Bouter et al. 2013). Taken together, the findings from human AD-brains, cell culture experiments and AD mouse models indicate a crucial role of $A\beta_{pE3-42}$ in the pathogenesis and disease progression of AD

4.1.1 The TBA42 mouse model

In transgenic mouse models a variety of $A\beta$ species are found, mimicking the situation in AD-patients. However, the effects of different species are hardly distinguishable. To further investigate $A\beta_{pE3-42}$ toxicity *in vivo* transgenic mouse models have been developed. The TBA42 model represents a transgenic mouse line that expresses N-truncated $A\beta_{3-42}$ with a glutamine residue at position 3 under the control of the Thy1.2 promotor sequence. The peptide is post transcriptionally converted into $A\beta_{pE3-42}$ by the glutaminyl cyclase (Wittnam et al. 2012). In the TBA2 mouse models, harboring the same DNA-construct, $A\beta_{pE3-42}$ expression induced an early lethal phenotype, limiting the usability of these lines in studying AD-mechanisms and therapeutic strategies (Wirhth et al. 2009). In the FAD42 model that was generated by crossing 5xFAD with TBA42 mice, an increase of the $A\beta_{pE3-42}$ dose induced an aggravated behavioral phenotype. In TBA42 mice $A\beta_{pE3-42}$ does not induce early lethality, however important AD-like hallmarks are produced. This AD-like phenotype is generated without relying on the expression of mutated genes that in humans cause early-onset familial forms of AD.

The aim of the present work was to extend previous findings, performing a detailed characterization of the TBA42 mouse model. For this purpose, the behavioral phenotype and hippocampal neurodegeneration were analyzed in the course of aging, testing male and female mice at 3, 6 and 12 months of age. TBA42 mice display a progressive neurodegeneration in the CA1 region of the hippocampus, where the highest transgene expression is observed. Furthermore, an age-dependent deficit in spatial learning, spatial reference memory and working memory is observed. These cognitive impairments are accompanied by sensorimotor deficits and a reduction of anxiety, resembling important hallmarks of Alzheimer disease.

4.1.2 Neuron loss in aged TBA42 mice

Hippocampal neuron loss and brain atrophy are major neuropathological hallmarks of AD-patient brains (West et al. 1994; Villemagne et al. 2013). APP single transgenic AD mouse models often failed to produce a neuron loss as it is seen in AD patients (Wirths and Bayer 2010). However, transgenic mouse lines with several mutations in the APP and the PS1 gene do exhibit neurodegeneration. APP/PS1KI mice display a neuron loss in the hippocampal CA1/CA2 region of more than 50 % at the age of 10 months (Casas et al. 2004, 2004; Breyhan et al. 2009). Additionally, 35 % of the neurons in the frontal cortex (Christensen et al. 2008) and 35 % of those in cholinergic nuclei were lost at the age of 12 months (Christensen et al. 2010). In the 5xFAD model, which harbors five different FAD mutations, an age dependent neuron loss was observed in the fifth cortical layer starting at 9 months. However, the total number of neurons in the hippocampus was unaltered, as measured by unbiased stereology (Jawhar et al. 2012). Interestingly $A\beta_{pE3-42}$ is present in both mouse lines. In APP/PS1KI mouse-brains a heterogeneous combination of N-terminally truncated $A\beta$ species was detected, appearing at 6 months of age (Casas et al. 2004), coinciding with the first neuronal loss (Wirths and Bayer 2010). In homozygous TBA 2.1 mice accumulation of $A\beta_{pE3-42}$ led to a loss of more than 40 % of hippocampal CA1 neurons (Alexandru et al. 2011). Interestingly, correlating with the observed neurodegeneration, $A\beta_{pE3-42}$ show the strongest relative increase in aggregation profiles in the hippocampus of APP/PS1KI mice (Breyhan et al. 2009). In the 5xFAD model $A\beta_{pE3-42}$ is found as a fraction of a variety of N-terminally truncated $A\beta$ peptides (Wittnam et al. 2012). While intraneuronal $A\beta$ was present in the fifth cortical layer of 5xFAD mice, it was absent in the CA1, linking the pattern of neurodegeneration to the distribution pattern of intraneuronal $A\beta$ (Eimer and Vassar 2013; Jawhar et al. 2012). Taking these findings into account, it is likely that the neuron loss observed in 5xFAD and APP/PS1KI mice to some extent is induced by $A\beta_{pE3-42}$ and intraneuronal $A\beta$ deposits rather than by plaque-bound $A\beta$.

Using unbiased stereological quantification, we found that TBA42 mice exhibit a significant 35 % neuron loss in the hippocampal CA1 region at the age of 12 months induced by the production of $A\beta_{pE3-42}$ (Meißner et al. 2015), corroborating previous findings on a severe neurological phenotype in TBA2.1, TBA2.2 and TBA2 mouse models expressing $A\beta_{pE3-42}$ (Alexandru et al. 2011; Wirths et al. 2009). Intraneuronal $A\beta_{pE3-42}$ deposition preceded neuronal loss since $A\beta_{pE3-42}$ is deposited starting in young animals (Wittnam et al. 2012), while neurodegeneration was only observed in aged animals. Strikingly, the observed neurodegeneration in TBA42 mice is induced by very low levels of $A\beta_{pE3-42}$, which were detected by mass spectrom-

etry (Wittnam et al. 2012). Intriguingly, in 12 month-old TBA42 mice the predominant intraneuronal A β staining was decreased and diffuse extracellular A β deposits were additionally detected. As neuron loss was present at this age, it is likely that A $\beta_{\text{pE3-42}}$ -positive neurons died beneath the burden of A $\beta_{\text{pE3-42}}$ toxicity. A similar course of events was shown for neurodegeneration observed in Tg4-42 mice, albeit a more severe neurodegeneration but similar intraneuronal pattern of A β distribution is observed in this model (Bouter et al. 2014).

The mechanism of A $\beta_{\text{pE3-42}}$ toxicity remains to be investigated further. Recently, Gunn and colleagues (2015) reported that A $\beta_{\text{pE3-42}}$ induces lipid peroxidation resulting in a loss of plasma membrane integrity in neuronal cell cultures. An altered ion homeostasis measured by an increase Ca²⁺-flux was also identified as a mechanism of toxicity mediated by A $\beta_{\text{pE3-42}}$. Moreover, Nussbaum et al. suggested a tau-dependent mechanism of A $\beta_{\text{pE3-42}}$ that relies on an interaction of A $\beta_{\text{pE3-42}}$ and tau while A $\beta_{\text{pE3-42}}$ is transported intracellularly (Nussbaum et al. 2012).

In order to extend the findings on neurodegeneration in TBA42 mice, it would be informative to perform detailed stereological analyses of the neuron number at different time points between 6 and 12 months to determine the exact onset of neurodegeneration. Additionally, neuron loss in other brain regions should be evaluated in order to decide if lower transgene expression is sufficient to induce neuronal death in these regions. Furthermore, homozygous TBA42 mice could be generated and analyzed to evaluate if neurodegeneration is dose-dependent as seen in the Tg4-42 model (Bouter et al. 2013).

4.1.3 Impaired motor function in TBA42 mice

AD is characterized predominantly by the progressive impairment of cognitive functions. In addition, patients also develop neuropsychiatric symptoms including motor dysfunctions, agitation and depression. Motor dysfunctions are a commonly observed feature of AD. Particularly late stage AD-patients exhibit motor impairments (Wirths and Bayer 2008). However, motor deficits are also observed in mild AD (Pettersson et al. 2005). In these early stages reduced motor function might even serve as a prognostic parameter for faster disease progression (Scarmeas et al. 2005). In transgenic mouse models of AD motor deficits are commonly observed (Wirths and Bayer 2008). Single transgenic APP models, for example, display an impairment in sensorimotor functions (Le Cudennec et al. 2008; Lee et al. 2004), bigenic APP/PS1 (Ewers et al. 2006). APP/PS1knock-in mice display a motor deficit starting at 6 months of age (Wirths et al. 2008), while in 5xFAD mice a motor deficit is seen starting from 9 months of age (Jawhar et al. 2012).

We found that $A\beta_{pE3-42}$ accumulation in TBA42 mice induces a robust motor dysfunction when compared to wildtype mice beginning at 6 months of age. This dysfunction was aggravated in the course of aging (Meißner et al. 2015). The sensorimotor function was tested using the balance beam, inverted grip hang and string suspension tests, which are all well-established. The decline in motor functions in the TBA42 model correlate with the presence of intraneuronal $A\beta_{pE3-42}$ in the motor cortex and the spinal cord, which was previously shown (Wittnam et al. 2012). Although neurodegeneration could not be observed, due to limitations in the quantification procedure, in the spinal cord, at least neuronal dysfunction in these regions most likely contributes to the observed motor phenotype in TBA42 mice. It was shown that the accumulation of N-truncated $A\beta$ in the spinal cord of APP/PS1KI mice was followed by axonal degeneration, characterized by the presence of axonal swellings and demyelination (Wirhth et al. 2007). This led to motor deficits in this model (Wirhth et al. 2008). In 5xFAD mice motor deficits were also correlated with the presence of axonal dysfunction (Jawhar et al. 2012). The severe motor dysfunctions in the TBA42 mouse line were detected before the onset of memory deficits. This progression pattern does not reflect the course of events in human AD-patients. Nevertheless, an important and clinically relevant attendant phenomenon of AD is resembled by the model.

4.1.4 Reduced anxiety behavior in the TBA42 model

On one hand anxiety is a neuropsychiatric feature that is commonly seen in AD patients (Porter et al. 2014), on the other hand however, disinhibition and agitation is observed in some patients (Lyketsos et al. 2002). In mice, correlates of these diametrically opposed disease manifestations can be tested using the elevated plus maze. An increased amount of time spent in the open arms of the maze stands for reduced anxiety and disinhibition, while increased anxiety is indicated by more time spent in the closed arms of the maze (Faure et al. 2011). Anxiety levels have been studied in a number of AD transgenic mouse models. 5xFAD (Jawhar et al. 2012), APP/PS1KI (Faure et al. 2011) and APP^{swe}+PS1/ Δ E9 (Lalonde et al. 2005) mice as well as single transgenic APP695^{swe} (Lalonde et al. 2003a) and PS1-A246E mice (Lalonde et al. 2003b) displayed reduced anxiety levels. In contrast the 3xTg-AD mouse model showed only a tendency towards increased anxiety (Sterniczuk et al. 2010) while anxiety levels were unaltered in APP23 mice (Lalonde et al. 2002). TBA42 mice displayed a reduction in anxiety levels in the elevated plus maze starting at 6 months of age, which was even more pronounced in 12 months old animals (Meißner et al. 2015).

Connectivity between different brain regions mediates the rather complex anxiety behavior, as it is tested in the elevated plus maze (Walf and Frye 2007). Hippocampus and amygdala (McHugh et al. 2004), as well as the prefrontal cortex (Lacroix et al. 2000) are involved in generation of anxiety behavior.

The observed anxiolysis and disinhibition in TBA42 mice is likely a consequence of neurodegeneration within the hippocampus, although abnormalities in other brain regions may contribute to the observed phenotype. This assumption is supported by the finding that anxiety levels are already elevated, while the neuron number of the CA1 is still unaltered. It could as well be hypothesized that synaptic dysfunction induced by $A\beta_{pE3-42}$ leads to anxiolysis in TBA42 mice.

4.1.5 Cognitive decline in aged TBA42 mice

Working memory, which, by definition, is "short-term memory for an object, stimulus or location within a testing session, but not typically between sessions" (Dudchenko 2004) is a cognitive function that is frequently affected in AD patients (Baddeley et al. 1991; Kirova et al. 2015). Working memory impairments, as indicated by a reduced alternation rate in the Y-maze or the cross maze task, were described in various transgenic mouse models including the 5xFAD model (Jawhar et al. 2012; Oakley et al. 2006) and the APP/PS1KI model (Wirhth et al. 2008). In the latter model this deficit is also associated with a neuron loss in the CA1 region of the hippocampus (Breyhan et al. 2009). A number of APP-transgenic mouse models did not display an impaired spatial working memory (Lalonde 2002; Karl et al. 2003; Savonenko et al. 2003). Interestingly, the Tg4-42 mouse model does not display an impaired spatial working memory, although a more pronounced neurodegeneration in the CA1 region was detected in the model (Dietrich 2015).

In TBA42 mice working memory was studied in order to correlate effects of the observed neurodegeneration in the CA1 region of the hippocampus. Spatial working memory in TBA42 mice was tested by calculating spontaneous alternation rates in the X-maze. When exploring a maze, due to their natural behavior, mice have the tendency to alternate their entries into the different arms (Dudchenko 2004). These spontaneous alternations were shown to rely on the interplay of different brain regions including the hippocampus, the prefrontal cortex, the septal region and the striatum (Lalonde 2002). TBA42 mice showed a decline in working memory, since their alternation rate in the X-maze was reduced (Meißner et al. 2015). Taken together, the findings on hippocampal neurodegeneration suggest that the working memory

impairment in aged TBA42 can at least partially be attributed to the neuron loss in the CA1 region, induced by A β _{pE3}-42 expression as the two events coincided and the hippocampus plays a crucial role in this form of short term memory. However dysfunctions in other brain regions might contribute to the observed deficit.

As opposed to the cross-maze, which addresses more basic cognitive functions, the Morris water maze (MWM) is a very sensitive and well-established test, which is suitable for assessing spatial learning and spatial reference memory in rodents (Morris 1984). The MWM is a widely used experiment to test AD-like cognitive impairment in mouse models. During the testing procedure mice learn to navigate a path to a submerged platform in a pool filled with opaque water. In contrast to other cognitive tests like the cross maze test, almost all established mouse models show an impairment in the MWM. A single mutation or the Swedish double mutation in the APP gene has been shown to be sufficient to induce deficits in transgenic mice, detectable by the MWM (Westerman et al. 2002; van Dam et al. 2003). 3xTg (Billings et al. 2005), APP/PS1KI (Webster et al. 2013). 5xFAD and Tg4-42 mice show an impairment in the task as well (Bouter et al. 2014). However, reflecting the findings in humans, the time course of cognitive decline in these models correlates poorly with plaque loads (Tanila 2012).

In TBA42 mice, we found an age-dependent deficit using the MWM. Young TBA42 mice performed indistinguishably from their wildtype littermates. Aged TBA42 mice however, displayed an impairment in spatial learning, as the distance travelled, while navigating a path to the submerged platform did not decrease significantly during the five days of acquisition training. A lack of target preference in the probe trial indicated an impairment in spatial reference memory (Meißner et al. 2015). It has to be stated that the performance in the Morris water maze is partially influenced by the motor deficits seen in TBA42 mice. Aged TBA42 mice swam significantly slower during all three testing stages. However, their swimming speed was sufficient to explore the testing apparatus entirely.

Spatial learning is particularly dependent on the integrity of the hippocampal formation (D'Hooze and De Deyn, P P 2001) and damage of the hippocampus largely affects performance in the acquisition training of the MWM (Smith et al. 1991). It was demonstrated that lesions encompassing 30 - 50 % of the hippocampus lead to an impairment of spatial memory, which was aggravated by increasing the lesion size (Broadbent et al. 2004).

These findings are in good agreement with the observations made in TBA42 mice. Here, an impairment in spatial learning and spatial reference memory is accompanied by a 35 % neuronal loss in the CA1 region of the hippocampus. However, contrasting findings were pub-

lished claiming that only 20 – 40 % of the hippocampus is sufficient maintain spatial learning (Moser et al. 1995), and Tg4-42 mice that displayed a similar extent of neurodegeneration in the CA1 were not impaired in memory function (Bouter et al. 2014). In addition to the hippocampus, it has been shown that other brain regions contribute to spatial learning in rodents. Lesion studies revealed that the thalamus (Savage et al. 1997), mammillary bodies (Santin et al. 1999), the amygdala (Decker et al. 1995) and different brain stem nuclei (Compton et al. 1995; Riekkinen and Sirvio 1990) influence this particular cognitive function.

Learning has additionally been attributed to hippocampal long term potentiation (LTP) (D'Hooge and De Deyn, P P 2001). It was shown that LTP was reduced by $A\beta_{pE3-42}$ expression in TBA2.1 mice (Alexandru et al. 2011). It would be informative to investigate long term potentiation in TBA42 mice to analyze if this contributes to learning and memory deficits in this model. In summary, it can be stated that the decline in spatial learning and spatial memory in aged TBA42 mice is induced by a hippocampal neuron loss, although it is possible that neurodegeneration in other brain regions and general neuronal dysfunction contribute to the observed deficits.

4.1.6 TBA42 is a valid model of AD

Animal models of AD are an important component in studying and understanding the mechanisms of disease *in vivo*. Several transgenic mouse models have been developed, each of which resemble some clinical or neuropathological features found in AD, including plaque and neurofibrillary tangle formation, gliosis, neurodegeneration, as well as cognitive and behavioral alterations (Elder et al. 2010). For example The first AD-mouse model that showed an AD-like pathology, PDAPP was generated by the expression of a human APP transgene containing an FAD-related mutation (V717F) under the control of the platelet derived growth factor (Games et al. 1995). The model exhibits plaques, surrounded by dystrophic neurites, reactive astrocytes and activated microglia (Reilly et al. 2003; Games et al. 1995). Furthermore, the model shows learning deficits (Chen et al. 2000) and synapse loss (Dodart et al. 2000). However APP single transgenic mouse models lack a neuron loss (Elder et al. 2010). Conversely, the 5xFAD or the APP/PS1KI model, in which a neuron loss is seen, rely on the combination of multiple mutations that individually are sufficient to induce AD in humans (Oakley et al. 2006; Jawhar et al. 2012; Casas et al. 2004). In addition to these inadequacies, the named examples model the genetically predetermined familial AD (FAD). However, FAD cases represent only a minor fraction of patients. Around 99 % of all AD cases are induced by a multifac-

torial pathogenic process of unknown etiology leading to sporadic AD (SAD) (Zetterberg and Mattsson 2014). There is an urgent need to model aspects of SAD in order to understand the underlying mechanisms.

An attempt to model SAD has been made by addressing a cerebral insulin resistant state that is found in AD patients (Steen et al. 2005; Talbot et al. 2012). By intracerebroventricular administration of streptozocin some aspects of an AD-like phenotype have been induced. In non-transgenic mice injected with streptozocin that develop such a cerebral insulin resistance (Chen et al. 2013), this leads to neuroinflammation, tau-hyperphosphorylation and behavioral deficits (Salkovic-Petrisic et al. 2009; Chen et al. 2013).

The TBA42 mouse model is a member of a new group of mouse models, which do not harbor mutations in the APP, PSEN-1 or PSEN-2 sequence, seen in FAD. Instead it expresses A β directly (Wittnam et al. 2012). It can therefore be seen as a model for sporadic AD. The model was developed based on the observation that A β_{pE3-42} is a highly toxic and abundant species found in AD-brains (Portelius et al. 2010; Russo et al. 2002). In TBA42 mice direct expression of A β induces intracellular accumulation of A β_{pE3-42} in hippocampal neurons, leading to an age dependent hippocampal neurodegeneration. A reduced anxiety and more importantly a cognitive decline appear to be induced by this neuron loss. In addition, A β_{pE3-42} accumulates in spinal cord neurons, which led to motor deficits. These deficits occurred even before the onset of cognitive deficits. Although important hallmarks of AD are developed by the model, plaque deposition and neurofibrillary tangle pathology is not seen. Additionally, the direct expression of A β does not reproduce the physiological pathway of A β generation by amyloidogenic processing of APP.

Taken together, these findings underline the importance of A β_{pE3-42} in the etiology and progression of AD by demonstrating its toxicity *in vivo* and make TBA42 a valid model to study AD in mice.

4.1.7 A β_{pE3-42} as a potential drug target

It was demonstrated that A β_{pE3-42} leads to neuron loss and cognitive decline in the TBA42 mouse model (Meißner et al. 2015). Since A β_{pE3-42} is more toxic than the full-length peptide, lowering the concentration of A β_{pE3-42} seems to be a promising treatment strategy to fight AD (Perez-Garmendia and Gevorkian 2013; Bayer and Wirths 2014). Two strategies to lower cerebral A β_{pE3-42} concentrations are conceivable. Firstly, limiting the conversion from unmodified

$A\beta$ to $A\beta_{pE3-42}$ by inhibiting the responsible enzymes is possible. Secondly, passive immunization against $A\beta_{pE3-42}$ appears to be auspicious in reversing $A\beta_{pE3-42}$ toxicity.

In AD mouse models oral treatment with a glutaminyl cyclase inhibitor resulted in the reduction of the $A\beta_{pE3-42}$, and $A\beta_{x-42}$ burden (Schilling et al. 2008). A phase two clinical study of the small molecule is ongoing. Moreover, treatment with the 9D5 antibody, recognizing $A\beta_{pEx-42}$ resulted in a significantly lowered plaque load in 5xFAD mice (Wirths et al. 2010). The therapeutic antibody Solanezumab (Eli Lilly) has been reported to recognize various N-terminally truncated $A\beta$ species (Imbimbo et al. 2012). Recently, it has been shown by our group that the biosimilar of this antibody detects $A\beta_{pE3-42}$ in TBA42 mice (Bouter et al. 2015). Although Phase 3 studies have failed to show an improvement in cognition (Doody et al. 2014), a positive effect was seen in the mild AD population of the study, which showed a slower disease progression (Siemers et al. 2015). Interestingly, the newly developed NT4X antibody, preferentially binds $A\beta_{pE3-42}$ among other N-truncated $A\beta$ species in cerebral blood vessels but binds only weakly to $A\beta$ plaques (Bouter et al. 2015). We could recently show that treatment with this antibody reduced $A\beta$ deposition in 5xFAD mice and even rescued neuron loss and behavioral deficits in Tg₄₋₄₂ mice (Antonios et al. 2015).

Together these findings from preclinical studies may suggest that $A\beta_{pE3-42}$ is a potential drug target in fighting or preventing AD.

4.2 Project II: Exploring in vivo effects of impaired A β clearance induced by knock-out of brain endothelial *LRP1* in 5xFAD mice

Autosomal dominant forms of AD are induced by the overproduction of toxic A β peptides (Hardy and Higgins 1992; Hardy and Selkoe 2002). These forms of the disease are induced by mutations in the APP or PSEN genes (Bettens et al. 2013). However, only a minor fraction of the patients is affected hereby. The vast majority of AD patients suffers from the late-onset form of the disease that is associated with a reduced clearance of A β from the brain, rather than by overproduction of A β (Bates et al. 2009; Mawuenyega et al. 2010).

Pathways of A β clearance are the cleavage by proteolytically active enzymes, the cellular uptake of A β followed by its proteasomal degradation (Wang et al. 2006), interstitial fluid bulk flow (Weller et al. 2008; Hawkes et al. 2012), cerebrospinal fluid absorption into the circulatory (Pollay 2010) system and efflux via the blood brain barrier (Tarasoff-Conway et al. 2015; Deane et al. 2009; Zlokovic 2011). The latter mechanism is addressed by the neurovascular hypothesis of Alzheimer's disease proposing that impaired clearance of A β by LRP1 at the BBB induces more A β -deposition, which leads to the progression of AD (Zlokovic 2005). A β is transported from the blood into brain by RAGE and from the brain into blood by LRP1 (Donahue et al. 2006).

The neurovascular hypothesis is corroborated by several studies underlining the importance of LRP1 in the BBB clearance of A β . Firstly, LRP1 brain levels naturally decrease during ageing (Shibata et al. 2000; Silverberg et al. 2010). Additionally, LRP1 levels are further decreased in the brains of AD patients (Shibata et al. 2000; Kang et al. 2000). Secondly, LRP1 substrates were identified as components of senile plaques (Rebeck et al. 1995). Thirdly, genetic risk factors of AD have been linked to a reduced clearance of A β by LRP1. This is the case for associations of variations in the *LRP1* gene and AD (Lambert et al. 1998; Christoforidis et al. 2005). Additionally, variants in *PICALM* that encodes the phosphatidylinositol binding clathrin assembly protein, are a well-established risk factor for AD (Harold et al. 2009). The protein has been shown to drive LRP1-mediated transcytosis (Zhao et al. 2015). Interestingly, a protective *PICALM* gene variant increases PICALM expression and thereby LRP1-mediated A β clearance (Lambert et al. 2013; Zhao et al. 2015). Moreover, apoE4 limits LRP1-mediated clearance of A β via the BBB (Bell et al. 2007; Deane et al. 2008)

Various experiments have been carried out to test the role of LRP1 in A β BBB clearance. Pharmacological inhibition of LRP1 does not limit BBB transport by LRP1 selectively (Qosa et al. 2014) and attempts study the role of LRP1 in AD by knocking out *LRP1* globally have failed and resulted in embryonic lethality, since the protein is essential for embryo implantation (Herz et al. 1992; Herz et al. 1993). A conditional knockout of *LRP1* in vascular smooth muscle cells of APP/PS1 mice, however, leads to an increased A β accumulation (Kanekiyo et al. 2012). Still, there are contrasting findings on the role of LRP1 in A β clearance by transport across the blood brain barrier (Ito et al. 2010; Yamada et al. 2008). These studies, on the basis of data obtained in *in-vitro* BBB models, come to the conclusion that LRP1 does not mediate transcytosis, but endocytosis and subsequent degradation of A β (Nazer et al. 2008).

The 5xFAD/*Lrp1*_{BE}^{-/-} mouse model of AD has been developed by the group of Prof. Pietrzik to address remaining issues and test the neurovascular hypothesis. The model combines the commonly used 5xFAD model, harboring five different AD mutations (Oakley et al. 2006), and a brain endothelial specific knockout model of *LRP1*. A β levels measured by enzyme-linked immunosorbent assay were significantly increased by this knockout (Storck et al. 2016). The aim of the present work was to assess the effects of *LRP1* knockout in vivo, evaluating the consequences on hippocampal A β plaque deposition and hippocampal gliosis, and testing spatial learning and spatial reference memory of the new mouse line.

4.2.1 Plaque pathology in 5xFAD/*Lrp1*_{BE}^{-/-}

Although, not correlating well with the clinical presentation and neurodegeneration that is observed in AD (Giannakopoulos et al. 1997), A β plaques are a major neuropathological hallmark of Alzheimer's disease (Thal et al. 2002). A β plaque deposition is adequately modeled in the murine 5xFAD model, which is predominantly characterized by widely distributed, plaque bound A β that is found in mouse brains starting at the age of 2 to 3 months (Jawhar et al. 2012; Oakley et al. 2006).

To evaluate whether *LRP1* knockout, which is followed by cerebral A β retention (Storck et al. 2016), eventually leads to an increased plaque deposition, plaques were stained immunohistochemically in 5xFAD/*Lrp1*_{BE}^{n/n} and 5xFAD/*Lrp1*_{BE}^{-/-} mice. A difference in plaque loads was not obvious (Storck et al. 2016). A standardized procedure was used to quantify the area covered with A β plaques within the hippocampus. However, no increase in plaque deposition in 5xFAD/*Lrp1*_{BE}^{-/-} mice could be measured, when compared to 5xFAD/*Lrp1*_{BE}^{n/n}. This finding was in good agreement with the results of immunoprecipitation and ELISA experiments,

showing that insoluble A β deposits were only significantly elevated for A β_{x-40} but not for A β_{x-42} . In contrast, both shorter A β_{x-40} and C-terminally truncated for A β_{x-42} were significantly elevated when soluble levels were analyzed. The A β_{1-42} /A β_{1-40} ratio was elevated (Storck et al. 2016). It has to be studied yet, if 5xFAD/*Lrp1*_{BE}^{-/-} mice start to develop higher plaque loads than 5xFAD/*Lrp1*_{BE}^{fl/fl} in the course of ageing.

4.2.2 Gliosis in 5xFAD/*Lrp1*_{BE}^{-/-} mice

In addition to A β plaque deposition, neuroinflammation is a hallmark of AD (Akiyama et al. 2000). Activated astrocytes and microglia facilitate A β clearance by cellular uptake (Wyss-Coray et al. 2003; Wyss-Coray et al. 2001). In Alzheimer's disease mouse models gliosis is a commonly observed feature. In TBA42 mice, for example, gliosis is observed in close proximity to A β accumulations (Wittnam et al. 2012). In 5xFAD mice hippocampal gliosis is observed starting in 2 months old animals and further increasing in older animals (Girard et al. 2014; Oakley et al. 2006).

In both, 5xFAD/*Lrp1*_{BE}^{-/-} and 5xFAD/*Lrp1*_{BE}^{fl/fl} mice a marked gliosis was observed (Storck et al. 2016). However, no quantitative difference in the amount of astrocytes and microglia, as measured by the area covered by GFAP and Iba1 immunoreactivity was found. It is known that gliosis in 5xFAD mice is proportional to plaque deposition. Additionally, the pattern of gliosis follows plaque distribution and reactive astrocytes surround A β plaques in this model (Oakley et al. 2006). Thus, the findings on unaltered gliosis in 5xFAD/*Lrp1*_{BE}^{-/-} are in good agreement with the findings on A β plaque deposition which was similarly unaffected.

4.2.3 Cognitive decline in 5xFAD/*Lrp1*_{BE}^{-/-} mice

To test the behavioral effects of increased accumulation of soluble A β in 5xFAD/*Lrp1*_{BE}^{-/-} mice, animals were subjected to the Morris water maze, testing spatial learning and spatial reference memory. Cognitive deficits have previously been reported for 5xFAD mice. At the age of 12 months mice have been reported to display a deficit in spatial learning and spatial reference memory (Bouter et al. 2014). Deficits in spatial working memory tested in the cross maze paradigm were reported to occur already in 6 months old animals (Jawhar et al. 2012).

In the present study we showed that 5xFAD/*Lrp1*_{BE}^{-/-} mice display a reduction in spatial learning when the acquisition training was analyzed. Compared to the control groups mice displayed significantly higher escape latencies. More obviously, spatial reference memory of

5xFAD/*Lrp1*_{BE}^{-/-} mice was impaired indicated by the absence of target preference in the probe trial of the MWM. The observed deficits cannot be separately explained by either the 5xFAD mutations or the knockout of *LRP1* in the cerebrovasculature, since 5xFAD/*Lrp1*^{BEfl/fl} and *Lrp1*_{BE}^{-/-} performed equally to, or only slightly poorer than wildtype animals. Instead, the two genetic modifications induced the deficits when they were combined. Thus inducible knockout of *LRP1* in the brain endothelium, resulting in increased cerebral A β accumulation (Storck et al. 2016), shifted the onset of cognitive decline in 5xFAD mice to an earlier point in time.

It is known that the concentrations of soluble A β species, rather than the amount of A β plaques is correlated to the extent of cognitive decline in animal models (Dodart et al. 2002) and in AD-patients (McDonald, Jessica M et al. 2010; McLean et al. 1999). A similar correlation was seen in the 5xFAD/*Lrp1*_{BE}^{-/-} mouse model. Concentrations of soluble A species are and the ratio of A β ₁₋₄₂/A β ₁₋₄₀ were elevated (Storck et al. 2016), which led to severe cognitive deficits, while the plaque load was unaltered, supporting the idea of the greater importance of soluble A β oligomers in AD-pathogenesis. For further investigations of the model it would be informative to test older animals. This way it could be analyzed whether longer-lasting disruption of BBB A β clearance by *LRP1* knockout leads to an increased divergence in the cognitive performance between 5xFAD/*Lrp1*_{BE}^{-/-} and control mice. In summary, the data collected in this work in combination with biochemical data on the function of LRP1 (Storck et al. 2016) highlight the significance of LRP1 in the clearance of A β across the BBB. Restoring and facilitating BBB clearance of A β is a promising approach for future treatments and prevention strategies of AD.

4.2.4 Restoring BBB clearance as a potential treatment and prevention of AD

Since the clearance of A β via the BBB is decreased in AD (Mawuenyega et al. 2010), restoring this function seems to be a promising approach in treating or even preventing AD (Ramanathan et al. 2015). In APP/PS1 mice an extract of the root of *Withania somnifera* induced an increased expression of LRP1 in microvessels of the brain and in the liver. The earlier increase of liver LRP1 is accompanied by the reversion of cerebral A β accumulation and behavioral deficits in the mice (Sehgal et al. 2012). The olive-oil derived oleocanthal also induced the expression of LRP1 in mice brain endothelial cells. This led to an increased clearance rate of radiolabeled A β , which was injected into the brains of wildtype mice (Abuznait et al. 2013).

In addition to classical active substances, gene therapy might be a possible strategy for addressing cerebrovascular LRP1 deficiency that is found in AD. Using Adeno-associated viral vectors the delivery of transgenic DNA to different components of the central nervous system can be achieved (Davidson et al. 2000). Especially brain endothelial cells could easily be targeted since they are directly accessible from the blood for adeno-associated viral vectors when applied intravenously (Chen et al. 2009; Varadi et al. 2012). Given that brain-endothelial LRP1 transports major amounts of A β across the blood brain barrier (Storck et al. 2016), gene therapy appears to be a promising approach. The newly developed 5xFAD/*Lrp1*_{BE}^{-/-} could serve as a valuable tool for testing this gene therapeutic approach in an AD mouse model.

5 Summary

According to the influential amyloid cascade hypothesis cerebral accumulation of A β is the key event in the pathogenesis of Alzheimer's disease. A β deposits occur as soluble forms, as well as insoluble forms. It is assumed that soluble and intraneuronal A β predominantly promotes development and progression of the disease. There is a large variety of A β species that differ in lengths and the presence of posttranscriptional modifications. The pyroglutamated and truncated isoform A $\beta_{\text{pE3-42}}$ is an especially toxic variant of the peptide. It was the aim of the present work to extend the knowledge on the role of A β in the development of the disease. For this purpose, two transgenic mouse models that address different aspects of the disorder, were characterized by analyzing age neuropathological and behavioral features.

In the first part of the thesis, an AD-like phenotype is demonstrated in the murine transgenic TBA42 model, which does not harbor mutated transgenes that are involved in A β generation by processing of its precursor protein. It is shown that direct expression of A $\beta_{\text{pE3-42}}$ in TBA42 mice leads to an age-dependent neurodegeneration in the hippocampal CA1 region of the hippocampus, which is intimately involved in cognition. This leads to a decline in memory function and altered anxiety levels. Moreover, accumulation of A $\beta_{\text{pE3-42}}$ induces a severe motor deficit, which even precedes the cognitive decline. Thus the toxicity of A $\beta_{\text{pE3-42}}$ is demonstrated *in vivo*. Taken together, these findings underline the importance of A $\beta_{\text{pE3-42}}$ in the etiology and progression of AD and make TBA42 a valid model to study mechanisms of AD progression and potential therapeutic strategies in mice.

The majority of AD cases occur sporadically and no overproduction of A β is found in these cases. In contrast, sporadic AD is characterized by the impairment of various mechanisms of A β clearance. Transport of A β across the blood brain is one important mechanism. According to the neurovascular hypothesis of AD an impaired blood brain barrier clearance by LRP1 leads to the retention of A β in the brain, resulting in a higher rate of A β deposition. In the second part, using the 5xFAD/*Lrp1*_{BE}^{-/-} model, in which soluble A β species are retained in the brain, the effect of a brain endothelial knockout of *LRP1* on cognition in an established AD mouse model is demonstrated. While the plaque load and gliosis is unaltered by the knockout, the onset of cognitive impairments is shifted to a younger age in 5xFAD/*Lrp1*_{BE}^{-/-} mice. Taken together these findings confirm the neurovascular hypothesis of AD, by highlighting the importance of LRP1-mediated blood brain barrier clearance of A β . 5xFAD/*Lrp1*_{BE}^{-/-} mice

could be used to test therapeutic approaches, which try to restore the impaired clearance of A β across the blood brain barrier.

In summary, both the TBA42 and the 5xFAD/*Lpl*_{BE}^{-/-} mouse model are valid AD models addressing features of sporadic AD.

6 Literature

- Abuznait AH, Qosa H, Busnena BA, El Sayed, Khalid A, Kaddoumi A (2013): Olive-oil-derived oleocanthal enhances beta-amyloid clearance as a potential neuroprotective mechanism against Alzheimer's disease: in vitro and in vivo studies. *ACS Chem Neurosci* 4, 973–982
- Akiyama H, Barger S, Barnum S, Bradt B, Bauer J, Cole GM, Cooper NR, Eikelenboom P, Emmerling M, Fiebich BL (2000): Inflammation and Alzheimer's disease. *Neurobiol Aging* 21, 383–421
- Albert MS, DeKosky ST, Dickson D, Dubois B, Feldman HH, Fox NC, Gamst A, Holtzman DM, Jagust WJ, Petersen RC (2011): The diagnosis of mild cognitive impairment due to Alzheimer's disease: recommendations from the National Institute on Aging-Alzheimer's Association workgroups on diagnostic guidelines for Alzheimer's disease. *Alzheimers Dement* 7, 270–279
- Alexandru A, Jagla W, Graubner S, Becker A, Bäuscher C, Kohlmann S, Sedlmeier R, Raber KA, Cynis H, Röncke R (2011): Selective Hippocampal neurodegeneration in transgenic mice expressing small amounts of truncated A β is induced by pyroglutamate-A β formation. *J Neurosci* 31, 12790–12801
- Allinson TMJ, Parkin ET, Turner AJ, Hooper NM (2003): ADAMs family members as amyloid precursor protein α -secretases. *J Neurosci Res* 74, 342–352
- Alzheimer A (1907): Über eine eigenartige Erkrankung der Hirnrinde. *Allgemeine Zeitschrift für Psychiatrie und psychisch-gerichtliche Medizin*. Band 64, 146–148
- Alzheimer A, Stelzmann RA, Schnitzlein HN, Murtagh FR (1995): An English translation of Alzheimer's 1907 paper, "Über eine eigenartige Erkrankung der Hirnrinde". *Clin Anat* 8, 429–431
- Andreasson U, Portelius E, Andersson ME, Blennow K, Zetterberg H (2007): Aspects of beta-amyloid as a biomarker for Alzheimer's disease. *Biomark Med* 1, 59–78
- Antonios G, Borgers H, Richard BC, Brauß A, Meißner J, Weggen S, Pena V, Pillot T, Davies SL, Bakrania P (2015): Alzheimer therapy with an antibody against N-terminal Abeta 4-X and pyroglutamate Abeta 3-X. *Sci Rep* 5, 17338
- Aprahamian I, Martinelli JE, Neri AL, Yassuda MS (2010): The accuracy of the Clock Drawing Test compared to that of standard screening tests for Alzheimer's disease: results from a study of Brazilian elderly with heterogeneous educational backgrounds. *Int Psychogeriatr* 22, 64–71
- Arai H, Ishiguro K, Ohno H, Moriyama M, Itoh N, Okamura N, Matsui T, Morikawa Y, Horikawa E, Kohno H et al. (2000): CSF phosphorylated tau protein and mild cognitive impairment: a prospective study. *Exp Neurol* 166, 201–203
- Baddeley AD, Bressi S, Della Sala S, Logie R, Spinnler H (1991): The decline of working memory in Alzheimer's disease. *Brain* 114, 2521–2542
- Bahar-Fuchs A, Clare L, Woods B (2013): Cognitive training and cognitive rehabilitation for mild to moderate Alzheimer's disease and vascular dementia. *Cochrane Database Syst Rev* 6, CD003260
- Bates KA, Verdile G, Li QX, Ames D, Hudson P, Masters CL, Martins RN (2009): Clearance mechanisms of Alzheimer's amyloid- β peptide: implications for therapeutic design and diagnostic tests. *Mol Psychiatry* 14, 469–486
- Bayer TA, Wirths O (2014): Focusing the amyloid cascade hypothesis on N-truncated Abeta peptides as drug targets against Alzheimer's disease. *Acta Neuropathol* 127, 787–801

- Bell RD, Sagare AP, Friedman AE, Bedi GS, Holtzman DM, Deane R, Zlokovic BV (2007): Transport pathways for clearance of human Alzheimer's amyloid β -peptide and apolipoproteins E and J in the mouse central nervous system. *J Cereb Blood Flow Metab* 27, 909–918
- Benilova I, Karran E, De Strooper B (2012): The toxic A β oligomer and Alzheimer's disease: an emperor in need of clothes. *Nat Neurosci* 15, 349–357
- Bentahir M, Nyabi O, Verhamme J, Tolia A, Horré K, Wiltfang J, Esselmann H, De Strooper B (2006): Presenilin clinical mutations can affect γ -secretase activity by different mechanisms. *J Neurochem* 96, 732–742
- Bettens K, Sleegers K, van Broeckhoven C (2013): Genetic insights in Alzheimer's disease. *Lancet Neurol* 12, 92–104
- Billings LM, Oddo S, Green KN, McGaugh JL, LaFerla FM (2005): Intraneuronal A β causes the onset of early Alzheimer's disease-related cognitive deficits in transgenic mice. *Neuron* 45, 675–688
- Birks J (2006): Cholinesterase inhibitors for Alzheimer's disease. *Cochrane Database Syst Rev*, CD005593
- Blazina L, MA LT, Rubin E (1995): The behavior rating scale for dementia of the Consortium to Establish a Registry for Alzheimer's Disease. *Am J psychiatry* 152, 1349–1357
- Blennow K, Hampel H (2003): CSF markers for incipient Alzheimer's disease. *Lancet Neurol* 2, 605–613
- Blennow K, Leon MJ de, Zetterberg H (2006): Alzheimer's disease. *Lancet* 368, 387–403
- Boucher P, Herz J (2011): Signaling through LRP1: Protection from atherosclerosis and beyond. *Biochem Pharmacol* 81, 1–5
- Bouter Y, Dietrich K, Wittnam JL, Rezaei-Ghaleh N, Pillot T, Papot-Couturier S, Lefebvre T, Sprenger F, Wirths O, Zweckstetter M (2013): N-truncated amyloid β (A β) 4–42 forms stable aggregates and induces acute and long-lasting behavioral deficits. *Acta Neuropathol* 126, 189–205
- Bouter Y, Kacprowski T, Weissmann R, Dietrich K, Borgers H, Brauß A, Sperling C, Wirths O, Albrecht M, Jensen LR (2014): Deciphering the molecular profile of plaques, memory decline and neuron loss in two mouse models for Alzheimer's disease by deep sequencing. *Front Aging Neurosci* 6, 75
- Bouter Y, Noguerola, JSL, Tucholla P, Crespi, Gabriela A N, Parker MW, Wiltfang J, Miles LA, Bayer TA (2015): Abeta targets of the biosimilar antibodies of Bapineuzumab, Crenezumab, Solanezumab in comparison to an antibody against N-truncated Abeta in sporadic Alzheimer disease cases and mouse models. *Acta Neuropathol*
- Braak H, Braak E (1991): Neuropathological staging of Alzheimer-related changes. *Acta Neuropathol* 82, 239–259
- Breyhan H, Wirths O, Duan K, Marcello A, Rettig J, Bayer TA (2009): APP/PS1KI bigenic mice develop early synaptic deficits and hippocampus atrophy. *Acta Neuropathol* 117, 677–685
- Broadbent NJ, Squire LR, Clark RE (2004): Spatial memory, recognition memory, and the hippocampus. *Proc Natl Acad Sci U S A* 101, 14515–14520
- Cabrejo L, Guyant-Maréchal L, Laquerrière A, Vercelletto M, De La Fournière, François, Thomas-Antérion C, Verny C, Letournel F, Pasquier F, Vital A (2006): Phenotype associated with APP duplication in five families. *Brain* 129, 2966–2976

- Carrière I, Fourrier-Reglat A, Dartigues J, Rouaud O, Pasquier F, Ritchie K, Ancelin M (2009): Drugs with anticholinergic properties, cognitive decline, and dementia in an elderly general population: the 3-city study. *Arch Intern Med* 169, 1317–1324
- Casas C, Sergeant N, Itier J, Blanchard V, Wirths O, van der Kolk, Nicolien, Vingtdoux V, van de Steeg, Evita, Ret G, Canton T et al. (2004): Massive CA1/2 neuronal loss with intraneuronal and N-terminal truncated A β 42 accumulation in a novel Alzheimer transgenic model. *Am J Pathol* 165, 1289–1300
- Chen G, Chen KS, Knox J, Inglis J, Bernard A, Martin SJ, Justice A, McConlogue L, Games D, Freedman SB (2000): A learning deficit related to age and β -amyloid plaques in a mouse model of Alzheimer's disease. *Nature* 408, 975–979
- Chen Y, Liang Z, Blanchard J, Dai C, Sun S, Lee MH, Grundke-Iqbal I, Iqbal K, Liu F, Gong C (2013): A non-transgenic mouse model (icv-STZ mouse) of Alzheimer's disease: similarities to and differences from the transgenic model (3xTg-AD mouse). *Mol Neurobiol* 47, 711–725
- Chen YH, Chang M, Davidson BL (2009): Molecular signatures of disease brain endothelia provide new sites for CNS-directed enzyme therapy. *Nat Med* 15, 1215–1218
- Christensen DZ, Kraus SL, Flohr A, Cotel M, Wirths O, Bayer TA (2008): Transient intraneuronal A β rather than extracellular plaque pathology correlates with neuron loss in the frontal cortex of APP/PS1KI mice. *Acta Neuropathol* 116, 647–655
- Christensen DZ, Bayer TA, Wirths O (2010): Intracellular A β triggers neuron loss in the cholinergic system of the APP/PS1KI mouse model of Alzheimer's disease. *Neurobiol Aging* 31, 1153–1163
- Christoforidis M, Schober R, Krohn K (2005): Genetic-morphologic association study: association between the low density lipoprotein-receptor related protein (LRP) and cerebral amyloid angiopathy. *Neuropathol Appl Neurobiol* 31, 11–19
- Chui DH, Dobo E, Makifuchi T, Akiyama H, Kawakatsu S, Petit A, Checler F, Araki W, Takahashi K, Tabira T (2001): Apoptotic neurons in Alzheimer's disease frequently show intracellular Abeta42 labeling. *J Alzheimers Dis* 3, 231–239
- Clarke DE, van Reekum R, Simard M, Streiner DL, Freedman M, Conn D (2007): Apathy in dementia: an examination of the psychometric properties of the apathy evaluation scale. *J Neuropsychiatry Clin Neurosci* 19, 57–64
- Cohen-Mansfield J (1997): Conceptualization of agitation: results based on the Cohen-Mansfield agitation inventory and the agitation behavior mapping instrument. *Int Psychogeriatr* 8, 309–315
- Colloby SJ, Perry EK, Pakrasi S, Pimlott SL, Wyper DJ, McKeith IG, Williams ED, O'Brien JT (2010): Nicotinic 123 I-5IA-85380 single photon emission computed tomography as a predictor of cognitive progression in alzheimer's disease and dementia with lewy Bodies. *Am J Geriatr Psychiatry* 18, 86–90
- Compton DM, Dietrich KL, Smith JS, Davis BK (1995): Spatial and non-spatial learning in the rat following lesions to the nucleus locus coeruleus. *Neuroreport* 7, 177–182
- Corder EH, Am Saunders, Strittmatter WJ, Schmechel DE, Gaskell PC, Small G, Roses AD, Haines JL, Pericak-Vance MA (1993): Gene dose of apolipoprotein E type 4 allele and the risk of Alzheimer's disease in late onset families. *Science* 261, 921–923
- Coulson EJ, Barrett GL, Storey E, Bartlett PF, Beyreuther K, Masters CL (1997): Down-regulation of the amyloid protein precursor of Alzheimer's disease by antisense oligonucleotides reduces neuronal adhesion to specific substrata. *Brain Res* 770, 72–80

- Cummins PM, O'Connor B (1998): Pyroglutamyl peptidase: an overview of the three known enzymatic forms. *Biochim Biophys Acta* 1429, 1–17
- Cynis H, Schilling S, Bodnar M, Hoffmann T, Heiser U, Saido TC, Demuth H (2006): Inhibition of glutaminyl cyclase alters pyroglutamate formation in mammalian cells. *Biochim Biophys Acta* 1764, 1618–1625
- Cynis H, Rahfeld J, Stephan A, Kehlen A, Koch B, Wermann M, Demuth H, Schilling S (2008a): Isolation of an isoenzyme of human glutaminyl cyclase: retention in the Golgi complex suggests involvement in the protein maturation machinery. *J Mol Biol* 379, 966–980
- Cynis H, Scheel E, Saido TC, Schilling S, Demuth H (2008b): Amyloidogenic Processing of Amyloid Precursor Protein: Evidence of a Pivotal Role of Glutaminyl Cyclase in Generation of Pyroglutamate-Modified Amyloid- β . *Biochemistry* 47, 7405–7413
- Dammers C, Gremer L, Reiss K, Klein AN, Neudecker P, Hartmann R, Sun N, Demuth H, Schwarten M, Willbold D (2015): Structural Analysis and Aggregation Propensity of Pyroglutamate A β (3–40) in Aqueous Trifluoroethanol. *PloS one* 10, e0143647
- Davidson BL, Stein CS, Heth JA, Martins I, Kotin RM, Derksen TA, Zabner J, Ghodsi A, Chiorini JA (2000): Recombinant adeno-associated virus type 2, 4, and 5 vectors: transduction of variant cell types and regions in the mammalian central nervous system. *Proc Natl Acad Sci U S A* 97, 3428–3432
- De Felice, Fernanda G, Wu D, Lambert MP, Fernandez SJ, Velasco PT, Lacor PN, Bigio EH, Jerecic J, Acton PJ, Shughrue PJ (2008): Alzheimer's disease-type neuronal tau hyperphosphorylation induced by A β oligomers. *Neurobiol Aging* 29, 1334–1347
- Deane R, Sagare A, Hamm K, Parisi M, Lane S, Finn MB, Holtzman DM, Zlokovic BV (2008): apoE isoform-specific disruption of amyloid beta peptide clearance from mouse brain. *J Clin Invest* 118, 4002–4013
- Deane R, Bell RD, Sagare A, Zlokovic BV (2009): Clearance of amyloid- β peptide across the blood-brain barrier: implication for therapies in Alzheimer's disease. *CNS Neurol Disord Drug Targets* 8, 16
- Decker MW, Curzon P, Brioni JD (1995): Influence of separate and combined septal and amygdala lesions on memory, acoustic startle, anxiety, and locomotor activity in rats. *Neurobiol Learn Mem* 64, 156–168
- Demuro A, Parker I, Stutzmann GE (2010): Calcium signaling and amyloid toxicity in Alzheimer disease. *J Biol Chem* 285, 12463–12468
- De Strooper B, Saftig P, Craessaerts K, Vanderstichele H, Guhde G, Annaert W, Figura K von, van Leuven F (1998): Deficiency of presenilin-1 inhibits the normal cleavage of amyloid precursor protein. *Nature* 391, 387–390
- DGN (2009): DGN Leitlinie Demenzen. Bonn: Deutsche Gesellschaft für Psychiatrie Psychotherapie und Nervenheilkunde (DGPPN), Deutsche Gesellschaft für Neurologie (DGN) <http://www.dgn.org/leitlinien/11-leitlinien-der-dgn/2341-II-15-2012-diagnose-und-therapie-von-demenzen>; Zugriff am 01.08.2015
- D'Hooze R, De Deyn, P P (2001): Applications of the Morris water maze in the study of learning and memory. *Brain Res Brain Res Rev* 36, 60–90
- Di Fede G, Catania M, Morbin M, Rossi G, Suardi S, Mazzoleni G, Merlin M, Giovagnoli AR, Prioni S, Erbetta A (2009): A recessive mutation in the APP gene with dominant-negative effect on amyloidogenesis. *Science* 323, 1473–1477

- Dieckmann M, Dietrich MF, Herz J (2010): Lipoprotein receptors-an evolutionarily ancient multifunctional receptor family. *Biol Chem* 391, 1341–1363
- Dietrich K: Impact of N-terminally truncated A β 4-42 on memory and synaptic plasticity-Tg4-42 a new mouse model of Alzheimer's disease. *Naturwiss. Diss. Göttingen* 2015
- Dineley KT, Westerman M, Bui D, Bell K, Ashe KH, Sweatt JD (2001): β -Amyloid activates the mitogen-activated protein kinase cascade via hippocampal $\alpha 7$ nicotinic acetylcholine receptors: in vitro and in vivo mechanisms related to Alzheimer's disease. *J Neurosci* 21, 4125–4133
- Dodart J, Mathis C, Saura J, Bales KR, Paul SM, Ungerer A (2000): Neuroanatomical abnormalities in behaviorally characterized APP V717F transgenic mice. *Neurobiol Dis* 7, 71–85
- Dodart J, Bales KR, Gannon KS, Greene SJ, DeMattos RB, Mathis C, DeLong CA, Wu S, Wu X, Holtzman DM (2002): Immunization reverses memory deficits without reducing brain Abeta burden in Alzheimer's disease model. *Nat Neurosci* 5, 452–457
- Donahue JE, Flaherty SL, Johanson CE, Duncan III, John A, Silverberg GD, Miller MC, Tavares R, Yang W, Wu Q, Sabo E (2006): RAGE, LRP-1, and amyloid-beta protein in Alzheimer's disease. *Acta Neuropathol* 112, 405–415
- Dong J, Atwood CS, Anderson VE, Siedlak SL, Smith MA, Perry G, Carey PR (2003): Metal binding and oxidation of amyloid- β within isolated senile plaque cores: Raman microscopic evidence. *Biochemistry* 42, 2768–2773
- Doody RS, Thomas RG, Farlow M, Iwatsubo T, Vellas B, Joffe S, Kieburtz K, Raman R, Sun X, Aisen PS (2014): Phase 3 trials of solanezumab for mild-to-moderate Alzheimer's disease. *N Engl J Med* 370, 311–321
- Dudchenko PA (2004): An overview of the tasks used to test working memory in rodents. *Neurosci Biobehav Rev* 28, 699–709
- Edbauer D, Winkler E, Haass C, Steiner H (2002): Presenilin and nicastrin regulate each other and determine amyloid β -peptide production via complex formation. *Proc Natl Acad Sci U S A* 99, 8666–8671
- Edison P, Archer HA, Gerhard A, Hinz R, Pavese N, Turkheimer FE, Hammers A, Tai YF, Fox N, Kennedy A (2008): Microglia, amyloid, and cognition in Alzheimer's disease: An [11C](R) PK11195-PET and [11C] PIB-PET study. *Neurobiol Dis* 32, 412–419
- Eimer WA, Vassar R (2013): Neuron loss in the 5XFAD mouse model of Alzheimer's disease correlates with intraneuronal Abeta42 accumulation and Caspase-3 activation. *Mol Neurodegener* 8
- Elder GA, Gama Sosa, Miguel A, Gasperi R de (2010): Transgenic mouse models of Alzheimer's disease. *Mt Sinai J Med* 77, 69–81
- Ellis RJ, Olichney JM, Thal LJ, Mirra SS, Morris JC, Beekly D, Heyman A (1996): Cerebral amyloid angiopathy in the brains of patients with Alzheimer's disease: the CERAD experience, Part XV. *Neurology* 46, 1592–1596
- Ewers M, Morgan DG, Gordon MN, Woodruff-Pak DS (2006): Associative and motor learning in 12-month-old transgenic APP+ PS1 mice. *Neurobiol Aging* 27, 1118–1128
- Fändrich M (2012): Oligomeric intermediates in amyloid formation: structure determination and mechanisms of toxicity. *J Mol Biol* 421, 427–440
- Farrer LA, Cupples LA, Haines JL, Hyman B, Kukull WA, Mayeux R, Myers RH, Pericak-Vance MA, Risch N, van Duijn CM (1997): Effects of age, sex, and ethnicity on the association between apolipoprotein E genotype and Alzheimer disease: a meta-analysis. *Jama* 278, 1349–1356

- Faure A, Verret L, Bozon B, El Tayara, N El Tannir, Ly M, Kober F, Dhenain M, Rampon C, Delatour B (2011): Impaired neurogenesis, neuronal loss, and brain functional deficits in the APPxPS1-Ki mouse model of Alzheimer's disease. *Neurobiol Aging* **32**, 407–418
- Ferri CP, Prince M, Brayne C, Brodaty H, Fratiglioni L, Ganguli M, Hall K, Hasegawa K, Hendrie H, Huang Y (2006): Global prevalence of dementia: a Delphi consensus study. *Lancet* **366**, 2112–2117
- Folstein MF, Folstein SE, McHugh PR (1975): "Mini-mental state": a practical method for grading the cognitive state of patients for the clinician. *J Psychiatr Res* **12**, 189–198
- Francis R, McGrath G, Zhang J, Ruddy DA, Sym M, Apfeld J, Nicoll M, Maxwell M, Hai B, Ellis MC (2002): aph-1 and pen-2 are required for Notch pathway signaling, γ -secretase cleavage of β APP, and presenilin protein accumulation. *Dev Cell* **3**, 85–97
- Frisoni GB, Bocchetta M, Ch  telat G, Rabinovici GD, de Leon, Mony J, Kaye J, Reiman EM, Scheltens P, Barkhof F, Black SE et al. (2013): Imaging markers for Alzheimer disease Which vs how. *Neurology* **81**, 487–500
- Furukawa K, Sopher BL, Rydel RE, Begley JG, Pham DG, Martin GM, Fox M, Mattson MP (1996): Increased Activity-Regulating and Neuroprotective Efficacy of α -Secretase-Derived Secreted Amyloid Precursor Protein Conferred by a C-Terminal Heparin-Binding Domain. *J Neurochem* **67**, 1882–1896
- Games D, Adams D, Alessandrini R, Barbour R, Berthelette P, Blackwell C, Carr T, Clemens J, Donaldson T, Gillespie F (1995): Alzheimer-type neuropathology in transgenic mice overexpressing V717F beta-amyloid precursor protein. *Nature* **373**, 523–527
- Genin E, Hannequin D, Wallon D, Slegers K, Hiltunen M, Combarros O, Bullido MJ, Engelborghs S, Deyn P de, Berr C (2011): APOE and Alzheimer disease: a major gene with semi-dominant inheritance. *Mol Psychiatry* **16**, 903–907
- Genius J, Klafki H, Benninghoff J, Esselmann H, Wiltfang J (2012): Current application of neurochemical biomarkers in the prediction and differential diagnosis of Alzheimer's disease and other neurodegenerative dementias. *Eur Arch Psychiatry Clin Neurosci* **262**, 71–77
- Giannakopoulos P, Hof PR, Michel J, Guimon J, Bouras C (1997): Cerebral cortex pathology in aging and Alzheimer's disease: a quantitative survey of large hospital-based geriatric and psychiatric cohorts. *Brain Res Brain Res Rev* **25**, 217–245
- Girard SD, Jacquet M, Baranger K, Migliorati M, Escoffier G, Bernard A, Khrestchatisky M, Feron F, Rivera S, Roman FS (2014): Onset of hippocampus-dependent memory impairments in 5XFAD transgenic mouse model of Alzheimer's disease. *Hippocampus* **24**, 762–772
- Gouras GK, Tsai J, Naslund J, Vincent B, Edgar M, Checler F, Greenfield JP, Haroutunian V, Buxbaum JD, Xu H et al. (2000): Intraneuronal A β 42 accumulation in human brain. *Am J Pathol* **156**, 15–20
- Goutte C, Tsunozaki M, Hale VA, Priess JR (2002): APH-1 is a multipass membrane protein essential for the Notch signaling pathway in *Caenorhabditis elegans* embryos. *Proc Natl Acad Sci U S A* **99**, 775–779
- Greenfield JP, Tsai J, Gouras GK, Hai B, Thinakaran G, Checler F, Sisodia SS, Greengard P, Xu H (1999): Endoplasmic reticulum and trans-Golgi network generate distinct populations of Alzheimer β -amyloid peptides. *Proc Natl Acad Sci U S A* **96**, 742–747
- Gunn AP, Wong BX, Johanssen T, Griffith JC, Masters CL, Bush AI, Barnham KJ, Duce JA, Cherny RA (2015): Amyloid-Beta Peptide A β 3pE-42 Induces Lipid Peroxidation, Membrane Permeabilization and Calcium-Influx in Neurons. *J Biol Chem* 10.1074/jbc.M115.655183

- Gupta R, Sen N (2016): Traumatic brain injury: a risk factor for neurodegenerative diseases. *Rev Neurosci* 27, 93–100
- Haass C, Selkoe DJ (2007): Soluble protein oligomers in neurodegeneration: lessons from the Alzheimer's amyloid β -peptide. *Nat Rev Mol Cell Biol* 8, 101–112
- Haass C, Schlossmacher MG, Hung AY, Vigo-Pelfrey C, Mellon A, Ostaszewski BL, Lieberburg I, Koo EH, Schenk D, Teplow DB (1992): Amyloid β -peptide is produced by cultured cells during normal metabolism. *Nature* 359, 322–325
- Hampel H, Broich K, Hoessler Y, Pantel J (2009): Biological markers for early detection and pharmacological treatment of Alzheimer's disease. *Dialogues Clin Neurosci* 11, 141
- Hampel H, Frank R, Broich K, Teipel SJ, Katz RG, Hardy J, Herholz K, Bokde ALW, Jessen F, Hoessler YC (2010): Biomarkers for Alzheimer's disease: academic, industry and regulatory perspectives. *Nat Rev Drug Discov* 9, 560–574
- Hampel H, Wilcock G, Andrieu S, Aisen P, Blennow K, Broich K, Carrillo M, Fox NC, Frisoni GB, Isaac M (2011): Biomarkers for Alzheimer's disease therapeutic trials. *Prog Neurobiol* 95, 579–593
- Hardy JA, Higgins GA (1992): Alzheimer's disease: the amyloid cascade hypothesis. *Science* 256, 184
- Hardy J, Selkoe DJ (2002): The amyloid hypothesis of Alzheimer's disease: progress and problems on the road to therapeutics. *Science* 297, 353–356
- Harigaya Y, Saido TC, Eckman CB, Prada CM, Shoji M, Younkin SG (2000): Amyloid beta protein starting pyroglutamate at position 3 is a major component of the amyloid deposits in the Alzheimer's disease brain. *Biochem Biophys Res Com* 276, 422–427
- Harold D, Abraham R, Hollingworth P, Sims R, Gerrish A, Hamshere ML, Pahwa JS, Moskvina V, Dowzell K, Williams A (2009): Genome-wide association study identifies variants at CLU and PICALM associated with Alzheimer's disease. *Nat Genet* 41, 1088–1093
- Haupt C, Leppert J, Röncke R, Meinhardt J, Yadav JK, Ramachandran R, Ohlenschläger O, Reymann KG, Görlach M, Fändrich M (2012): Structural Basis of β -Amyloid-Dependent Synaptic Dysfunctions. *Angew Chem Int Ed Engl* 124, 1608–1611
- Hawkes CA, Sullivan PM, Hands S, Weller RO, Nicoll, James A R, Carare RO (2012): Disruption of arterial perivascular drainage of amyloid-beta from the brains of mice expressing the human APOE epsilon4 allele. *PloS one* 7, e41636
- Herz J, Clouthier DE, Hammer RE (1992): LDL receptor-related protein internalizes and degrades uPA-PAI-1 complexes and is essential for embryo implantation. *Cell* 71, 411–421
- Herz J, Clouthier DE, Hammer RE (1993): Correction: LDL receptor-related protein internalizes and degrades uPA-PAI-1 complexes and is essential for embryo implantation. *Cell* 73, 428
- Holtzman DM, Bales KR, Tenkova T, Fagan AM, Parsadanian M, Sartorius LJ, Mackey B, Olney J, McKeel D, Wozniak D (2000): Apolipoprotein E isoform-dependent amyloid deposition and neuritic degeneration in a mouse model of Alzheimer's disease. *Proc Natl Acad Sci U S A* 97, 2892–2897
- Holtzman DM, Morris JC, Goate AM (2011): Alzheimer's disease: the challenge of the second century. *Sci Transl Med* 3, 77sr1
- Hu Y, He S, Wang X, Duan Q, Khatoon S, Iqbal K, Grundke-Iqbal I, Wang J (2002): Elevated levels of phosphorylated neurofilament proteins in cerebrospinal fluid of Alzheimer disease patients. *Neurosci Lett* 320, 156–160

- Huang K, Liu Y, Cheng W, Ko T, Wang AH (2005): Crystal structures of human glutaminyl cyclase, an enzyme responsible for protein N-terminal pyroglutamate formation. *Proc Natl Acad Sci U S A* 102, 13117–13122
- Hung AY, Koo EH, Haass C, Selkoe DJ (1992): Increased expression of beta-amyloid precursor protein during neuronal differentiation is not accompanied by secretory cleavage. *Proc Natl Acad Sci U S A* 89, 9439–9443
- Hutton M, Lendon CL, Rizzu P, Baker M, Froelich S, Houlden H, Pickering-Brown S, Chakraverty S, Isaacs A, Grover A (1998): Association of missense and 5'-splice-site mutations in tau with the inherited dementia FTDP-17. *Nature* 393, 702–705
- Imbimbo BP, Ottonello S, Frisardi V, Solfrizzi V, Greco A, Seripa D, Pilotto A, Panza F (2012): Solanezumab for the treatment of mild-to-moderate Alzheimer's disease. *Expert Rev Clin Immunol* 8, 135–149
- Ito S, Ueno T, Ohtsuki S, Terasaki T (2010): Lack of brain-to-blood efflux transport activity of low-density lipoprotein receptor-related protein-1 (LRP-1) for amyloid- β peptide (1-40) in mouse: involvement of an LRP-1-independent pathway. *J Neurochem* 113, 1356–1363
- Iwatsubo T, Odaka A, Suzuki N, Mizusawa H, Nukina N, Ihara Y (1994): Visualization of A β 42 (43) and A β 40 in senile plaques with end-specific A β monoclonals: evidence that an initially deposited species is A β 42 (43). *Neuron* 13, 45–53
- Jack CR, Knopman DS, Jagust WJ, Petersen RC, Weiner MW, Aisen PS, Shaw LM, Vemuri P, Wiste HJ, Weigand SD (2013): Tracking pathophysiological processes in Alzheimer's disease: an updated hypothetical model of dynamic biomarkers. *Lancet Neurol* 12, 207–216
- Jawhar S, Wirths O, Bayer TA (2011): Pyroglutamate amyloid- β (A β): a hatchet man in Alzheimer disease. *J Biol Chem* 286, 38825–38832
- Jawhar S, Trawicka A, Jenneckens C, Bayer TA, Wirths O (2012): Motor deficits, neuron loss, and reduced anxiety coinciding with axonal degeneration and intraneuronal A β aggregation in the 5XFAD mouse model of Alzheimer's disease. *Neurobiol Aging* 33, 196–e29
- Jellinger KA, Paulus W, Wrocklage C, Litvan I (2001): Traumatic brain injury as a risk factor for Alzheimer disease. Comparison of two retrospective autopsy cohorts with evaluation of ApoE genotype. *BMC Neurol* 1, 3
- Jin M, Shepardson N, Yang T, Chen G, Walsh D, Selkoe DJ (2011): Soluble amyloid β -protein dimers isolated from Alzheimer cortex directly induce Tau hyperphosphorylation and neuritic degeneration. *Proc Natl Acad Sci U S A* 108, 5819–5824
- Kales HC, Kim HM, Zivin K, Valenstein M, Seyfried LS, Chiang C, Cunningham F, Schneider LS, Blow FC (2014): Risk of mortality among individual antipsychotics in patients with dementia. *Am J psychiatry*
- Kandalepas PC, Vassar R (2012): Identification and biology of β -secretase. *J Neurochem* 120, 55–61
- Kanekiyo T, Liu C, Shinohara M, Li J, Bu G (2012): LRP1 in brain vascular smooth muscle cells mediates local clearance of Alzheimer's amyloid-beta. *J Neurosci* 32, 16458–16465
- Kanekiyo T, Cirrito JR, Liu C, Shinohara M, Li J, Schuler DR, Shinohara M, Holtzman DM, Bu G (2013): Neuronal clearance of amyloid- β by endocytic receptor LRP1. *J Neurosci* 33, 19276–19283
- Kang DE, Saitoh T, Chen X, Xia Y, Masliah E, La Hansen, Thomas RG, Thal LJ, Katzman R (1997): Genetic association of the low-density lipoprotein receptor-related protein gene (LRP), and apolipoprotein E receptor, with late-onset Alzheimer's disease. *Neurology* 49, 56–61

- Kang DE, Pietrzik CU, Baum L, Chevallier N, Merriam DE, Kounnas MZ, Wagner SL, Troncoso JC, Kawas CH, Katzman R (2000): Modulation of amyloid beta-protein clearance and Alzheimer's disease susceptibility by the LDL receptor-related protein pathway. *J Clin Invest* 106, 1159–1166
- Karas G, Scheltens P, Rombouts S, van Schijndel R, Klein M, Jones B, van der Flier, Wiesje, Vrenken H, Barkhof F (2007): Precuneus atrophy in early-onset Alzheimer's disease: a morphometric structural MRI study. *Neuroradiology* 49, 967–976
- Karch CM, Cruchaga C, Goate AM (2014): Alzheimer's disease genetics: from the bench to the clinic. *Neuron* 83, 11–26
- Karl T, Pabst R, Hörsten S von (2003): Behavioral phenotyping of mice in pharmacological and toxicological research. *Exp Toxicol Pathol* 55, 69–83
- Kasuga K, Shimohata T, Nishimura A, Shiga A, Mizuguchi T, Tokunaga J, Ohno T, Miyashita A, Kuwano R, Matsumoto N (2009): Identification of independent APP locus duplication in Japanese patients with early-onset Alzheimer disease. *J Neurol Neurosurg Psychiatry* 80, 1050–1052
- Kirova A, Bays RB, Lagalwar S (2015): Working Memory and Executive Function Decline across Normal Aging, Mild Cognitive Impairment, and Alzheimer's Disease. *Biomed Res Int* 2015, 748212
- Kivipelto M, Helkala EL, Laakso MP, Hanninen T, Hallikainen M, Alhainen K, Soininen H, Tuomilehto J, Nissinen A (2001): Midlife vascular risk factors and Alzheimer's disease in later life: longitudinal, population based study. *BMJ* 322, 1447–1451
- Kivipelto M, Ngandu T, Fratiglioni L, Viitanen M, Kareholt I, Winblad B, Helkala E, Tuomilehto J, Soininen H, Nissinen A (2005): Obesity and vascular risk factors at midlife and the risk of dementia and Alzheimer disease. *Arch Neurol* 62, 1556–1560
- Klein WL (2002): Abeta toxicity in Alzheimer's disease: globular oligomers (ADDLs) as new vaccine and drug targets. *Neurochem Int* 41, 345–352
- Klunk WE, Engler H, Nordberg A, Wang Y, Blomqvist G, Holt DP, Bergström M, Savitcheva I, Huang G, Estrada S (2004): Imaging brain amyloid in Alzheimer's disease with Pittsburgh Compound-B. *Ann Neurol* 55, 306–319
- Knauer MF, Soreghan B, Burdick D, Kosmoski J, Glabe CG (1992): Intracellular accumulation and resistance to degradation of the Alzheimer amyloid A4/beta protein. *Proc Natl Acad Sci U S A* 89, 7437–7441
- Kumar-Singh S, Theuns J, van Broeck B, Pirici D, Vennekens K, Corsmit E, Cruts M, Dermaut B, Wang R, van Broeckhoven C (2006): Mean age-of-onset of familial alzheimer disease caused by presenilin mutations correlates with both increased A β 42 and decreased A β 40. *Hum Mutat* 27, 686–695
- Kumar S, Rezaei-Ghaleh N, Terwel D, Thal DR, Richard M, Hoch M, Mc Donald, Jessica M, Wüllner U, Glebov K, Heneka MT (2011): Extracellular phosphorylation of the amyloid β -peptide promotes formation of toxic aggregates during the pathogenesis of Alzheimer's disease. *EMBO J* 30, 2255–2265
- Kuo Y, Webster S, Emmerling MR, Lima N de, Roher AE (1998): Irreversible dimerization/tetramerization and post-translational modifications inhibit proteolytic degradation of A β peptides of Alzheimer's disease. *Biochim Biophys Acta* 1406, 291–298
- Lacroix L, Spinelli S, Heidbreder CA, Feldon J (2000): Differential role of the medial and lateral prefrontal cortices in fear and anxiety. *Behav Neurosci* 114, 1119
- LaFerla FM, Troncoso JC, Strickland DK, Kawas CH, Jay G (1997): Neuronal cell death in Alzheimer's disease correlates with apoE uptake and intracellular Abeta stabilization. *J Clin Invest* 100, 310

- Lalonde R (2002): The neurobiological basis of spontaneous alternation. *Neurosci Biobehav Rev* 26, 91–104
- Lalonde R, Dumont M, Staufenbiel M, Sturchler-Pierrat C, Strazielle C (2002): Spatial learning, exploration, anxiety, and motor coordination in female APP23 transgenic mice with the Swedish mutation. *Brain Res* 956, 36–44
- Lalonde R, Lewis TL, Strazielle C, Kim H, Fukuchi K (2003a): Transgenic mice expressing the β APP 695 SWE mutation: effects on exploratory activity, anxiety, and motor coordination. *Brain Res* 977, 38–45
- Lalonde R, Qian S, Strazielle C (2003b): Transgenic mice expressing the PS1-A246E mutation: effects on spatial learning, exploration, anxiety, and motor coordination. *Behav Brain Res* 138, 71–79
- Lalonde R, Kim HD, Maxwell JA, Fukuchi K (2005): Exploratory activity and spatial learning in 12-month-old APP 695 SWE/co+PS1/ Δ DeltaE9 mice with amyloid plaques. *Neurosci Lett* 390, 87–92
- Lambert J, Wavrant-De Vrièze F, Amouyel P, Chartier-Harlin M (1998): Association at LRP gene locus with sporadic late-onset Alzheimer's disease. *Lancet* 351, 1787–1788
- Lambert JC, Ibrahim-Verbaas CA, Harold D, Naj AC, Sims R, Bellenguez C, DeStafano AL, Bis JC, Beecham GW, Grenier-Boley B (2013): Meta-analysis of 74,046 individuals identifies 11 new susceptibility loci for Alzheimer's disease. *Nat Genet* 45, 1452–1458
- Le Cudennec C, Faure A, Ly M, Delatour B (2008): One-year longitudinal evaluation of sensorimotor functions in APP751SL transgenic mice. *Genes Brain Behav* 7, 83–91
- Lee CD, Landreth GE (2010): The role of microglia in amyloid clearance from the AD brain. *J Neural Transm* 117, 949–960
- Lee K, Lee SH, Kim H, Song J, Yang S, Paik SG, Han P (2004): Progressive cognitive impairment and anxiety induction in the absence of plaque deposition in C57BL/6 inbred mice expressing transgenic amyloid precursor protein. *J Neurosci Res* 76, 572–580
- Leibson CL, Rocca WA, Hanson VA, Cha R, Kokmen E, O'Brien PC, Palumbo PJ (1997): Risk of dementia among persons with diabetes mellitus: a population-based cohort study. *Am J Epidemiol* 145, 301–308
- Lesné SE, Sherman MA, Grant M, Kuskowski M, Schneider JA, Bennett DA, Ashe KH (2013): Brain amyloid- β oligomers in ageing and Alzheimer's disease. *Brain*, awt062
- Levy ML, Cummings JL, Fairbanks LA, Bravi D, Calvani M, Carta A (1996): Longitudinal assessment of symptoms of depression, agitation, and psychosis in 181 patients with Alzheimer's disease. *Am J psychiatry* 153, 1438–1443
- Lyketsos CG, Lopez O, Jones B, Fitzpatrick AL, Breitner J, DeKosky S (2002): Prevalence of neuropsychiatric symptoms in dementia and mild cognitive impairment: results from the cardiovascular health study. *Jama* 288, 1475–1483
- Martinelli JE, Cecato JF, Bartholomeu D, Montiel JM (2014): Comparison of the diagnostic accuracy of neuropsychological tests in differentiating Alzheimer's disease from mild cognitive impairment: can the montreal cognitive assessment be better than the cambridge cognitive examination? *Dement Geriatr Cogn Dis Extra* 4, 113–121
- Masters CL, Simms G, Weinman NA, Multhaup G, McDonald BL, Beyreuther K (1985): Amyloid plaque core protein in Alzheimer disease and Down syndrome. *Proc Natl Acad Sci U S A* 82, 4245–4249

- Mattson MP (1997): Cellular Actions of γ -Amyloid Precursor Protein and Its Soluble and Fibrillogenic Derivatives. *Physiol Rev* 77
- Mattson MP, Guo ZH, Geiger JD (1999): Secreted Form of Amyloid Precursor Protein Enhances Basal Glucose and Glutamate Transport and Protects Against Oxidative Impairment of Glucose and Glutamate Transport in Synaptosomes by a Cyclic GMP-Mediated Mechanism. *J Neurochem* 73, 532–537
- Mattsson N, Zetterberg H, Hansson O, Andreasen N, Parnetti L, Jonsson M, Herukka S, van der Flier, Wiesje M, Blankenstein MA, Ewers M (2009): CSF biomarkers and incipient Alzheimer disease in patients with mild cognitive impairment. *Jama* 302, 385–393
- Mawuenyega KG, Sigurdson W, Ovod V, Munsell L, Kasten T, Morris JC, Yarasheski KE, Bateman RJ (2010): Decreased clearance of CNS β -amyloid in Alzheimer's disease. *Science* 330, 1774
- Mayeux R, Stern Y (2012): Epidemiology of Alzheimer disease. *Cold Spring Harb Perspect Med* 2
- McDonald, Jessica M, Savva GM, Brayne C, Welzel AT, Forster G, Shankar GM, Selkoe DJ, Ince PG, Walsh DM (2010): The presence of sodium dodecyl sulphate-stable A β dimers is strongly associated with Alzheimer-type dementia. *Brain* 133, 1328–1341
- McHugh SB, Deacon RM, Rawlins JN, Bannerman DM (2004): Amygdala and ventral hippocampus contribute differentially to mechanisms of fear and anxiety. *Behav Neurosci* 118, 63
- McKhann GM, Knopman DS, Chertkow H, Hyman BT, Jack CR, Kawas CH, Klunk WE, Koroshetz WJ, Manly JJ, Mayeux R (2011): The diagnosis of dementia due to Alzheimer's disease: recommendations from the National Institute on Aging-Alzheimer's Association workgroups on diagnostic guidelines for Alzheimer's disease. *Alzheimers Dement* 7, 263–269
- McLean CA, Cherny RA, Fraser FW, Fuller SJ, Smith MJ, Vbeyreuther K, Bush AI, Masters CL (1999): Soluble pool of A β amyloid as a determinant of severity of neurodegeneration in Alzheimer's disease. *Ann Neurol* 46, 860–866
- McShane R, Areosa Sastre A, Minakaran N (2006): Memantine for dementia. *Cochrane Database Syst Rev*, CD003154
- Meißner JN, Bouter Y, Bayer TA (2015): Neuron Loss and Behavioral Deficits in the TBA42 Mouse Model Expressing N-Truncated Pyroglutamate Amyloid- β 3–42. *J Alzheimers Dis* 45, 471–482
- Miller DL, Papayannopoulos IA, Styles J, Bobin SA, Lin YY, Biemann K, Iqbal K (1993): Peptide Compositions of the Cerebrovascular and Senile Plaque Core Amyloid Deposits of Alzheimer's Disease. *Arch Biochem Biophys* 301, 41–52
- Milward EA, Papadopoulos R, Fuller SJ, Moir RD, Small D, Beyreuther K, Masters CL (1992): The amyloid protein precursor of Alzheimer's disease is a mediator of the effects of nerve growth factor on neurite outgrowth. *Neuron* 9, 129–137
- Mirra SS, Heyman A, McKeel D, Sumi SM, Crain BJ, Brownlee LM, Vogel FS, Hughes JP, van Belle G, Berg L (1991): The Consortium to Establish a Registry for Alzheimer's Disease (CERAD). Part II. Standardization of the neuropathologic assessment of Alzheimer's disease. *Neurology* 41, 479–486
- Mitchell AJ (2009): A meta-analysis of the accuracy of the mini-mental state examination in the detection of dementia and mild cognitive impairment. *J Psychiatr Res* 43, 411–431
- Moechars D, Dewachter I, Lorent K, Reversé D, Baekelandt V, Naidu A, Tesseur I, Spittaels K, Van Den Haute, Chris, Checler F (1999): Early phenotypic changes in transgenic mice that overexpress different mutants of amyloid precursor protein in brain. *J Biol Chem* 274, 6483–6492

- Moestrup SK, Gliemann J, Pallesen G (1992): Distribution of the α 2-macroglobulin receptor/low density lipoprotein receptor-related protein in human tissues. *Cell Tissue Res* 269, 375–382
- Montine TJ, Phelps CH, Beach TG, Bigio EH, Cairns NJ, Dickson DW, Duyckaerts C, Frosch MP, Masliah E, Mirra SS (2012): National Institute on Aging-Alzheimer's Association guidelines for the neuropathologic assessment of Alzheimer's disease: a practical approach. *Acta Neuropathol* 123, 1–11
- Mori H, Takio K, Ogawara M, Selkoe DJ (1992): Mass spectrometry of purified amyloid beta protein in Alzheimer's disease. *J Biol Chem* 267, 17082–17086
- Mori H, Ishii K, Tomiyama T, Furiya Y, Sahara N, Asano S, Endo N, Shirasawa T, Takio K (1994): Racemization: its biological significance on neuropathogenesis of Alzheimer's disease. *Tohoku J Exp Med* 174, 251–262
- Morris R (1984): Developments of a water-maze procedure for studying spatial learning in the rat. *J Neurosci Methods* 11, 47–60
- Moser M, Moser EI, Forrest E, Andersen P, Morris RG (1995): Spatial learning with a minislab in the dorsal hippocampus. *Proc Natl Acad Sci U S A* 92, 9697–9701
- Mucke L, Abraham CR, Masliah E (1996): Neurotrophic and neuroprotective effects of hAPP in transgenic Micea. *Ann N Y Acad Sci* 777, 82–88
- Mungas D, Harvey D, Reed BR, Jagust WJ, DeCarli C, Beckett L, Mack WJ, Kramer JH, Weiner MW, Schuff N (2005): Longitudinal volumetric MRI change and rate of cognitive decline. *Neurology* 65, 565–571
- Munson GW, Roher AE, Kuo Y, Gilligan SM, Reardon CA, Getz GS, LaDu MJ (2000): SDS-stable complex formation between native apolipoprotein E3 and β -amyloid peptides. *Biochemistry* 39, 16119–16124
- Nakagawa T, Zhu H, Morishima N, Li E, Xu J, Yankner BA, Yuan J (2000): Caspase-12 mediates endoplasmic-reticulum-specific apoptosis and cytotoxicity by amyloid- β . *Nature* 403, 98–103
- Näslund J, Schierhorn A, Hellman U, Lannfelt L, Roses AD, Tjernberg LO, Silberring J, Gandy SE, Winblad B, Greengard P (1994): Relative abundance of Alzheimer A beta amyloid peptide variants in Alzheimer disease and normal aging. *Proc Natl Acad Sci U S A* 91, 8378–8382
- Nazer B, Hong S, Selkoe DJ (2008): LRP promotes endocytosis and degradation, but not transcytosis, of the amyloid- β peptide in a blood-brain barrier in vitro model. *Neurobiol Dis* 30, 94–102
- Nickerson DA, Taylor SL, Fullerton SM, Weiss KM, Clark AG, Stengård JH, Salomaa V, Boerwinkle E, Sing CF (2000): Sequence diversity and large-scale typing of SNPs in the human apolipoprotein E gene. *Genome Res* 10, 1532–1545
- Noguchi A, Matsumura S, Dezawa M, Tada M, Yanazawa M, Ito A, Akioka M, Kikuchi S, Sato M, Ideno S (2009): Isolation and characterization of patient-derived, toxic, high mass amyloid β -protein (A β) assembly from Alzheimer disease brains. *J Biol Chem* 284, 32895–32905
- Nussbaum JM, Schilling S, Cynis H, Silva A, Swanson E, Wangsanut T, Tayler K, Wiltgen B, Hatami A, Röncke R (2012): Prion-like behaviour and tau-dependent cytotoxicity of pyroglutamylated amyloid- β . *Nature* 485, 651–655
- Oakley H, Cole SL, Logan S, Maus E, Shao P, Craft J, Guillozet-Bongaarts A, Ohno M, Disterhoft J, van Eldik L (2006): Intraneuronal β -amyloid aggregates, neurodegeneration, and neuron loss in transgenic mice with five familial Alzheimer's disease mutations: potential factors in amyloid plaque formation. *J Neurosci* 26, 10129–10140

- Olson MI, Shaw C (1969): Presenile dementia and Alzheimer's disease in mongolism. *Brain* 92, 147–156
- Ownby RL, Crocco E, Acevedo A, John V, Loewenstein D (2006): Depression and risk for Alzheimer disease: systematic review, meta-analysis, and metaregression analysis. *Arch Gen Psychiatry* 63, 530–538
- Perez-Garmendia R, Gevorkian G (2013): Pyroglutamate-Modified Amyloid Beta Peptides: Emerging Targets for Alzheimer's Disease Immunotherapy. *Curr Neuroparmacol* 11, 491–498
- Petersen RC (2004): Mild cognitive impairment as a diagnostic entity. *J Intern Med* 256, 183–194
- Pettersson AF, Olsson E, Wahlund L (2005): Motor function in subjects with mild cognitive impairment and early Alzheimer's disease. *Dement Geriatr Cogn Disord* 19, 299–304
- Pike CJ, Walencewicz AJ, Glabe CG, Cotman CW (1991): In vitro aging of β -amyloid protein causes peptide aggregation and neurotoxicity. *Brain Res* 563, 311–314
- Pike CJ, Overman MJ, Cotman CW (1995): Amino-terminal deletions enhance aggregation of β -amyloid peptides in vitro. *J Biol Chem* 270, 23895–23898
- Plassman BL, Havlik RJ, Steffens DC, Helms MJ, Newman TN, Drosdick D, Phillips C, Gau BA, Welsh-Bohmer KA, Burke JR (2000): Documented head injury in early adulthood and risk of Alzheimer's disease and other dementias. *Neurology* 55, 1158–1166
- Pollay M (2010): The function and structure of the cerebrospinal fluid outflow system. *Cerebrospinal Fluid Res* 7, 9
- Portelius E, Bogdanovic N, Gustavsson MK, Volkman I, Brinkmalm G, Zetterberg H, Winblad B, Blennow K (2010): Mass spectrometric characterization of brain amyloid beta isoform signatures in familial and sporadic Alzheimer's disease. *Acta Neuropathol* 120, 185–193
- Porter VR, Buxton WG, Fairbanks LA, Strickland T, O'Connor SM, Rosenberg-Thompson S, Cummings JL (2014): Frequency and characteristics of anxiety among patients with Alzheimer's disease and related dementias. *J Neuropsychiatry Clin Neurosci*
- Prelli F, Castano E, Glenner GG, Frangione B (1988): Differences between vascular and plaque core amyloid in Alzheimer's disease. *J Neurochem* 51, 648–651
- Qiu C, Winblad B, Marengoni A, Klarin I, Fastbom J, Fratiglioni L (2006): Heart failure and risk of dementia and Alzheimer disease: a population-based cohort study. *Arch Intern Med* 166, 1003–1008
- Qiu C, Ronchi D de, Fratiglioni L (2007): The epidemiology of the dementias: an update. *Curr Opin Psychiatry* 20, 380–385
- Qosa H, Abuasal BS, Romero IA, Weksler B, Couraud P, Keller JN, Kaddoumi A (2014): Differences in amyloid- β clearance across mouse and human blood-brain barrier models: Kinetic analysis and mechanistic modeling. *Neuropharmacology* 79, 668–678
- Ramanathan A, Nelson AR, Sagare AP, Zlokovic BV (2015): Impaired vascular-mediated clearance of brain amyloid beta in Alzheimer's disease: the role, regulation and restoration of LRP1. *Front Aging Neurosci* 7, 136
- Raux G, Guyant-Marechal L, Martin C, Bou J, Penet C, Brice A, Hannequin D, Frebourg T, Campion D (2005): Molecular diagnosis of autosomal dominant early onset Alzheimer's disease: an update. *J Med Genet* 42, 793–795

- Rebeck GW, Harr SD, Hyman BT, Strickland DK (1995): Multiple, diverse senile plaque-associated proteins are ligands of an apolipoprotein e receptor, the α 2-macroglobulin receptor/low-density-lipoprotein receptor—related protein. *Ann Neurol* 37, 211–217
- Reddy PH, Beal MF (2008): Amyloid beta, mitochondrial dysfunction and synaptic damage: implications for cognitive decline in aging and Alzheimer's disease. *Trends Mol Med* 14, 45–53
- Reilly JF, Games D, Rydel RE, Freedman S, Schenk D, Young WG, Morrison JH, Bloom FE (2003): Amyloid deposition in the hippocampus and entorhinal cortex: quantitative analysis of a transgenic mouse model. *Proc Natl Acad Sci U S A* 100, 4837–4842
- Reisberg B, Auer SR, Monteiro IM (1997): Behavioral pathology in Alzheimer's disease (BEHAVE-AD) rating scale. *Alzheimer Dis Assoc Disord* 8, 301–308
- Reitz C, Brayne C, Mayeux R (2011): Epidemiology of Alzheimer disease. *Nat Rev Neurol* 7, 137–152
- Reitz C, Mayeux R (2014): Alzheimer disease: epidemiology, diagnostic criteria, risk factors and biomarkers. *Biochem Pharmacol* 88, 640–651
- Ridder DA, Lang M, Salinin S, Roderer J, Struss M, Maser-Gluth C, Schwaninger M (2011): TAK1 in brain endothelial cells mediates fever and lethargy. *J Exp Med* 208, 2615–2623
- Riekkinen P, Sirvio J (1990): Interaction between raphe dorsalis and nucleus basalis magnocellularis in spatial learning. *Brain Res* 527, 342–345
- Rohlmann A, Gotthardt M, Hammer RE, Herz J (1998): Inducible inactivation of hepatic LRP gene by cre-mediated recombination confirms role of LRP in clearance of chylomicron remnants. *J Clin Invest* 101, 689–695
- Rolland Y, Pillard F, Klapouszczak A, Reynish E, Thomas D, Andrieu S, Rivière D, Vellas B (2007): Exercise Program for Nursing Home Residents with Alzheimer's Disease: A 1-Year Randomized, Controlled Trial. *J Am Geriatr Soc* 55, 158–165
- Rovelet-Lecrux A, Hannequin D, Raux G, Le Meur N, Laquerrière A, Vital A, Dumanchin C, Feuillette S, Brice A, Vercelletto M (2006): APP locus duplication causes autosomal dominant early-onset Alzheimer disease with cerebral amyloid angiopathy. *Nat Genet* 38, 24–26
- Rovelet-Lecrux A, Frebourg T, Tuominen H, Majamaa K, Campion D, Remes AM (2007): APP locus duplication in a Finnish family with dementia and intracerebral haemorrhage. *J Neurol Neurosurg Psychiatry* 78, 1158–1159
- Rowe CC, Ng S, Ackermann U, Gong SJ, Pike K, Savage G, Cowie TF, Dickinson KL, Maruff P, Darby D (2007): Imaging β -amyloid burden in aging and dementia. *Neurology* 68, 1718–1725
- Russo C, Violani E, Salis S, Venezia V, Dolcini V, Damonte G, Benatti U, D'Arrigo C, Patrone E, Carlo P (2002): Pyroglutamate-modified amyloid β -peptides-A β N3 (pE)-strongly affect cultured neuron and astrocyte survival. *J Neurochem* 82, 1480–1489
- Saido TC, Iwatsubo T, Mann DMA, Shimada H, Ihara Y, Kawashima S (1995): Dominant and differential deposition of distinct β -amyloid peptide species, A β N3 (pE), in senile plaques. *Neuron* 14, 457–466
- Salkovic-Petrisic M, Osmanovic J, Grunblatt E, Riederer P, Hoyer S (2009): Modeling sporadic Alzheimer's disease: the insulin resistant brain state generates multiple long-term morphobiological abnormalities including hyperphosphorylated tau protein and amyloid-beta. *J Alzheimers Dis* 18, 729–750
- Santin LJ, Rubio S, Begega A, Arias JL (1999): Effects of mammillary body lesions on spatial reference and working memory tasks. *Behav Brain Res* 102, 137–150

- Savage LM, Sweet AJ, Castillo R, Langlais PJ (1997): The effects of lesions to thalamic lateral internal medullary lamina and posterior nuclei on learning, memory and habituation in the rat. *Behav Brain Res* 82, 133–147
- Savonenko AV, Xu GM, Price DL, Borchelt DR, Markowska AL (2003): Normal cognitive behavior in two distinct congenic lines of transgenic mice hyperexpressing mutant APP SWE. *Neurobiol Dis* 12, 194–211
- Scarmeas N, Albert M, Brandt J, Blacker D, Hadjigeorgiou G, Papadimitriou A, Dubois B, Sarazin M, Wegesin D, Marder K (2005): Motor signs predict poor outcomes in Alzheimer disease. *Neurology* 64, 1696–1703
- Scheuner D, Eckman C, Jensen M, Song X, Citron M, Suzuki N, Bird TD, Hardy J, Hutton M, Kukull W (1996): Secreted amyloid β -protein similar to that in the senile plaques of Alzheimer's disease is increased in vivo by the presenilin 1 and 2 and APP mutations linked to familial Alzheimer's disease. *Nat Med* 2, 864–870
- Schilling S, Hoffmann T, Manhart S, Hoffmann M, Demuth H (2004): Glutaminyl cyclases unfold glutamyl cyclase activity under mild acid conditions. *FEBS Lett* 563, 191–196
- Schilling S, Lauber T, Schaupp M, Manhart S, Scheel E, Böhm G, Demuth H (2006): On the seeding and oligomerization of pGlu-amyloid peptides (in vitro). *Biochemistry* 45, 12393–12399
- Schilling S, Zeitschel U, Hoffmann T, Heiser U, Francke M, Kehlen A, Holzer M, Hutter-Paier B, Prokesch M, Windisch M et al. (2008): Glutaminyl cyclase inhibition attenuates pyroglutamate A β and Alzheimer's disease-like pathology. *Nat Med* 14, 1106–1111
- Schlenzig D, Manhart S, Cinar Y, Kleinschmidt M, Hause G, Willbold D, Funke SA, Schilling S, Demuth H (2009): Pyroglutamate formation influences solubility and amyloidogenicity of amyloid peptides. *Biochemistry* 48, 7072–7078
- Schmitz C, Hof PR (2005): Design-based stereology in neuroscience. *Neuroscience* 130, 813–831
- Schmitz C, Rutten BPF, Pielen A, Schäfer S, Wirths O, Tremp G, Czech C, Blanchard V, Multhaup G, Rezaie P (2004): Hippocampal neuron loss exceeds amyloid plaque load in a transgenic mouse model of Alzheimer's disease. *Am J Pathol* 164, 1495–1502
- Schneider LS, Mangialasche F, Andreasen N, Feldman H, Giacobini E, Jones R, Mantua V, Mecocci P, Pani L, Winblad B (2014): Clinical trials and late-stage drug development for Alzheimer's disease: an appraisal from 1984 to 2014. *J Intern Med* 275, 251–283
- Sehgal N, Gupta A, Valli RK, Joshi SD, Mills JT, Hamel E, Khanna P, Jain SC, Thakur SS, Ravindranath V (2012): *Withania somnifera* reverses Alzheimer's disease pathology by enhancing low-density lipoprotein receptor-related protein in liver. *Proc Natl Acad Sci U S A* 109, 3510–3515
- Seitz DP, Adunuri N, Gill SS, Gruneir A, Herrmann N, Rochon P (2011): Antidepressants for agitation and psychosis in dementia. *Cochrane Database Syst Rev*, CD008191
- Selkoe DJ (1998): The cell biology of β -amyloid precursor protein and presenilin in Alzheimer's disease. *Trends Cell Biol* 8, 447–453
- Selkoe DJ (2000): Toward a Comprehensive Theory for Alzheimer's Disease. Hypothesis: Alzheimer's Disease Is Caused by the Cerebral Accumulation and Cytotoxicity of Amyloid β -Protein. *Ann N Y Acad Sci* 924, 17–25
- Selkoe DJ, Wolfe MS (2007): Presenilin: running with scissors in the membrane. *Cell* 131, 215–221
- Selkoe DJ, Abraham CR, Podlisny MB, Duffy LK (1986): Isolation of low-molecular-weight proteins from amyloid plaque fibers in Alzheimer's disease. *J Neurochem* 46, 1820–1834

- Sergeant N, Bombois S, Ghestem A, Drobecq H, Kostanjevecki V, Missiaen C, Wattez A, David J, Vanmechelen E, Sergheraert C (2003): Truncated beta-amyloid peptide species in pre-clinical Alzheimer's disease as new targets for the vaccination approach. *J Neurochem* 85, 1581–1591
- Seubert P, Vigo-Pelfrey C, Esch F, Lee M, Dovey H, Davis D, Sinha S, Schiossmacher M, Whaley J, Swindlehurst C (1992): Isolation and quantification of soluble Alzheimer's β -peptide from biological fluids. *Nature* 359, 325–327
- Sevalle J, Amoyel A, Robert P, Fournie-Zaluski M, Roques B, Checler F (2009): Aminopeptidase A contributes to the N-terminal truncation of amyloid beta-peptide. *J Neurochem* 109, 248–256
- Shankar GM, Li S, Mehta TH, Garcia-Munoz A, Shepardson NE, Smith I, Brett FM, Farrell MA, Rowan MJ, Lemere CA (2008): Amyloid- β protein dimers isolated directly from Alzheimer's brains impair synaptic plasticity and memory. *Nat Med* 14, 837–842
- Shibata M, Yamada S, Kumar SR, Calero M, Bading J, Frangione B, Holtzman DM, Miller CA, Strickland DK, Ghiso J (2000): Clearance of Alzheimer's amyloid- β 1-40 peptide from brain by LDL receptor-related protein-1 at the blood-brain barrier. *J Clin Invest* 106, 1489
- Shin J, Kepe V, Barrio JR, Small GW (2010): The merits of FDDNP-PET imaging in Alzheimer's disease. *J Alzheimers Dis* 26, 135–145
- Shoghi-Jadid K, Small GW, Agdeppa ED, Kepe V, Ercoli LM, Siddarth P, Read S, Satyamurthy N, Petric A, Huang S (2002): Localization of neurofibrillary tangles and beta-amyloid plaques in the brains of living patients with Alzheimer disease. *Am J Geriatr Psychiatry* 10, 24–35
- Siemers ER, Sundell KL, Carlson C, Case M, Sethuraman G, Liu-Seifert H, Dowsett SA, Pontecorvo MJ, Dean RA, Demattos R (2015): Phase 3 solanezumab trials: Secondary outcomes in mild Alzheimer's disease patients. *Alzheimers Dement*
- Silverberg GD, Messier AA, Miller MC, Machan JT, Majmudar SS, Stopa EG, Donahue JE, Johanson CE (2010): Amyloid efflux transporter expression at the blood-brain barrier declines in normal aging. *J Neuropathol Exp Neurol* 69, 1034–1043
- Sisodia SS (1992): Beta-amyloid precursor protein cleavage by a membrane-bound protease. *Proc Natl Acad Sci U S A* 89, 6075–6079
- Sivanandam TM, Thakur MK (2012): Traumatic brain injury: a risk factor for Alzheimer's disease. *Neurosci Biobehav Rev* 36, 1376–1381
- Slegers K, Brouwers N, Gijssels I, Theuns J, Goossens D, Wauters J, Del-Favero J, Cruts M, van Duijn, Cornelia M, van Broeckhoven C (2006): APP duplication is sufficient to cause early onset Alzheimer's dementia with cerebral amyloid angiopathy. *Brain* 129, 2977–2983
- Smith DH, Okiyama K, Thomas MJ, Claussen B, McIntosh TK (1991): Evaluation of memory dysfunction following experimental brain injury using the Morris water maze. *J Neurotrauma* 8, 259–269
- Steen E, Terry BM, Rivera EJ, Cannon JL, Neely TR, Tavares R, Xu XJ, Wands JR, de la Monte, Suzanne M (2005): Impaired insulin and insulin-like growth factor expression and signaling mechanisms in Alzheimer's disease—is this type 3 diabetes? *J Alzheimers Dis* 7, 63–80
- Sterniczuk R, Antle MC, LaFerla FM, Dyck RH (2010): Characterization of the 3xTg-AD mouse model of Alzheimer's disease: part 2. Behavioral and cognitive changes. *Brain Res* 1348, 149–155
- Storck SE, Meister S, Nahrath J, Meissner JN, Schubert N, Di Spiezio A, Baches S, Vandenbroucke RE, Bouter Y, Prikulis I (2016): Endothelial LRP1 transports amyloid-beta1-42 across the blood-brain barrier. *J Clin Invest* 126, 123–136

- Storey E, Spurck T, Pickett-Heaps J, Beyreuther K, Masters CL (1996): The amyloid precursor protein of Alzheimer's disease is found on the surface of static but not actively motile portions of neurites. *Brain Res* 735, 59–66
- Strittmatter WJ, Saunders AM, Schmechel D, Pericak-Vance M, Enghild J, Salvesen GS, Roses AD (1993): Apolipoprotein E: high-avidity binding to beta-amyloid and increased frequency of type 4 allele in late-onset familial Alzheimer disease. *Proc Natl Acad Sci U S A* 90, 1977–1981
- Sunderland T, Hill JL, Mellow AM, Lawlor BA, Gundersheimer J, Newhouse PA, Grafman JH (1989): Clock drawing in Alzheimer's disease. *J Am Geriatr Soc* 37, 725–729
- Takasugi N, Tomita T, Hayashi I, Tsuruoka M, Nüimura M, Takahashi Y, Thinakaran G, Iwatsubo T (2003): The role of presenilin cofactors in the γ -secretase complex. *Nature* 422, 438–441
- Talbot K, Wang H, Kazi H, Han L, Bakshi KP, Stucky A, Fuino RL, Kawaguchi KR, Samoyedny AJ, Wilson RS (2012): Demonstrated brain insulin resistance in Alzheimer's disease patients is associated with IGF-1 resistance, IRS-1 dysregulation, and cognitive decline. *J Clin Invest* 122, 1316–1338
- Tanila H (2012): Wading pools, fading memories—place navigation in transgenic mouse models of Alzheimer's disease. *Front Aging Neurosci* 4
- Tarasoff-Conway JM, Carare RO, Osorio RS, Glodzik L, Butler T, Fieremans E, Axel L, Rusinek H, Nicholson C, Zlokovic BV (2015): Clearance systems in the brain-implications for Alzheimer disease. *Nat Rev Neurol* 11, 457–470
- Thal DR, Rüb U, Orantes M, Braak H (2002): Phases of A β -deposition in the human brain and its relevance for the development of AD. *Neurology* 58, 1791–1800
- Thinakaran G, Koo EH (2008): Amyloid precursor protein trafficking, processing, and function. *J Biol Chem* 283, 29615–29619
- Tomiyama T, Nagata T, Shimada H, Teraoka R, Fukushima A, Kanemitsu H, Takuma H, Kuwano R, Imagawa M, Ataka S (2008): A new amyloid β variant favoring oligomerization in Alzheimer's-type dementia. *Ann Neurol* 63, 377–387
- van Dam D, D'Hooze R, Staufenbiel M, van Ginneken C, van Meir F, De Deyn, Peter P (2003): Age-dependent cognitive decline in the APP23 model precedes amyloid deposition. *Eur J Neurosci* 17, 388–396
- Varadi K, Michelfelder S, Korff T, Hecker M, Trepel M, Katus HA, Kleinschmidt JA, Muller OJ (2012): Novel random peptide libraries displayed on AAV serotype 9 for selection of endothelial cell-directed gene transfer vectors. *Gene Ther* 19, 800–809
- Vassar R, Bennett BD, Babu-Khan S, Kahn S, Mendiaz EA, Denis P, Teplow DB, Ross S, Amarante P, Loeloff R (1999): β -Secretase cleavage of Alzheimer's amyloid precursor protein by the transmembrane aspartic protease BACE. *Science* 286, 735–741
- Villemagne VL, Burnham S, Bourgeat P, Brown B, Ellis KA, Salvado O, Szoek C, Macaulay SL, Martins R, Maruff P (2013): Amyloid beta deposition, neurodegeneration, and cognitive decline in sporadic Alzheimer's disease: a prospective cohort study. *Lancet Neurol* 12, 357–367
- Walf AA, Frye CA (2007): The use of the elevated plus maze as an assay of anxiety-related behavior in rodents. *Nat Protoc* 2, 322–328
- Wang D, Dickson DW, Malter JS (2006): beta-Amyloid degradation and Alzheimer's disease. *J Biomed Biotechnol* 2006
- Webster SJ, Bachstetter AD, Van Eldik, Linda J (2013): Comprehensive behavioral characterization of an APP/PS-1 double knock-in mouse model of Alzheimer's disease. *Alzheimers Res Ther* 5, 28

- Weder ND, Aziz R, Wilkins K, Tampi RR (2007): Frontotemporal dementias: a review. *Ann Gen Psychiatry* 6, 1–10
- Weller RO, Subash M, Preston SD, Mazanti I, Carare RO (2008): Perivascular drainage of amyloid-beta peptides from the brain and its failure in cerebral amyloid angiopathy and Alzheimer's disease. *Brain Pathol* 18, 253–266
- West MJ, Slomianka L, Gundersen HJ (1991): Unbiased stereological estimation of the total number of neurons in the subdivisions of the rat hippocampus using the optical fractionator. *Anat Rec* 231, 482–497
- West MJ, Coleman PD, Flood DG, Troncoso JC (1994): Differences in the pattern of hippocampal neuronal loss in normal ageing and Alzheimer's disease. *Lancet* 344, 769–772
- Westerman MA, Cooper-Blacketer D, Mariash A, Kotilinek L, Kawarabayashi T, Younkin LH, Carlson GA, Younkin SG, Ashe KH (2002): The relationship between A β and memory in the Tg2576 mouse model of Alzheimer's disease. *J Neurosci* 22, 1858–1867
- Willem M, Tahirovic S, Busche MA, Ovsepian SV, Chafai M, Kootar S, Hornburg D, Evans LDB, Moore S, Daria A (2015): γ -Secretase processing of APP inhibits neuronal activity in the hippocampus. *Nature* 526, 443–447
- Wirths O, Bayer TA (2008): Motor impairment in Alzheimer's disease and transgenic Alzheimer's disease mouse models. *Genes Brain Behav* 7, 1–5
- Wirths O, Bayer TA (2010): Neuron loss in transgenic mouse models of Alzheimer's disease. *Int J Alzheimers Dis* 2010
- Wirths O, Multhaup G, Bayer TA (2004): A modified β -amyloid hypothesis: intraneuronal accumulation of the β -amyloid peptide—the first step of a fatal cascade. *J Neurochem* 91, 513–520
- Wirths O, Weis J, Kayed R, Saido TC, Bayer TA (2007): Age-dependent axonal degeneration in an Alzheimer mouse model. *Neurobiol Aging* 28, 1689–1699
- Wirths O, Breyhan H, Schäfer S, Roth C, Bayer TA (2008): Deficits in working memory and motor performance in the APP/PS1ki mouse model for Alzheimer's disease. *Neurobiol Aging* 29, 891–901
- Wirths O, Breyhan H, Cynis H, Schilling S, Demuth H, Bayer TA (2009): Intraneuronal pyroglutamate-A β 3–42 triggers neurodegeneration and lethal neurological deficits in a transgenic mouse model. *Acta Neuropathol* 118, 487–496
- Wirths O, Erck C, Martens H, Harmeier A, Geumann C, Jawhar S, Kumar S, Multhaup G, Walter J, Ingelsson M (2010): Identification of low molecular weight pyroglutamate A β oligomers in Alzheimer disease: a novel tool for therapy and diagnosis. *J Biol Chem* 285, 41517–41524
- Witnam JL, Portelius E, Zetterberg H, Gustavsson MK, Schilling S, Koch B, Demuth H, Blennow K, Wirths O, Bayer TA (2012): Pyroglutamate amyloid β (A β) aggravates behavioral deficits in transgenic amyloid mouse model for Alzheimer disease. *J Biol Chem* 287, 8154–8162
- World Health Organization: International Statistical Classification of Diseases and Related Health Problems 10th Revision (G30.-), www.icd-code.de/icd/code/F00.-*.html, Zugriff am 01.08.2015
- Wyss-Coray T, Lin C, Yan F, Yu GQ, Rohde M, McConlogue L, Masliah E, Mucke L (2001): TGF- β 1 promotes microglial amyloid-beta clearance and reduces plaque burden in transgenic mice. *Nat Med* 7, 612–618
- Wyss-Coray T, Loike JD, Brionne TC, Lu E, Anankov R, Yan F, Silverstein SC, Husemann J (2003): Adult mouse astrocytes degrade amyloid-beta in vitro and in situ. *Nat Med* 9, 453–457

- Yamada K, Hashimoto T, Yabuki C, Nagae Y, Tachikawa M, Strickland DK, Liu Q, Bu G, Basak JM, Holtzman DM (2008): The low density lipoprotein receptor-related protein 1 mediates uptake of amyloid beta peptides in an in vitro model of the blood-brain barrier cells. *J Biol Chem* 283, 34554–34562
- Yamin G (2009): NMDA receptor-dependent signaling pathways that underlie amyloid β -protein disruption of LTP in the hippocampus. *J Neurosci Res* 87, 1729–1736
- Yan R, Bienkowski MJ, Shuck ME, Miao H, Tory MC, Pauley AM, Brashler JR, Stratman NC, Mathews WR, Buhl AE (1999): Membrane-anchored aspartyl protease with Alzheimer's disease β -secretase activity. *Nature* 402, 533–537
- Yu G, Nishimura M, Arawaka S, Levitan D, Zhang L, Tandon A, Song Y, Rogaeva E, Chen F, Kawarai T (2000): Nicastrin modulates presenilin-mediated notch/glp-1 signal transduction and β APP processing. *Nature* 407, 48–54
- Zempel H, Thies E, Mandelkow E, Mandelkow E (2010): A β oligomers cause localized Ca²⁺ elevation, missorting of endogenous Tau into dendrites, Tau phosphorylation, and destruction of microtubules and spines. *J Neurosci* 30, 11938–11950
- Zetterberg H, Mattsson N (2014): Understanding the cause of sporadic Alzheimer's disease. *Expert Rev Neurother* 14, 621–630
- Zhao Z, Sagare AP, Ma Q, Halliday MR, Kong P, Kisler K, Winkler EA, Ramanathan A, Kanekiyo T, Bu G (2015): Central role for PICALM in amyloid-beta blood-brain barrier transcytosis and clearance. *Nat Neurosci* 18, 978–987
- Ziegler U, Doblhammer G (2009): Prävalenz und Inzidenz von Demenz in Deutschland-Eine Studie auf Basis von Daten der gesetzlichen Krankenversicherungen von 2002. *Gesundheitswesen* 71, 281–290
- Zlokovic BV (2005): Neurovascular mechanisms of Alzheimer's neurodegeneration. *Trends Neurosci* 28, 202–208
- Zlokovic BV (2011): Neurovascular pathways to neurodegeneration in Alzheimer's disease and other disorders. *Nat Rev Neurosci* 12, 723–738
- Zlokovic BV, Deane R, Sagare AP, Bell RD, Winkler EA (2010): Low-density lipoprotein receptor-related protein-1: a serial clearance homeostatic mechanism controlling Alzheimer's amyloid β -peptide elimination from the brain. *J Neurochem* 115, 1077–1089

Acknowledgements

First and foremost, I want to thank Prof. Dr. Thomas A. Bayer for giving me the opportunity to work in his laboratory and carry out this thesis under his supervision. I am extremely grateful to his encouragement and would like to thank him for discussing my projects and letting me work very independently.

I especially would like to thank Dr. Yvonne Bouter for her mentorship and supervision. She was always reachable and greatly involved in the design of my studies. I would also like to thank her for discussing my results and insightful feedback.

I would also like to thank PD Dr. Oliver Wirths who was always reachable when questions concerning my work occurred. I thank Petra Tucholla for excellent technical and logistical support. Additionally, I would like to thank Nils Schubert for the good collaboration in the LRP1 project.

I am very grateful to the Jacob-Henle-Programm for experimental medicine by the university medicine Göttingen. The program allowed me to concentrate on my work in the laboratory, providing financial support and indispensable background knowledge. In this context I especially would like to thank Dr. Werner Albig.

I would also like to thank the German National Academic Foundation (Studienstiftung des Deutschen Volkes) for financial support and an interesting summer academy on Alzheimer's disease with Prof. Dr. Marcus Fändrich and Prof. Dr. Dietmar Thal.

I thank Helene Sophie Meißner for proof reading the thesis.

Curriculum vitae

I was born on the 18th of June 1991 as the third child of my parents Andreas Siegfried and Heide Meißner in Göttingen. Here I visited Lohberg-Grundschule from 1997 to 2001 and Hainberg-Gymnasium from 2001 to 2010. Here I was awarded the Allgemeine Hochschulreife (very good (1.3)).

From August 2010 to April 2011 I did community service in the protestant hospital Neu Beth-lehem in Göttingen.

In April 2011 I began to study human medicine at the Georg-August-Universität Göttingen. In March 2013 I completed the ersten Abschnitt der ärztlichen Prüfung (very good (1.5)). From August 2013 to October 2014 I participated in the Jacob-Henle-Programm für experimentelle Medizin of the Georg-August-Universität Göttingen and started my experimental work in the Division of Molecular Psychiatry, Department of Psychiatry and Psychotherapy under the direction of Prof. Dr. rer. nat. T. A. Bayer in February 2014. I was supervised by Dr. rer. nat. Yvonne Bouter. I have been a fellow of the German National Academic Foundation since January 2014.